ISSN 3083-7219 (Print)
ISSN 3083-7227 (Online)

№1
(150)
2026

ТЕОРІЯ І ПРАКТИКА МЕТАЛУРГІЇ

THEORY AND PRACTICE OF METALLURGY

ТЕОРІЯ І ПРАКТИКА МЕТАЛУРГІЇ

№1
(150)
2026

НАУКОВО-ВИРОБНИЧИЙ ЖУРНАЛ

Видається з березня 1997 року
Виходить 4 рази на рік

Засновник і видавець: Український державний університет науки і технологій

Дніпро
2026

УДК 669:620.2:621

Журнал зареєстровано в Національній раді України з питань телебачення і радіомовлення як друковане медіа. Рішення № 924 від 28.09.2023. Ідентифікатор медіа: R30-01392.
Наказом Міністерства освіти і науки України №157 від 09.02.2021 р. журнал включено до категорії «Б» переліку наукових фахових видань України за спеціальностями:

133 – Галузеве машинобудування;
136 – Металургія;
161 – Хімічні технології

РЕДАКЦІЙНА КОЛЕГІЯ

***Пройдак Юрій Сергійович*,** доктор технічних наук, професор, проректор з наукової роботи, Український державний університет науки і технологій, Україна – **головний редактор**

***Камкіна Людмила Володимирівна*,** доктор технічних наук, професор, завідувач кафедри теоретичних основ металургійних процесів, Український державний університет науки і технологій, Україна

***Білодіденко Сергій Валентинович*,** доктор технічних наук, професор, завідувач кафедри галузевого машинобудування, Український державний університет науки і технологій, Україна

***Єрьомін Олександр Олегович*,** доктор технічних наук, професор, завідувач кафедри екології, теплотехніки та охорони праці, Український державний університет науки і технологій, Україна

***Узлов Костянтин Іванович*,** доктор технічних наук, професор, професор, Український державний університет науки і технологій, Україна

***Кавалек Анна Малгожата*,** доктор технічних наук, декан факультету інженерії продукції та технології матеріалів, Ченстоховська Політехніка, Польща

Карбовничек Мирослав, доктор технічних наук, професор, завідувач кафедри чорної металургії, Гірничо-металургійна академія ім. Станіслава Сташиця, Польща

***Лежнєв Сергій Николаевич*,** кандидат наук, доцент, доцент кафедри металургії та гірничої справи, Рудненський індустріальний інститут, Казахстан

Лобода Петро Іванович, доктор технічних наук, професор, академік НАН України, науковий керівник кафедри високотемпературних матеріалів та порошкової металургії, Навчально-науковий інститут матеріалознавства та зварювання імені Є.О. Патона Національного технічного університету України «Київський політехнічний інститут імені Ігоря Сікорського» (НН ІМЗ ім. Є.О. Патона), Україна

Молчанов Лавр Сергійович, кандидат технічних наук, доцент, зав. відділом фізико-технічних проблем металургії сталі, Інститут чорної металургії ім. З.І. Некрасова НАН України, Україна

***Муравйова Ірина Геннадіївна*,** доктор технічних наук, професор, Провідний науковий співробітник, Інститут чорної металургії ім. З.І. Некрасова НАН України

***Тогобицька Дар'я Миколаївна*,** доктор технічних наук, професор, провідний науковий співробітник відділу фізико-хімічних проблем металургійних процесів, Інститут чорної металургії ім. З.І. Некрасова НАН України, Україна

Матеріали публікуються мовою оригіналу та ліцензуються відповідно до Creative Commons Attribution 4.0 International (CC BY 4.0).

Автори зберігають авторські права на опубліковані статті та надають видавцеві невиключне право на публікацію статті з посиланням на нього, як на оригінального видавця, у разі повторного використання, а також на розповсюдження статті у будь-якій формі та на будь-яких носіях.

Автори можуть укладати окремі додаткові договори про невиключне поширення опублікованої статті (наприклад, розміщення її в інституційному репозитарії або публікація в книзі) із зазначенням її первинної публікації в цьому журналі з обов'язковим зазначенням doi статті.

THEORY AND PRACTICE OF METALLURGY

No. 1
(150)
2026

SCIENTIFIC AND PRODUCTION JOURNAL

Issued since March 1997
Released 4 times a year

Founder and Publisher: Ukrainian State University of Science and Technologies

Dnipro
2026

UDC 669:620.2:621

The Journal is registered as a print media outlet by the National Council of Television and Radio Broadcasting of Ukraine. Decision No. 924, dated September 28, 2023. Media Identifier: R30-01392.

By the order of the Ministry of Education and Science of Ukraine No. 157 from 09.02.2021 p. the journal is included in category "B" of the list of scientific professional publications of Ukraine, by specialties:

133 - Industry engineering;
136 - Metallurgy;
161 - Chemical technologies

EDITORIAL BOARD

Proidak Yurii Serhiiovych, D. Sc. (Tech.), Professor, Vice-Rector for scientific work, Ukrainian State University of Science and Technologies, Ukraine - ***Editor in Chief***

Kamkina Liudmyla Volodymyrivna**,** D. Sc. (Tech.), Professor, Head of the Department of Theoretical Basis of Metallurgical Processes, Ukrainian State University of Science and Technologies, Ukraine

Bilodidenko Serhii Valentynovych**,** D. Sc. (Tech.), Professor, Head of the Department of Industrial Mechanical Engineering, Ukrainian State University of Science and Technologies, Ukraine

Yeromin Oleksandr Olehovych**,** D. Sc. (Tech.), Professor, Professor, Head of the Department of Ecology, Heat Engineering, Occupational Safety and Health, Ukrainian State University of Science and Technologies, Ukraine

Uzlov Kostiantyn Ivanovych**,** D. Sc. (Tech.), Professor, Professor, Ukrainian State University of Science and Technologies, Ukraine

Kawalek Anna Małgorzata, D. Sc. (Tech.), Dean of the Faculty of Production Engineering and Materials Technology, Częstochowa University Of Technology, Poland

Karbowniczek Miroslaw**,** D. Sc. (Tech.), Professor, Head of the Department of Ferrous Metallurgy, AGH University of Science & Technology, Krakow, Poland

Lezhniev Serhii Nykolaevych**,** PhD, Associate Professor, Associate Professor of the Department of Metallurgy and Mining, Rudny Industrial Institute, Kazakhstan

Loboda Petro Ivanovych**,** D. Sc. (Tech.), Professor, Academician of the National Academy of Sciences of Ukraine, Head of the Department of High-Temperature Materials and Powder Metallurgy, National Technical University of Ukraine “Igor Sikorsky Kyiv Polytechnic Institute”, Ukraine

Molchanov Lavr Serhiiovych**,** PhD, Associate Professor, Head of the Department of Physical and Technical Problems of Steel Metallurgy, Iron and Steel Institute of Z. I. Nekrasov National Academy of Sciences of Ukraine, Ukraine

Muraviova Iryna Hennadiivna**,** D. Sc. (Tech.), Professor, Senior Researcher, Iron and Steel Institute of Z. I. Nekrasov National Academy of Sciences of Ukraine, Ukraine

Tohobytska Daria Mykolaivna**,** D. Sc. (Tech.), Professor, Senior Researcher of the Department of Physical and Technical Problems of Steel Metallurgy, Iron and Steel Institute of Z. I. Nekrasov National Academy of Sciences of Ukraine, Ukraine

Articles are published in their original language and licensed under Creative Commons Attribution 4.0 International (CC BY 4.0).

Authors retain copyright of the published papers and grant to the publisher the non-exclusive right to publish the article, to be cited as its original publisher in case of reuse, and to distribute it in all forms and media.

Authors can enter the separate, additional contractual arrangements for non-exclusive distribution of the published paper (e.g., post it to an institutional repository or publish it in a book), with an indication of its primary publication in this journal and the mandatory indication of the article's doi.

ISSN 3083-7219 (Print), ISSN 3083-7227 (Online)
Теорія і практика металургії, 2026, № 1
Theory and Practice of Metallurgy, 2026, No. 1

https://doi.org/10.15802/tpm.1.2026.01

UDC 669.15'74-198:669.046.5:536.7

Gasik M. M.

Thermodynamic equilibrium of high-carbon ferromanganese smelting

ORCID: 0000-0002-5782-7987. Aalto University Foundation, Espoo, Finland
Email: michael.gasik@aalto.fi

Гасик М. М.

Термодинамічна рівновага процесу виплавки високовуглецевого феромарганцю

ORCID: 0000-0002-5782-7987. Університетська Фундація Аалто, Еспоо, Фінляндія
Email: michael.gasik@aalto.fi

Abstract. *The goal of this study is to carry our detailed thermodynamic analysis of FeMn fluxless smelting process in submerged arc furnaces (SAF) using realistic plant data and compare the calculation results with industrial outcomes. Modern thermodynamic databases FactSAGE was deployed to assess equilibria inside separate phases and between them at 1400-1800°C for two FeMn78 alloys with different phosphorus content. Phases (metal, slag and gas) compositions were calculated with metal recovery value for manganese as well as through-recovery of manganese in both working slag and metal. It was found that temperature of the process 1500-1525°C predicts maximal recovery of manganese into the alloy. The outcomes allowed combination of blended manganese agglomerates, ores, return tails to be efficiently composed and converted into materials streams, which can be fed into the thermodynamic calculations. Such approach allows flexibility to optimize different scenarios in high-carbon ferromanganese fluxless smelting. The correlation of the calculations with industrial plant outcomes was found to be very good. The method gives a good basis to check behavior of different components and elements in the furnace, distribution of them between the phases (gas, metal, slag) and identify the pathways for improvement of the process leading to higher yield and quality. With the same thermodynamic database parameter similar approach can be used for other manganese ferroalloys.*
Keywords: *ferromanganese, thermodynamics, slag, metal, equilibria, metal recovery.*

Анотація. *Задачею роботи було проведення термодинамічного аналізу процесу виплавки високовуглецевого феромарганцю безфлюсовим методом у дугових печах з використанням реальних заводських даних і порівняння їх з результатами. Сучасна термодинамічна база даних FactSAGE була застосована для розрахунків рівноваги окремих фаз і між фазами в інтервалі температур 1400-1800°C для двох типів феромарганцю ФМн78 з різним вмістом фосфору. Склад окремих фаз і загалом всій системи було розраховано разом з виходом металу (прямого вилучення марганцю у стоп) і повного вилучення марганцю (металева і шлакова фази разом). Оптимальну температуру процесу було визначено у 1500-1525°C коли вилучення марганцю у металеву фазу максимальне. Процес розрахунку дозволяє комбінувати різні суміші агломератів, руд, хвостів і зворотних матеріалів для реалізації різних сценаріїв при виробництві феромарганцю. Отримані результати показали дуже добру кореляцію із даними заводського виробництва феромарганцю зокрема у хімічному складі металу, прямого і загального вилучення марганцю. Метод таким чином дозволяє оцінку поведінки різних компонентів і елементів у печі, їх розподіл між фазами (газ, метал, шлак) і визначення шляхів покращення процесу щодо виходу металу і його якості. Така ж сама база термодинамічних даних може бути застосована і для оптимізації інших марганцевих феросплавів. Дана робота демонструє, що коректне використання термодинамічних баз даних дозволяє зробити досить вірну оцінку характеристик процесу і якості феросплаву. Такі розрахунки ефективно заміняють спрощені калькуляції балансу шихти і енергії, даючи гнучкість у оптимізації феросплавного виробництва.*
Ключові слова: *феромарганець, термодинаміка, шлак, метал, рівновага, вихід металу.*

Introduction. Manganese-based ferroalloys such as ferromanganese (FeMn) and silicomanganese (FeSiMn) are essential components of modern steelmaking [1-3]. They are commercially produced by the carbothermic reduction of manganese oxide ores in submerged arc furnaces (SAFs) having in three-phase submerged arc furnaces, which have a three-electrode (Søderberg or self-baking type) circular or a six-electrode rectangular geometry, rated from about 20 to 90 MVA power capacity [1-4]. High carbon ferromanganese, one of the most used ferroalloy, typically contains around 72-82% Mn and 6-7% C, balance being Fe, Si and impurities. As in other ferroalloys, phosphorus is such an impurity which needs to be carefully controlled due to its negative impact in steelmaking [3, 5].

Literature analysis. A typical charge for FeMn production is composed of manganese ores, concen-

© Gasik M. M., 2026
© Гасик М. М. , 2026

This is an Open Access article under the CC BY 4.0 license https://creativecommons.org/licenses/by/4.0/

trates, agglomerates and returned tails depending on the quality of these raw materials - blending Mn-sources from different origins is a common practice for instance, to obtain a specific Mn/Fe ratio in the metal and limited phosphorus content [1, 3, 5, 6]. Manganese ores with a high content of phosphorus (0.18–0.22%) cannot be usually enriched by mechanical methods with simultaneous phosphorus removal and it passes into manganese concentrates, agglomerates – and finally into the alloy, decreasing its quality [1, 2, 7]. Ukrainian standard DSTU 3547-97 limits phosphorus content in high-carbon FeMn78 alloy to 0.10% (grade A) and 0.70% (grade B) [6].

Fluxes (dolomite, limestone) and carbonaceous agents (coke) and reusable waste (where applicable) are added according to expected desired composition of the alloy and the slag. These basic fluxes are commonly added to give the slag suitable chemical properties, smelting temperature, and viscosity to secure good furnace operation and a high manganese yield [3, 5]. High-carbon ferromanganese FeMn78 is commonly produced essentially by a flux-less process, which is more cost-effective over flux process [1, 3]. The resulting high-manganese slag (>35% Mn) is used at the next stage as the raw material in the charge for smelting silicomanganese with lower phosphorus content, which increases the through-recovery of manganese [1, 3, 5]. It is known that the phosphorus capacity of slags in this process is much depending not only on slag and metal compositions but also gas phase such as oxygen potential [8, 9]. Interactions between the slag, metal and gas phase are rather complex inside the SAF, depending on the location, temperature zones distribution and reaction and transport kinetics [10, 11]. Ferromanganese smelting practice therefore has accumulated engineering parameters linked to the core reactions of MnO reduction as the leading targeted force in the process [12].

Because many parameters of the smelting are not under direct observation, thermodynamic modeling was used to predict the process, mass and energy balances, and to correlate them with the experimental data. Earlier studies have used simplified schematics based on regular solution models [13]. This approach has limitations coming from the solution model itself as well as from the lack of parameters counting for multi-phase equilibrium. Later modeling was extended for application of thermodynamic databases allowed differences in mineral phase composition and specific interactions beyond the regular solution [14]. Also, recently a similar thermodynamic analysis to produce high-carbon FeMn using a SAF process was compared with the plant operation conditions to obtain a simplified simulation model [15]. Whereas being more detailed, this model was eventually limited to one temperature (1400°C) and charge composition. Such conditions are sufficiently replicable in the lab, but they do not reflect industrial practice.

Objectives of this work. The goal of this study is to carry out detailed thermodynamic analysis of FeMn smelting process using realistic plant data and compare the calculation results with industrial outcomes. If the correlation is sufficient, this gives a good basis to check behavior of different components and elements in the furnace, distribution of them between the phases (gas, metal, slag) and identify the pathways for improvement of the process leading to high yield and quality.

Materials and methods. For calculations of the expected equilibria in the conditions of a SAF the following assumptions have been made. First, only the thermodynamic equilibrium is considered, without kinetics of the process which imposes an ideally mixed reactor model. The temperature range was selected as 1400-1800°C and 1 atm of total pressure as it is typical for FeMn smelting. Charge materials mineral compositions (Table 1) were converted into oxides, including those minerals present in coke ash, and the sum of oxides was normalized to 100% (Table 2). One exception was done for phosphorus – it was entered into calculations as apatite $Ca_3(PO_4)_2$ because using P_2O_5 as a starting compound lead to immediate removal of all phosphorus into gas phase. Volatile sulfur and moisture were ignored, and losses-on-heating (LOH) were assumed to be only due to presence of carbonates (when all CO_2 is converted to the gas phase before melting but remained in the system). The composition of the briquettes from returns was approximated by 'diluted' ferromanganese adjusted to the experimental composition provided from the plant lab. Finally, the slag-metal waste (SMW) was represented by a mixture of ferromanganese scrap with RMS – re-workable manganese slag [1, 3] (Table 1).

Four phases considered in these calculations are gas, liquid metal, slag (with oxides originating from the coke ash) and – at the entry – coke as carbonaceous reducing agent. Possible transfer of materials from the electrodes (carbon) and lining (oxides) was neglected. For these phases the activity parameters were used if known, and otherwise an approximation has been deployed (the gas is also assumed to be ideal, and dust contribution was not counted).

The reaction between these phases was without restrictions on the transfer of elements from phase to phase (i.e., free mass exchange between all phases is assumed). Each analogous component (oxide or element) of the charge is combined (ore and non-ore components, Table 1) and converted into oxides and elements, Table 2. Phases (oxide, metal, gas) are first brought to equilibrium separately, assuming no interaction between them (i.e. testing for stability and the formation of metastable phases and immiscibility zones). After local phase equilibrium was calculated, all these phases are mixed as 4 streams at a constant temperature for calculations of the total equilibrium. In this work, thermodynamic software 'FactSAGE 6.0' (GTT Technologies GmbH, Germany) was used with the standard '*FToxid*' (slag melt database) and author's own '*OptiDB09*' metal melt database with optimized thermodynamic interaction parameters. Calculated data were obtained in tabulated form and as plots shown below.

Results. Numerical example for 1600°C for FeMn78P20 alloy is shown in Table 3. The total weight of all phases will be 3,310.8 kg (the initial mass in Table 2 is 3328 kg), i.e., with a discrepancy of only 0.52%. In this case, the coke carbon is completely consumed by reduction. The total mass of all components is 77800 mol, with a calculated enthalpy change of +114.48 kJ/mol, entropy of +78.72 kJ/mol, and free energy change of -51.637 kJ/mol (as it is negative it reflects the smelting process is thermodynamically favorable).

Figure 1 displays weight composition of the equilibrium gas phase (only major constituents shown). It is seen that whilst CO is the leading compound (as expected), transfer of manganese into gas phase is significant over 1500°C. At higher temperatures 1700-1800°C there is also increase of SiO and Mg(gas), but there is not much phosphorus compared to other species (note logarithmic scale).

Figure 2 shows components of the slag phase, reflecting the dominance of MnO and SiO_2 as major constituents, with the maximal MnO content to be reached around 1600°C. Increasing temperature lowers MnO content in the slag, but it does not improves Mn extraction into the metal phase (Fig. 3) - rather it accelerates manganese losses to the gas phase, decrease in C and an increase in Si in the alloy. Noteworthy, the mass of silicon in the metal changes only slightly at higher temperatures, but due to Mn evaporation losses, its mass fraction increases. Similar tendencies are also seen for FeMn78P70 alloy composition.

Discussion. The recovery of manganese into the metal and overall (through) one have been calculated as ratios of Mn in metal to total manganese input in the system, and respectively for Mn in metal and slag vs. total entered manganese (Fig. 4 for both alloys). There are slight differences related to various input compositions (for FeMn78P70 there was more MnO in the raw materials), but the trends are similar.

Table 1. Used original raw materials compositions including blended ores and agglomerates for smelting of ferromanganese.

Raw materials	**SiO_2**	**CaO**	**MgO**	**P**	**Al_2O_3**	**MnO**	**P_2O_5**	**Fe_2O_3**	**$MnCO_3$**	**$CaCO_3$**	**C**	**Si**	**Fe**	**Mn**
Agglomerates														
AMNV-1	15	4.4	1.2		3	64.8	0.490	3.86						
AMNV-2	26.1	8	2.4		3	50.0	0.420	3.14						
AMNV-1A	10.1	3.6	0.7		3	65.4	0.327	5.43						
AMNV-2П	21.8	10.1	5.1		3	50.1	0.233	2.86						
Mn ores														
KK48NZh	9.3	0.8	0.5		1.2	48.9	0.098	6.14	24.88	2.00				
KK28	13.6	6.3	4.8		2.1	0.5	0.152	1.71	57.94	15.75				
KK37	5.5	13.3	3.1		0.3	44.9	0.058	9.43	6.46	33.25				
Slags														
RMS	30.3	8.5	2.3		10.6	43.5	0.007	0.34						
Waste slag	50.3	16.8	5.1		7.9	15.0	0.140							
SMW	9.09	2.55	0.69	0.126	3.18	13.05					4.55	0.63	10.09	54.6
Coke 10% ash	5.14	1.41	0.22	1.67	1.28			1.75			85.46			
Limestone	1		1							98				
Iron ore	3.5	0.5	0.5		3.5			92						
Quarzite	97.8	0.5	0.2		1			0.5						
FeMn (0.18%P)											6.5	0.9	14.42	78

Table 2. Normalized raw materials input (kg) used in calculations. Note that initial gas phase (mainly CO_2) originates from the carbonate components decomposition.

Ferroalloy type:	**FeMn78P20**	**FeMn78P70**
Oxide phase (with coke ash oxides):		
SiO_2	307.708	389.123
CaO	45.826	106.311
MgO	18.271	27.969
Al_2O_3	63.121	93.097
MnO	1524.963	1804.059
P_2O_5	4.789	10.047
Fe_2O_3	169.616	239.358
$MnCO_3$	452.187	127.554
$CaCO_3$	36.347	10.253
Metal phase:		
Mn	256.130	256.130
Fe	47.351	47.351
P	0.591	0.591
Si	2.955	2.955
C	21.344	21.344
Coke: C solid	376.801	358.858
Total mass, kg	**3328**	**3495**

These data were compared with the real averaged ferroalloys plant numbers (Table 4). It is noteworthy that the calculated values surprisingly well match the plant data for Mn recovery, despite some differences in Si and C content, as well as the composition of the gas phase. Significant loss of manganese under industrial conditions is likely much compensated by Mn gas condensation or absorption in the layer of unreacted charge, where solid-phase reduction and accumulation of manganese in a new metallic phase can occur, subsequently entering the metal bath.

Table 3. Example for equilibrium at 1600°C for FeMn78P20 alloy (in % wt.; for slag phase shown in % mol.)

Phase	Mass/volume	Composition
Gas	32204 mol, 4950.2 m^3, 997.26 kg	88.99 CO, 10.963 Mn, $1.736\cdot10^{-2}$ CO_2, $1.61\cdot10^{-2}$ Mg, $1.21\cdot10^{-2}$ SiO, $3.71\cdot10^{-5}$ Fe, $2.26\cdot10^{-5}$ Ca, $4.4\cdot10^{-7}$ Al, $1.33\cdot10^{-7}$ Si, $9.72\cdot10^{-9}$ P, $8.45\cdot10^{-9}$ MgO, $1.75\cdot10^{-9}$ Al_2O, $1.63\cdot10^{-9}$ AlO, $2.43\cdot10^{-10}$ CaO, $6.57\cdot10^{-13}$ O_2
Metal	29126 mol, 1174.8 kg	14.128 Fe, 72.289 Mn, 0.233 P, 4.38 Si, 8.97 C
Slag	16740 mol, 1138.8 kg	2.67 MgO, $2.95\cdot10^{-4}$ FeO, 66.318 MnO, 20.25 SiO_2, 7.05 CaO, 3.7 Al_2O_3, $1.71\cdot10^{-7}$ Fe_2O_3, $9.77\cdot10^{-10}$ $Ca_3(PO_4)_2$, $7.9\cdot10^{-3}$ Mn_2O_3, $3.44\cdot10^{-4}$ SiC

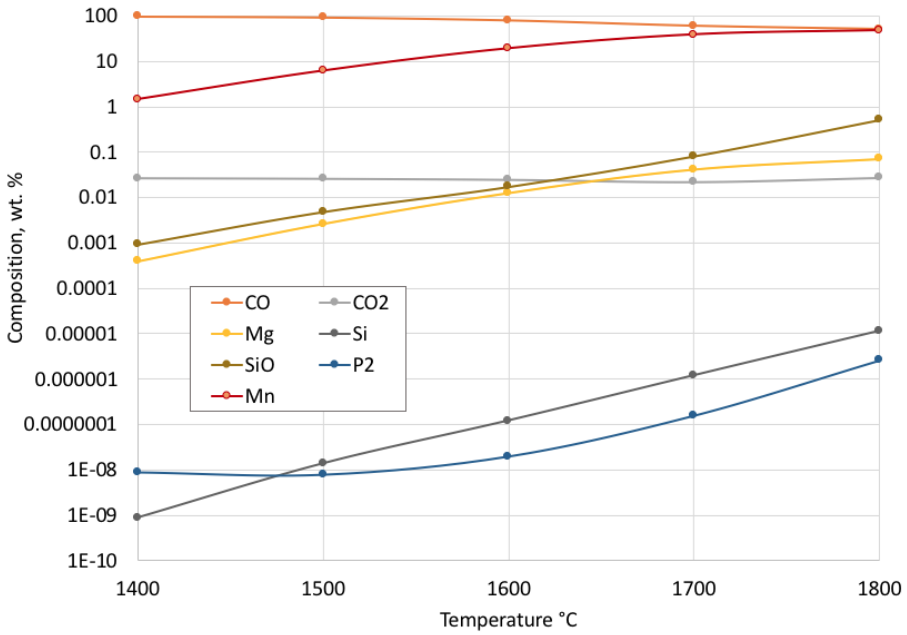

Fig. 1. Gas phase components for FeMn78P20 smelting at different temperatures.

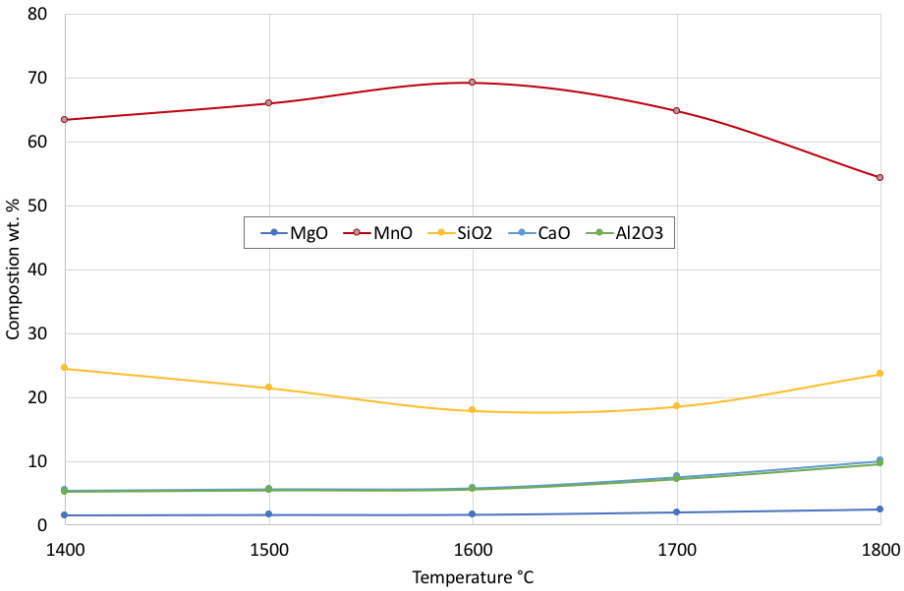

Fig. 2. Slag phase major components for FeMn78P20 at different temperatures.

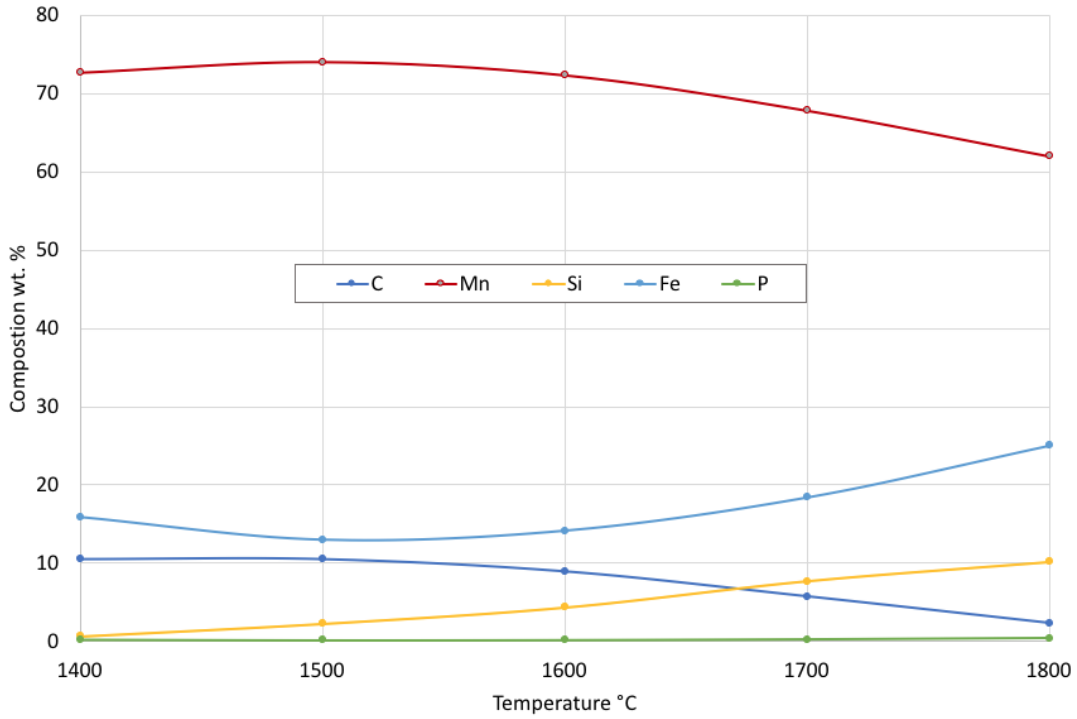

Fig. 3. Metal phase components for FeMn78P20 smelting at different temperatures.

Table 4. Comparison of calculated and experimental plant data.

Parameter	C	Si	Mn	P	Fe	Mn recovery into metal	FeMn yield, kg	Slag yield, kg/t alloy
FeMn78P20								
Calculated:	7.3	1.5	73.9	0.21	17.1	57.2	1161	1155
Plant data:	6.5	0.9	78.0	0.18	12.6	62.1	1000	1254
FeMn78P70								
Calculated:	6.8	2.3	72.6	0.39	17.9	60.0	1341	1100
Plant data:	6.1	1.9	78.6	0.41	14.5	60.2	1000	1540

If this correlation validity is accepted, one can estimate the expected temperatures of the smelting process when the manganese recovery is matched to the experimental data of Table 4. For Fig. 4 this leads to ~1525°C for FeMn78P20 and 1500-1520°C for FeMn78P70. The lower yield of the convertible manganese slag in calculations compared to the plant data (Table 4) is related to the expected higher metal yield. This could also be explained due to the higher recovery of silicon, iron, and carbon into the melt, which somewhat reduces the fraction of manganese.

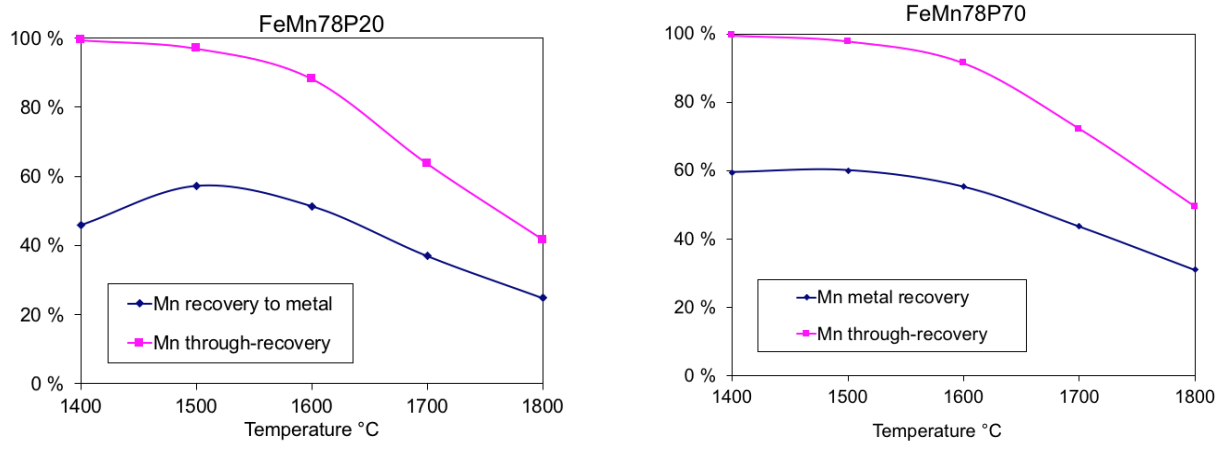

a b

Fig. 4. Manganese recovery calculated by thermodynamic equilibration at different temperatures for FeMn78P20 (a) and FeMn78P70 (b).

Conclusions. The results of calculations with updated thermodynamic data for ferromanganese smelting and their comparison with experimental (plant) values have demonstrated a very good correlation. They also show several variables that are hardly observed directly in industrial practice (e.g. expected temperature in the reaction zone or immediate gas phase composition). Equilibration predicts a higher degree of carbon and silicon conversion into the metal and virtually almost complete removal of phosphorus from the slag in this fluxless process. Significant manganese loss at elevated temperatures and negligible phosphorus loss were predicted but they could not be directly confirmed with experimental data. Very low concentrations of high-oxidation oxides (Fe_2O_3, Mn_2O_3) and SiC in the slag are consistent with literature and experimental practice. If manganese recovery is taken as a target feature parameter, average temperature of 1500-1525°C looks being an optimal range for this process, as further temperature increase will lead to more manganese losses. This range is higher than was previously analyzed 1400°C in alternative study [15].

Such calculations can be carried out excluding manganese as a component of the gas phase; however, to approximate the calculation to real conditions, a more accurate knowledge of air consumption as a reaction component is necessary (for example dilution of the gas phase with nitrogen can significantly shift the equilibrium of all reactions which involve gas products).

This work proves that careful assessment of input parameters and use of proper thermodynamic databases are valuable tools for estimation of the process features and resulting products quality, which could help smelting plants to manage better production. Embedded thermodynamic calculations are efficiently replacing manually set calculation procedures [3] or simplified models [13] for charge and energy demands in the process without assumptions for losses or phase partition.

References

1. Gasik, M. I. (1992). *Manganese*. Metallurgya
2. Gasik, M. I., Lyakishev, N. P., & Gasik, M. M. (2009). *Physical chemistry and technology of ferroalloys*. Sistemnye Technologii
3. Gasik, M. I., Dashevskii, V. Ya., & Bizhanov A. (2020). *Ferroalloys Theory and Practice.* Springer, Cham (Switzerland). https://doi.org/10.1007/978-3-030-57502-1
4. Gladkikh, V. A., Gasik, M. I., Ovcharuk, V. N., & Proydak, Yu. S. (2007). Ferroalloy electric furnaces. System Technologies
5. Olsen, S., Tangstad M., & Lindstad T. (2007). *Production of manganese ferroalloys*. Tapir Forlag
6. Velichko, B. F., Gavrilov, V. A., Gasik, M. I., et al. (1996). *Metallurgy of manganese of Ukraine*. Technika
7. Gvelisiani, G. G., Baratashvili, I. B., & Tsagareishvili, D. Sh. (1982). *Thermodynamics of the interaction of manganese with phosphorus.* Metsniereba
8. Maramba, B., & Eric, R. H. (2008). Phosphide capacities of ferromanganese smelting slags. Minerals Engin. 21, 132–137. https://doi.org/10.1016/j.mineng.2007.07.012
9. Yuanchi, D., Shangxing, G., & Chen, E. (1997). Control of oxygen potential and its effect on dephosphorization in ferromanganese. In: Proc. Eighth Intern. Ferroalloy Congr. INFACON 8, Bejing, China, 255–258
10. Shaojun, C., & Kuangdi, X. (2023). Ferromanganese. In: Xu, K. (eds) ECPH Encyclopedia Mining & Metallurgy. Springer, Singapore. https://doi.org/10.1007/978-981-19-0740-1_1023-1
11. Lee, Y. E., & Kolbeinsen, L. (2021). Behavior of slag in ferromanganese and silicomanganese smelting process. *Metall. Mater. Trans B*52, 3142–3150. https://doi.org/10.1007/s11663-021-02242-2
12. Coetsee, T. (2018) MnO reduction in high carbon ferromanganese production: practice and theory. *Miner. Process. Extr. Metall. Rev*., 39, 351–358. https://doi.org/10.1080/08827508.2018.1459618
13. Li, H., Morris, A. E., & Robertson, D. G. C. (1998). Thermodynamic model for MnO-containing slags and gas-slag-metal equilibrium in ferromanganese smelting. Metallurgical and Materials Transactions B, 29(6), 1181–1191. https://doi.org/10.1007/s11663-998-0040-z
14. Kutsyn, V. S., Gasik, M. M., & Gasik, M. I. (2012). Thermodynamic computer modeling of phase transformations in complex oxide systems, equivalent to manganese agglomerates made by existing and developed technologies. *Metall. Mining Ind*., 4(3), 16–24
15. Nam, J., van Ende, M-A., & Jung, I. H. (2022). Ferromanganese production in a submerged arc furnace: thermodynamic and energy balance analysis. *JOM*, 74(4), 1624-1632. https://doi.org/10.1007/s11837-021-05121-y

Надіслано до редакції / Received: 02.01.2026
Прорецензовано / Peer-Reviewed: 14.02.2026
Прийнято до друку / Accepted: 16.03.2026
Опубліковано / Published: 30.03.2026

ISSN 3083-7219 (Print), ISSN 3083-7227 (Online)
Теорія і практика металургії, 2026, № 1
Theory and Practice of Metallurgy, 2026, No. 1

https://doi.org/10.15802/tpm.1.2026.02

UDC 621.771.014:621.7.019:672.6

Kolisnyk K. D.

Effect of deformation degree during drawing out on the quality of heavy-duty hook forgings

ORCID: 0009-0004-2030-1123. National Technical University “Kharkiv Polytechnic Institute”, Ukraine
Email: kolesnik2195@gmail.com

Колісник К. Д.

Вплив ступеня деформації під час витяжки на якість важких поковок з гаком

ORCID: 0009-0004-2030-1123. Національний технічний університет
«Харківський політехнічний інститут», Україна
Email: kolesnik2195@gmail.com

Abstract. *This study investigates the influence of the degree of deformation during the drawing out forging operation on the distribution pattern of plastic strain in billets intended for manufacturing high-capacity lifting hooks. The primary objective is to determine the optimal deformation degree that enhances the uniformity of plastic strain distribution across the forging's cross-section. The research was conducted using numerical modeling of the sequential upsetting and drawing out processes, accounting for the continuity of the technological cycle. Drawing out was performed using the "ring" method (circumferential rotation) with a rotation angle of 15° and a relative feed of 0.5. Three deformation degrees per pass were analyzed: 10%, 15%, and 20%. To quantitatively assess strain uniformity, the nonuniformity coefficient C_n was employed, defined as the ratio of equivalent strain values at control points to the maximum equivalent strain within the cross-section. It was established that increasing the deformation degree from 10% to 20% raises the level of accumulated plastic strain and improves its uniformity across the cross-section. The most uniform strain distribution was achieved at a deformation degree of 20%, where the minimum nonuniformity coefficient value was 0.54. This indicates a 46% reduction in strain nonuniformity (since C_n=0.54 corresponds to nonuniformity reduced to 54% of the reference maximum difference). The obtained results can be applied in the development of rational technological regimes for forging high-capacity lifting hooks with enhanced requirements for quality and reliability.*
Keywords: *drawing out, upsetting, degree of deformation, plastic strain, strain nonuniformity coefficient, high-capacity lifting hook forging.*

Анотація. *У цьому дослідженні досліджується вплив ступеня деформації під час операції витяжного кування на характер розподілу пластичної деформації в заготовках, призначених для виготовлення великовантажних вантажопідйомних гаків. Основною метою є визначення оптимального ступеня деформації, який підвищує рівномірність розподілу пластичної деформації по поперечному перерізу поковки. Дослідження проводилося з використанням числового моделювання послідовних процесів висадки та витяжки з урахуванням безперервності технологічного циклу. Витяжка виконувалася методом "кільця" (окружне обертання) з кутом повороту 15° та відносною подачею 0,5. Було проаналізовано три ступені деформації за прохід: 10%, 15% та 20%. Для кількісної оцінки рівномірності деформації використовувався коефіцієнт нерівномірності Cn, який визначається як відношення значень еквівалентної деформації в контрольних точках до максимальної еквівалентної деформації в межах поперечного перерізу. Було встановлено, що збільшення ступеня деформації з 10% до 20% підвищує рівень накопиченої пластичної деформації та покращує її рівномірність по поперечному перерізу. Найбільш рівномірний розподіл деформації був досягнутий при ступені деформації 20%, де мінімальне значення коефіцієнта неоднорідності становило 0,54. Це свідчить про зменшення неоднорідності деформації на 46% (оскільки Cn=0,54 відповідає неоднорідності, зменшеній до 54% від контрольної максимальної різниці). Отримані результати можуть бути застосовані при розробці раціональних технологічних режимів кування високовантажних вантажопідйомних гаків з підвищеними вимогами до якості та надійності.*
Ключові слова: *витяжка, осаджування, ступінь деформації, пластична деформація, коефіцієнт неоднорідності деформації, кування високовантажного вантажопідйомного гака.*

Introduction. High-capacity lifting hooks are critical components in hoisting and transportation systems, operating under variable and impact loads. The operational reliability of such components is determined by a combination of factors, among which the structural homogeneity of the metal, the absence of internal defects, and a favorable orientation of the fibrous structure play a key role. These characteristics are primarily formed during the forging process.

One of the key parameters influencing the formation of the structure and quality of forged products is the pattern of plastic strain distribution throughout

© Kolisnyk K. D., 2026
© Колісник К. Д., 2026

This is an Open Access article under the CC BY 4.0 license https://creativecommons.org/licenses/by/4.0/

the billet volume. Strain nonuniformity can lead to the formation of internal defects and premature failure of the component. For critical parts, particularly high-capacity lifting hooks, achieving uniform deformation penetration (thorough working) of the metal is one of the primary technological challenges.

In the technology for manufacturing single-horn (single-prong) lifting hooks, a combined forming scheme is employed, which includes preliminary upsetting of the billet followed by drawing out [1]. Upsetting ensures the breakdown of the cast structure and a substantial reduction in internal porosity of the metal, while the drawing out operation imparts the required shape and length to the billet, creating a favorable fiber orientation [2, 3]. At the same time, the degree of deformation during drawing out significantly affects the pattern of its distribution throughout the metal volume and can either improve or impair the structural homogeneity of the final product.

Despite the considerable number of studies on metal forming processes, the specific influence of the degree of deformation during drawing out—performed after preliminary upsetting—on the nonuniformity of plastic strain in billets for single-horn high-capacity lifting hooks remains insufficiently explored. Establishing quantitative relationships for the distribution of plastic strain will enable the justification of rational technological forging regimes and improve the quality of the finished products.

Literature Review and Problem. Upsetting is a fundamental operation in the forging of large critical forgings, as it ensures thorough working (penetration) of the metal. This process breaks down the cast structure, heals internal defects, and promotes the formation of a homogeneous microstructure, which is crucial for the strength of the final product. However, as demonstrated by the results in [4], the upsetting process is accompanied by significant nonuniformity in the stress-strain state (SSS), which directly depends on the initial shape of the billet. Furthermore, work [5] has established that the pattern of metal flow is substantially influenced by friction conditions and the temperature-velocity regimes of processing.

Therefore, to achieve uniform strain distribution, it is effective to use billets of special (profiled or contoured) shapes and intensified processing regimes. In particular, work [6] has demonstrated that the application of profiled billets helps to distribute deformation more homogeneously and prevent the formation of internal cracks. Additionally, enhanced quality can be achieved through complex loading schemes. As shown in study [7], the combination of deformations and varying stresses ensures better working (penetration) of the metal structure throughout the entire billet volume. This not only improves its strength but also enables effective control of product quality in open-die forging.

The primary formation of quality and strength in large forgings occurs during the drawing out forging operation. In study [8], based on numerical modeling, it was established that when processing large forgings with flat dies, insufficient working (penetration) of the central zone in the billet's cross-section persists, necessitating improvements in the feed and reduction parameters. The relevance of seeking new technological solutions to enhance the drawing out process is confirmed in work [9], which analyzes modern forging regimes from the perspective of improving metal quality and production energy efficiency.

One of the most interesting approaches to improving metal quality is proposed by the authors of work [10]. They demonstrated that the use of dies with unconventional (asymmetric) shapes induces intense internal twisting of the metal, which significantly enhances the breakdown of coarse structures compared to conventional drawing out. A logical extension of this idea is presented in work [11], where the authors suggested replacing preliminary upsetting with billet profiling using wedge-shaped dies prior to drawing out. According to their findings, this approach enables through-working of the metal, reduces press force requirements, and saves processing time.

In modern practice, combined forging technologies are increasingly employed. For example, as demonstrated in work [12], the application of a double "upsetting–drawing out" cycle represents one of the most effective methods for eliminating internal defects. This combination of operations not only changes the shape of the billet but also enables targeted control over the restoration of the metal microstructure in the core of heavy forgings.

At the same time, improving the forging process—even when using special convex dies—always carries the risk of compromising the integrity of the product. Studies [14, 15] demonstrate that critical stresses arising at high degrees of deformation during drawing out can lead to crack formation.

Thus, the analysis of global experience confirms that achieving high-quality and safe products, such as lifting hooks, requires finding an optimal balance between improving metal working and preserving the structural integrity of the material. This necessitates detailed computer modeling to determine rational degrees of deformation, which constitutes the primary objective of the present work.

Purpose and objectives of the research. The objective of this work is to investigate the influence of the degree of deformation during the drawing-out forging operation—performed after preliminary upsetting of the billet—on the distribution of plastic strain and to evaluate the nonuniformity of deformation throughout the volume of the billet for high-capacity lifting hooks.

Materials and Methods of Research. The object of the study was a cylindrical billet made of steel 1020 (equivalent to Ukrainian grade steel 20), with an initial diameter of 470 mm and height of 940 mm. Steel 1020 is a low-carbon steel commonly used for forging heavy-duty lifting hooks due to its good hot workability, moderate strength, and suitability for subsequent heat treatment.

Numerical simulation of the forging processes was

performed using the QForm UK software package [15] based on the finite element method (FEM). The modeling accounted for the sequential continuity of the technological cycle: preliminary upsetting followed by drawing out.

The forging operations (upsetting and drawing out) were simulated under isothermal conditions at a constant temperature of 1150°C. This temperature corresponds to the typical hot forging range for low-carbon steels like 1020/20, ensuring high ductility, low flow stress, and effective deformation without excessive cracking risk.

Upsetting was performed using flat upsetting plates (dies): the lower plate was fixed, while the upper plate moved vertically downward.

The degree of deformation during upsetting was set at 50% reduction of the initial billet height (from 940 mm to 470 mm).

This stage aimed to achieve preliminary deformation penetration (thorough working) of the metal structure prior to the subsequent drawing-out operation, thereby breaking down the initial cast microstructure, closing internal porosity, and promoting overall homogeneity.

The results obtained after the upsetting stage were used as initial conditions for the subsequent modeling of the drawing-out processes. This approach ensured the continuity of the technological process and the accurate reproduction of real forging conditions.

The 3D model of the initial billet, its position between the plates prior to upsetting, and the state after upsetting are presented in Figure 1.

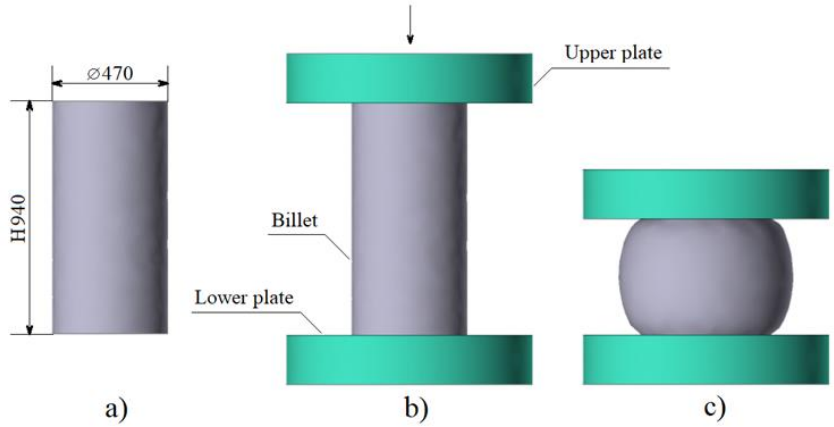

Figure 1 – 3D model of the upsetting operation: (a) initial cylindrical billet (D=470 mm, H=940 mm); (b) billet position before upsetting; (c) billet state after upsetting.

Subsequently, numerical modeling of the drawing-out forging operation was performed. The initial state for this stage was the billet with the already formed distribution of plastic strain obtained after the upsetting stage. This approach ensured the continuity of the technological process and the accurate reproduction of real forging conditions.

The drawing out of the billet was carried out using flat dies with dimensions 400 × 1000 × 500 mm. The "ring" method (circumferential rotation drawing) was selected, which involves sequential reductions of the billet accompanied by rotation (canting) by an angle α = 15°. A relative feed s/h = 0.5 was applied only after a full rotation of the billet (i.e., after completing the 360° circumferential pass).

The schematic diagram and 3D model of the drawing-out process are presented in Figure 2.

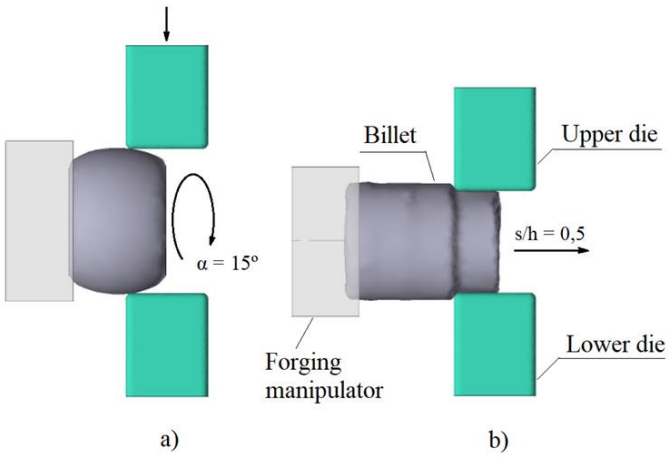

Figure 2 – 3D model of the drawing-out forging operation: (a) initial state of the billet and canting scheme (α = 15°); (b) drawing-out stage and relative feed (s/h = 0.5).

To investigate the influence of the degree of deformation during the drawing-out forging operation on the quality of lifting hook forgings, three modeling variants were performed with different deformation de-

grees per pass: 10%, 15%, and 20%. For each variant, three sequential drawing-out passes were carried out. After the third pass, the accumulated equivalent plastic strain was determined, and the pattern of its distribution in the cross-section—specifically in the central region of the billet — was analyzed.

This approach enabled the establishment of the relationship between the degree of deformation after the third drawing-out pass and the uniformity of plastic strain distribution. This uniformity is a decisive parameter in ensuring the quality of high-capacity lifting hook forgings.

To evaluate the uniformity of plastic strain distribution, the method for predicting volumetric nonuniformity was applied, with detailed justification provided in work [16]. In each analyzed cross-section, four radial lines were drawn, positioned at 45° angles to one another. Along each line, seven control points were marked, symmetrically arranged relative to the center of the section and the zones of maximum equivalent plastic strain (Figure 3). Within this approach, the nonuniformity coefficient C_n was determined for the strain distribution.

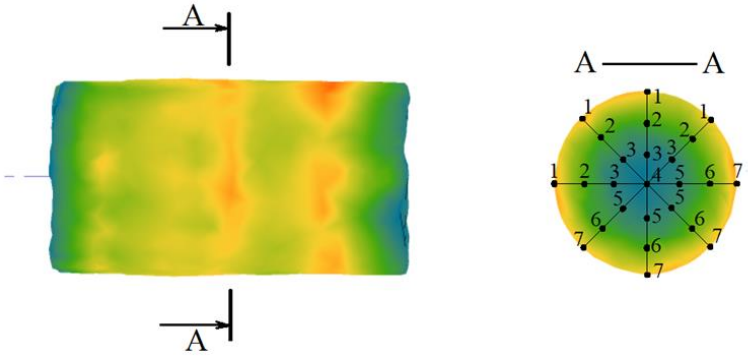

Figure 3 – Schematic of radial lines and control points arrangement in the billet cross-section during drawing out.

The nonuniformity coefficient C_n was calculated as the ratio of the equivalent plastic strain value at each control point in the cross-section to the maximum equivalent plastic strain value within the corresponding cross-section. This definition confines C_n to the range from 0 to 1. Values close to 1 indicate a more uniform distribution of plastic strain across the section.

Figure 4 illustrates the distribution of plastic strain in the central cross-section of the billet after the upsetting stage. The maximum values of plastic strain are concentrated in the central zone, reaching 1, while a gradual decrease is observed toward the surface zone, with minimum values of 0.6. Thus, the range of plastic strain variation across the cross-section is 0.6–1 indicating the presence of nonuniformity in the deformation state.

The plastic strain distribution formed after upsetting determines the initial state of the billet prior to drawing out and influences both the subsequent strain values and the uniformity of its distribution during the drawing-out process.

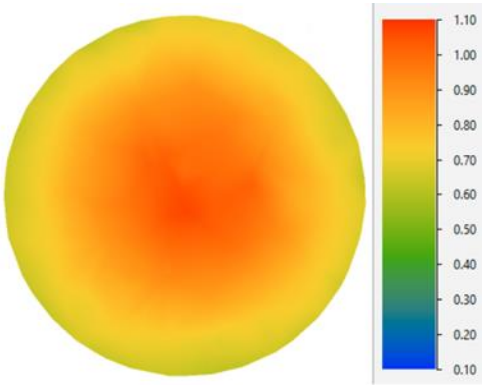

Figure 4 – Distribution of plastic strain in the cross-section of the billet after upsetting.

Figure 5 presents the distribution of plastic strain in the central cross-section of the billet after the third drawing-out pass for deformation degrees per pass of 10%, 15%, and 20%. As can be seen from the contour plots, increasing the deformation degree leads to a more uniform strain distribution across the section, with the most homogeneous pattern observed at 20% (Figure 5c).

At a deformation degree of 10 % per pass (Figure 5a), the plastic strain values vary within the range of 2 to 8, indicating pronounced strain nonuniformity and insufficient working of the central zone.Increasing the deformation degree to 15% (Figure 5b) results in a rise of the minimum strain values to 3.1, while the maximum values remain around 8. This suggests improved deformation penetration in the internal layers of the metal. The most thorough deformation working is observed at a deformation degree of 20% (Figure 5c), where the minimum strain values reach 7.1 and the maximum values attain 13. At this level, the strain distribution along the radius becomes significantly more uniform.

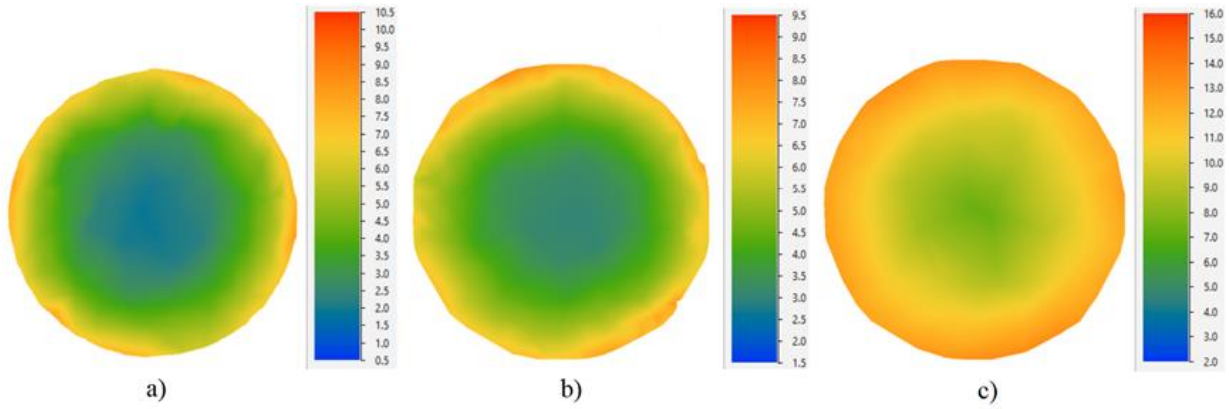

Figure 5. Distribution of plastic strain in the billet cross-section after the third drawing-out pass at different deformation degrees per pass: (a) ε = 10%; (b) ε = 15%; (c) ε = 20%.

The obtained results clearly demonstrate the significant influence of the deformation degree during billet drawing out and confirm the advisability of applying higher deformation degrees to achieve more complete working (penetration) throughout the billet volume. The summarized results of the numerical analysis are presented in Table 1, which includes the minimum and maximum values of plastic strain, as well as the calculated nonuniformity coefficient C_n for each variant of the deformation degree during drawing out.

Table 1. Plastic strain characteristics and nonuniformity coefficient after the third drawing out pass for different deformation degrees per pass.

Deformation degree per pass, ε (%)	Minimum equivalent plastic strain, ε min	Maximum equivalent plastic strain, ε max	Nonuniformity coefficient, C_n
10	2	8	0.25
15	3.1	8	0.38
20	7.1	13	0.54

Figure 6 presents graphs of the nonuniformity coefficient C_n distribution along the measurement lines in the cross-section of billets with different deformation degrees after the third drawing-out pass.

Analysis of the graphs made it possible to establish the pattern of distribution of the deformation nonuniformity coefficient C_n as a function of the billet deformation degree. For all variants, the curves exhibit a characteristic symmetric shape: the maximum C_n values are observed at the outermost (peripheral) points (points 1 and 7), while the minimum values occur in the central zone of the cross-section (points 3–5).

It was established that increasing the deformation degree leads to a rise in the nonuniformity coefficient C_n values in the central zone of the billet. At a deformation degree of 10% per pass (Figure 6a), the minimum C_n value in the central zone is 0.25. When the deformation degree is increased to 15% (Figure 6b), the coefficient rises to 0.38. At a deformation degree of 20% (Figure 6c), the K_n value reaches 0.54.

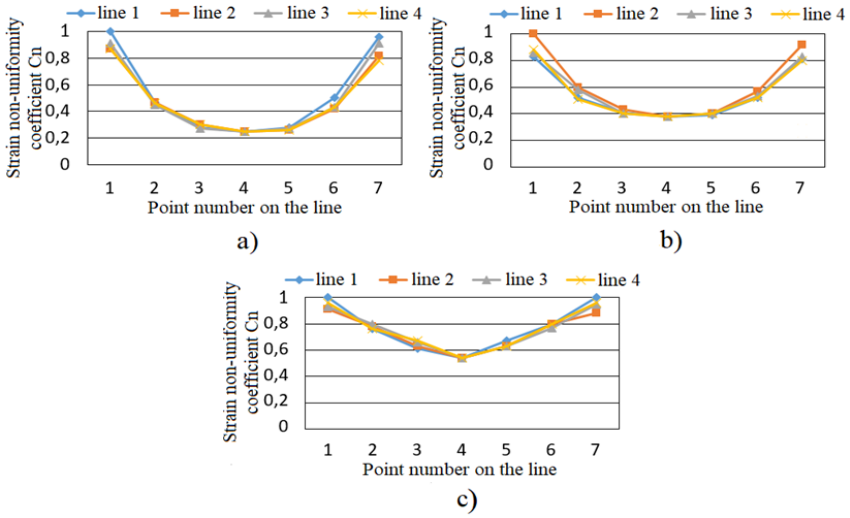

Figure 6. Graphs of the deformation nonuniformity coefficient Cn distribution after the third drawing-out pass for billets with different deformation degrees per pass: (a) ε = 10%; (b) ε = 15%; (c) ε = 20%.

In this case, the billet processed with a deformation degree of 20% per pass (Figure 6c) exhibits the most uniform plastic strain distribution. The minimum value of the nonuniformity coefficient is C_n = 0.54. Since values of the coefficient close to unity correspond to a more uniform strain distribution, the obtained result indicates that the deformation nonuniformity is reduced to 54%.

Conclusions. In this study, numerical modeling of the drawing out processes following preliminary billet upsetting was performed to investigate the influence of the deformation degree in the drawing out forging operation on the pattern of plastic strain distribution and to evaluate deformation nonuniformity throughout the volume of billets intended for high-capacity lifting hooks.

It was established that after upsetting, the billet exhibits nonuniform plastic strain distribution, with values decreasing from the center to the surface within the range of 0.6–1. This initial strain distribution is critical, as it determines the subsequent metal quality and the uniformity of structural working during the drawing-out stage.

The key role of the deformation degree during drawing out has been demonstrated: increasing the deformation per pass from 10% to 20% ensures a transition from pronounced nonuniformity to stable and thorough working of the entire metal volume. In particular, the minimum strain values increase more than threefold (from 2.0 to 7.1).

Analysis of the nonuniformity coefficient C_n confirmed that the central zone of the billet cross-section is the most difficult to deform. However, raising the deformation degree to 20% allows the uniformity in the central zone to increase from 0.25 to 0.54. This result indicates that the deformation nonuniformity is reduced to 54%.

The obtained findings can be used to develop rational technological regimes for open-die forging of high-capacity lifting hooks with enhanced requirements for structural uniformity, mechanical properties, and operational reliability.

References

1. Zhang, X., Li, Y., & Wang, J. (2012). Forging process for single-horn hook (Patent No. CN102764849A). China National Intellectual Property Administration. https://patents.google.com/patent/CN102764849A

2. Altan, T., Ngaile, G., & Shen, G. (2005). Cold and hot forging: Fundamentals and applications. ASM International. https://doi.org/10.31399/asm.tb.chffa.t53700001. Available from: http://ressources.unit.eu/cours/MediaMef3/module-forgeage-materiaux/res/Cold_and_Hot_Forging_Fundamentals_and_Applications.pdf

3. Hosford, W. F., & Caddell, R. M. (2011). *Metal forming: Mechanics and metallurgy*. Cambridge University Press.

4. Dourandish, S., Champliaud, H., Morin, J.-B., & Jahazi, M. (2024). Numerical simulation and experimental validation of microstructure evolution during the upsetting process of a large-size martensitic stainless steel forging. International Journal of Material Forming, 17, 38. https://doi.org/10.1007/s12289-024-01840-0

5. Obiko, J., Shongwe, M. B., & Malatji, N. (2025). On the effect of deformation conditions on the metal flow behavior during upsetting process using finite element simulation DEFORM-3D software. *International Journal on Interactive Design and Manufacturing*. https://doi.org/10.1007/s12008-024-02051-2

6. Markov, O. E., Zlygorev, V. N., Gerasimenko, O. V., Khvashchynskyi, A. S., & Zhytnikov, R. Yu. (2019). Development of recommendations for computer-aided design of profiled upsetting workpieces. *Mechanics and Advanced Technologies*, 86(2). https://doi.org/10.20535/2521-1943.2019.86.181050

7. Volokitina, I. E., Naizabekov, A. B., Panin, V. E., & Panin, A. V. (2023). Methods for improving the quality of forgings obtained by forging through intensifying shear or alternating strain. *Progress in Physics of Metals*, 24(4), 764–791. https://doi.org/10.15407/ufm.24.04.764

8. Chen, K., Yang, Y., Shao, G., & Liu, K. (2011). Simulation of large forging flat-anvil stretching process and its optimization. *Journal of Shanghai Jiaotong University (Science)*, 16(2), 199–202. https://doi.org/10.1007/s12204-011-1121-8

9. Pop, E. A. (2024). Research on stretching by forging. Scientific Bulletin Series D: Mining, Mineral Processing, Non-Ferrous Metallurgy, Geology & Environmental Engineering, 38, p. 27.

10. Banaszek, G., Berski, S., & Dyja, H. (2011). Numerical analysis of the torsion stretch forging operation in asymmetric anvils. *Metallurgical and Mining Industry*, 3(7), 98-101.

11. Markov, O. E., Perig, A. V., Zlygoriev, V. N., Markova, M. A., & Kosilov, M. S. (2017). Development of forging processes using intermediate workpiece profiling before drawing: research into strained state. Journal of the Brazilian Society of Mechanical Sciences and Engineering, 39(11), 4649–4665. https://doi.org/10.1007/s40430-017-0812-y

12. Su, J. H., Chen, Y. W., Chen, Y. Y., & Shi, Y. L. (2011). Defect recovery and control in heavy forgings by two times upsetting and stretching process. *Advanced Materials Research*, 291, 706-709. https://doi.org/10.4028/www.scientific.net/amr.291-294.706

13. Kukuryk, M. (2020). Analysis of deformation and prediction of cracks in the cogging process for die steel at elevated temperatures. Materials, 13(24), 5589. https://doi.org/10.3390/ma13245589

14. Kukuryk, M. (2021). Analysis of deformation, the stressed state and fracture predictions for cogging shafts with convex anvils. *Materials*, 14(11), 3113. https://doi.org/10.3390/ma14113113

15. QForm UK. (2026). Web-site: https://qform3d.com/

16. Chukhlib, V., Ashkelianets, A., Gubskii, S., O. Petrov, O., Duvanskii, O., Palienko, V., & Okun, A. (2021). Development of a technological concept for designing forging processes taking into account the influence of the deformation mode on the quality of forging pieces. Bulletin of the National Technical University “KhPI”. *Series: Hydraulic machines and hydraulic units*, 1, 95-103. https://doi.org/10.20998/2411-3441.2021.1.12. Available from: https://repository.kpi.kharkov.ua/server/api/core/bitstreams/689f51f9-c801-43c0-8475-db40cbef7ce5/content

Надіслано до редакції / Received: 05.01.2026
Прорецензовано / Peer-Reviewed: 22.02.2026
Прийнято до друку / Accepted: 16.03.2026
Опубліковано / Published: 30.03.2026

ISSN 3083-7219 (Print), ISSN 3083-7227 (Online)
Теорія і практика металургії, 2026, № 1
Theory and Practice of Metallurgy, 2026, No. 1

https://doi.org/10.15802/tpm.1.2026.03

UDC 629.4.027.2:621.83.06:621.7/9

Biriukov S. V.[1,*]***, Chukhlib V. L.***[2]

Development of the technology for manufacturing the bracket for mounting the reducer of the metropolitane cars

[1] ORCID: 0009-0005-6403-5880. National Technical University “Kharkiv Polytechnic Institute”, Ukraine
[2] ORCID: 0000-0001-6176-0917. National Technical University “Kharkiv Polytechnic Institute”, Ukraine
* Email: Serhii.Biriukov@mit.khpi.edu.ua

Бірюков С. В.[1,*]***, Чухліб В. Л.***[2]

Розробка технології виготовлення кронштейну кріплення редуктора вагону метрополітену

[1] ORCID: 0009-0005-6403-5880. Національний технічний університет «Харківський політехнічний інститут», Україна
[2] ORCID: 0000-0001-6176-0917. Національний технічний університет «Харківський політехнічний інститут», Україна
* Email: Serhii.Biriukov@mit.khpi.edu.ua

Abstract. *This article discusses the developed technology for manufacturing a gearbox mounting bracket used on rolling stock in domestic metro systems. The article also analyses the design of this bracket and the malfunctions that may occur during operation. The specific nature of metro rolling stock operation, characterised by high traffic intensity, frequent acceleration and braking cycles, and significant dynamic loads, places increased demands on the reliability of each structural element of its running gear. Since a significant part of the bogie parts are manufactured using metal pressure processing methods, the issue of improving the quality of stamped forgings becomes a relevant technical task that affects the safety of passenger transport and the accident-free operation of vehicles. This article analyses other works related to improving the mechanical characteristics of products and increasing their quality, which depend on the parameters and methods of their production. The traditional forging technology discussed above usually involves a multi-stage process that includes the use of rolling grooves for preliminary distribution of metal along the axis of the blank. However, this approach increases the size of the stamping equipment and requires more passes, which leads to higher energy costs and production costs. The authors proposed abandoning the use of a rolling groove, since it is possible to manufacture this forging without changing the geometry of the blank before bending.The results of this work can be used by technologists and engineers in the machine-building industry as one of the promising ways to improve and rationalise the stamping of forgings with similar geometry, since by reducing the number of stamping passes, it is possible to reduce the cost of production and manufacture of dies without significantly affecting the stress-strain state of the resulting forging. The expediency of using computer modelling in the design of production technology is also indicated, as it allows all stages of production to be investigated without significant financial costs and ways to improve and rationalise technological operations to be identified, which will have an impact on improving the quality of manufactured products in the future.*
Keywords: *production technology, stamping, forging, stamping groove, underground railway, gearbox mounting bracket.*

Анотація. *В даній статті розглянуто розроблену технологію виготовлення кронштейну кріплення редуктора, що експлуатується на рухомому складі вітчизняних метрополітенів. Також в роботі була проаналізована конструкція цього кронштейну та несправності, які можуть виникати при експлуатації. Адже специфіка роботи рухомого складу метрополітену, що характеризується високою інтенсивністю руху, частими циклами розгону та гальмування, а також значними динамічними навантаженнями, висуває підвищені вимоги до надійності кожного конструкційного елемента його ходової частини. Оскільки значна частина деталей візка вагону виготовляється методами обробки металів тиском, питання покращення якості штампованих поковок стає актуальним технічним завданням, що впливає на забезпечення безпеки пасажирських перевезень та безаварійну експлуатацію транспортних засобів. У даній статті зроблено аналіз інших робіт, що стосуються поліпшення механічних характеристик виробів та підвищення їх якості, що залежать від параметрів та методів їх виробництва. Традиційна технологія виготовлення поковки, що була розглянута, зазвичай передбачає багатостадійний процес, що включає використання підкатувальних рівчаків для попереднього розподілу металу вздовж осі заготовки. Однак, такий підхід збільшує габарити штампового оснащення та вимагає більшої кількості переходів, що веде до зростання енерговитрат та собівартості. Авторами було запропоновано відмовитися від використання підкатувального рівчака, оскільки для виготовлення даної поковки можливо не змінювати геометрію заготовки перед її згинанням. Результати даної роботи можуть бути використані технологами та інженерами машинобудівної галузі, як один із перспективних шляхів поліпшення та*

© Biriukov S.V., Chukhlib V.L., 2026
© Бірюков С.В., Чухліб В.Л., 2026

This is an Open Access article under the CC BY 4.0 license https://creativecommons.org/licenses/by/4.0/

раціоналізації штампування поковок схожої геометрії, оскільки за рахунок зменшення кількості штампувальних переходів можливо зменшити витрати на виробництво та виготовлення штампів, без суттєвого впливу на напружено-деформований стан отриманої поковки. Також вказано на доцільність застосування комп'ютерного моделювання в проектуванні технології виробництва, адже це дозволяє дослідити всі етапи виробництва без значних фінансових кладень та виявити шляхи покращення та раціоналізації технологічних операцій, що матиме вплив на покращення якості виготовляємої продукції в подальшому.
Ключові слова: *технологія виробництва, штампування, поковка, штампувальний рівчак, метрополітен, кронштейн кріплення редуктора.*

Introduction. The modern transport engineering industry requires new approaches to production, as scientific and technological progress moves forward, production processes are automated, and equipment is improved. The development and optimisation of production is also facilitated by the use of computer technology, which allows production processes to be simulated before they are implemented in the enterprise, making it possible to identify 'weak' points in the technological chain of operations. These studies, conducted using specialised software such as QForm, Abaqus, SolidWorks, and ANSYS Mechanical, help specialists improve production efficiency, because the earlier an error is detected in the product life cycle, the cheaper it will be to correct it.

When manufacturing running gear components for transport, they undergo many technological operations to get from a blank to a finished part that meets all the specified requirements, standards and tolerances. The running gear of rail transport, namely bogies, consists of parts, most of which are manufactured using metal pressure processing. Accordingly, by pre-modelling these processes, it is possible to predict ways to improve the technology for manufacturing these parts. In particular, the modelling of stamping processes has broad prospects in modern industry, allowing the analysis of product manufacturing in the early stages of its life cycle.

Analysis of literature data and problem statement. The running gear of railway and metro rolling stock consists of many components, the details of which are manufactured using pressure processing technology, in particular, volumetric hot stamping. Since the transportation of passengers and cargo by rail accounts for a significant share of Ukraine's total passenger and freight traffic [1], it is appropriate to improve the quality of manufactured parts, as they affect not only the reliability and strength of the entire structure, but also traffic safety. Specialists in the field of production offer various ways to improve and optimise production processes in order to improve the characteristics of products, including their quality.

In [2], the authors conducted a study aimed at assessing the quality of forgings depending on the forging parameters. It was found that after manufacturing and heat treatment, surface cracks appeared in the forgings, which subsequently affected their reliability and mechanical properties. One of the causes of cracking is the wear of dies and damage during the forging process, which contributes to the formation of non-metallic oxide inclusions and the transfer of surface defects to forgings.

Work is also underway to optimise production processes. In particular, in [3], the hot forging process was modelled in the QFORM software package, which allowed the authors to reduce material and energy costs for forming by using the minimum number of forming passes and a low-power forging hammer. Modelling showed that by combining the blanking and upsetting passes, it is possible to achieve a more favourable blank profile, which improves the metal forming conditions for the selected stamping dies used to produce the forging under study.

In modern research on metal pressure treatment, the creation of new approaches to forging and the rationalisation of its modes are relevant. One of the ways to improve this process is the work [4-7] related to predicting the quality of forgings depending on the deformation mode during forging. This approach in the forging process allows not only to analyse the unevenness of metal deformation during pressure treatment, but also to establish more rational modes of this treatment in order to obtain a uniform distribution of mechanical properties in the product, which will undoubtedly improve its quality and reliability.

Also, in [4], a method was proposed for predicting the unevenness of metal deformation during forging, which allows for a more uniform stress-strain state of the forging, affecting the uniformity of the distribution of mechanical properties in the metal.

Thus, modern research in the field of mechanical engineering mainly concerns the optimisation and rationalisation of production processes, increasing their efficiency, as well as improving the mechanical characteristics and quality of parts manufactured, in particular by stamping. The solution to these problems is greatly facilitated by the use of specialised computer programs, such as QForm [8], which allow the parameters of the manufacturing process to be researched, analysed and improved at the technology development stage. However, the problem lies in finding ways to improve production, as technologies are being modernised and technical progress is not standing still. Accordingly, the 'classic' production schemes that existed earlier are now being supplemented or revised in the context of modern approaches and production equipment.

Purpose and objectives of the research. The purpose of this work is to develop a technology for manufacturing a gearbox mounting bracket used on rolling stock of domestic metros. The authors set themselves the task of investigating the possibility of simplifying the manufacture of this bracket by applying a technology that differs slightly from the classic technology for manufacturing forgings with a curved axis.

Materials and research methods. One of the main components of a rail transport trolley is its traction transmission, which is usually attached to the trolley frame using brackets and suspension. Accordingly, the design of the mounting brackets must meet all the reliability and strength criteria established for them under operating conditions.

For example, the rolling stock of the Kharkiv Metro uses a gearbox mounting bracket consisting of a cylindrical part and an eyelet. This bracket is welded into the crossbeam of the trolley frame [9], as shown in Figure 1.

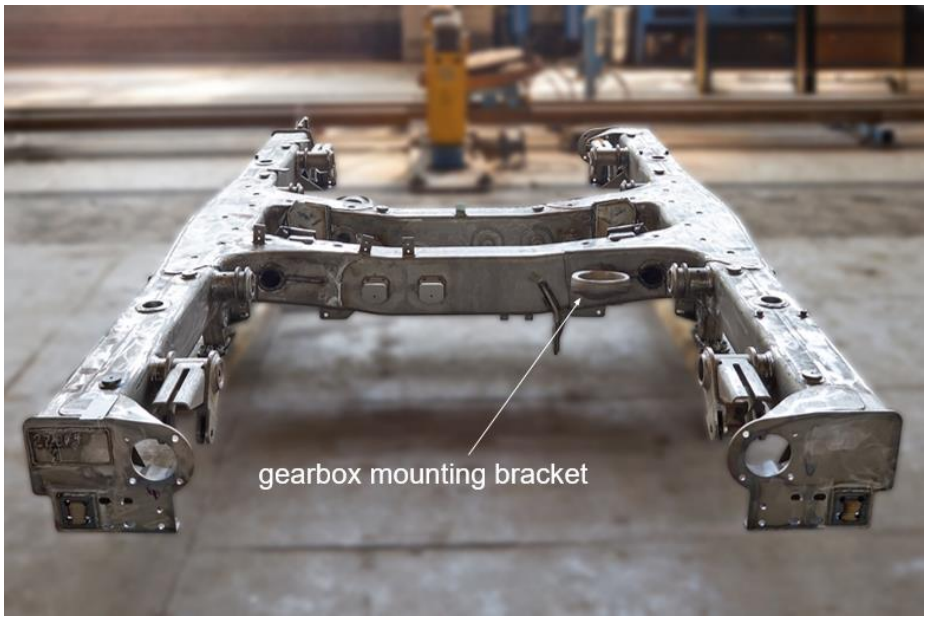

Fig. 1 – Bracket for mounting the gearbox of a 81-717 series carriage bogie.

The eye of this bracket is tilted towards the horizon at an angle of 18º, and the axle of the gearbox suspension is deflected at the same angle to ensure the smallest vertical deflection between the shafts of the traction motor and the gearbox gear when the axle springs are loaded.

This bracket is a very important element of the car's running gear and, accordingly, has high reliability requirements, since its failure, as shown in Figure 2, will significantly affect traffic safety and is unacceptable during operation [10, 11]. To prevent such cases, the bogie is equipped with a comprehensive safety device [12] that prevents the reduction gear suspension elements from falling onto the rail track in the event of their breakage or breakage of the mounting bracket.

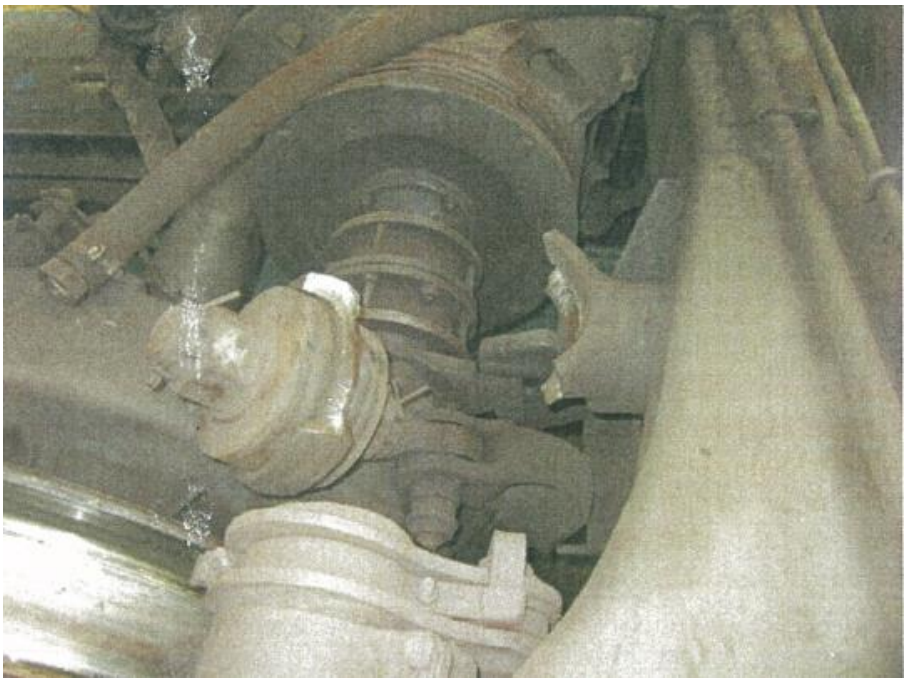

Fig. 2 – Breakage of the gearbox mounting bracket on an E-type carriage.

Many elements of a railway carriage bogie are manufactured using metal pressure processing methods. The gearbox mounting bracket is no exception. The production technology for this bracket involves hot volumetric stamping [13]. A cylindrical blank is used to manufacture the forging for this part.

Research results. The model of the bracket and its forging are shown in Figure 3. This forging belongs to the group of forgings with a curved axis [14].

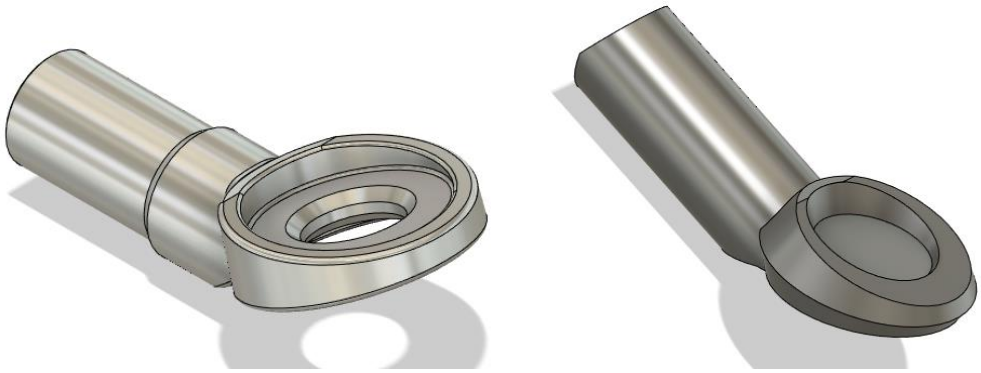

a) b)

Fig. 3 – Model of bracket a) and its forging b).

Such forgings are stamped using an appropriate combination of die grooves [15]. The classic technology for manufacturing this forging, which has a curved axis, involves the following sequence of stamping passes: rolling groove – bending groove – preliminary groove – final groove.

The authors propose simplifying the production technology for such a forging, namely, not using a roll-up groove, but deforming the cylindrical blank first in a bending groove, and then in the preliminary and final grooves. This decision was made in accordance with the calculated blank (diameter diagram) and its cross-section diagram. These diagrams, shown in Figure 4, were constructed after the forging was unfolded, since its axis has an 18º bend in the area of the lug.

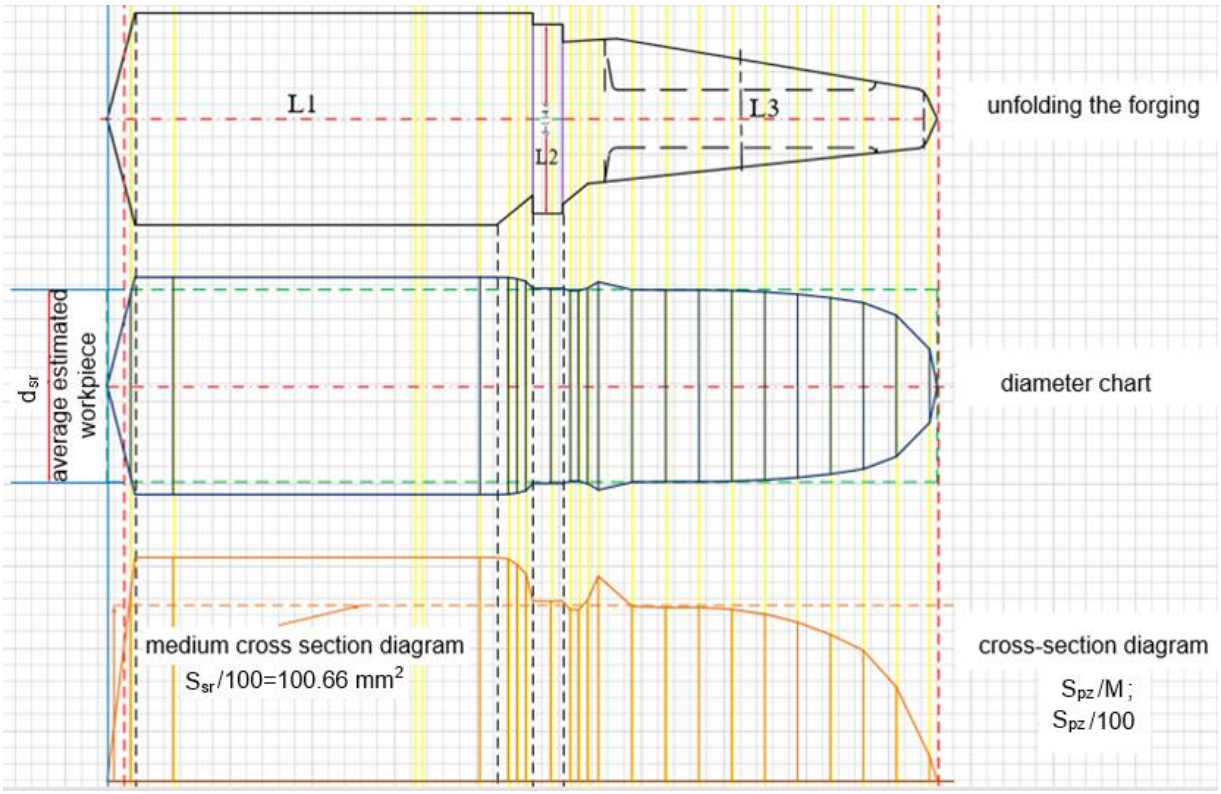

Fig. 4 – Calculated blank and its cross-section diagram.

Since the diameter profile is close to rectangular in shape, it was proposed to abandon the rolling groove for the production of this bracket.

Discussion of results. The development of production technology for any part involves a combination of die grooves that must be used to obtain the re-

quired shape of the forging. The use of modern approaches to the development of forging manufacturing technology, in particular computer modelling, allows for a broader analysis of hot volumetric stamping processes and the identification of ways to improve production, which can have a positive impact on its cost-effectiveness, efficiency and quality. It is this analysis that is promising in the context of this work, which requires a more thorough consideration of the proposed production technology.

This work proposes a way to rationalise stamping processes by minimising the number of passes, which reduces production costs while maintaining the required characteristics of the forging. The authors justify the feasibility of introducing digital modelling systems for virtual testing of technologies. This approach allows identifying the potential for improving operations without additional financial investments, ensuring high quality of products in the future.

Conclusions. A technology has been developed for the production of a gearbox mounting bracket, which is manufactured by metal pressure treatment, namely hot volumetric stamping. Based on the obtained calculated blank and its cross-section diagram, it is proposed to abandon the rolling groove, which is usually used, in particular, for the production of forgings with a curved axis.

Based on the developed technology, it is necessary to conduct a more detailed analysis and modelling to study its impact on the quality characteristics of forgings.

References

1. Stasiuk, O. M., Chmyrova, L. Yu., & Fediai, N. O. (2020). Freight and passenger transportation markets in Ukraine: problems and trends. *Efektyvna ekonomika*, 9. https://doi.org/10.32702/2307-2105-2020.9.54
2. Grega, M. & Brezinova, J., 2025. Evaluation of the quality of forgings depending on the technological parameters of production. *Machines. Technologies. Materials*, 8, 280-284.
3. Husachuk, D. A., Klymenko, O. D., Parfentieva, I. O., Dmytriiuk, M. V., Imbirovych, N. Yu., Feshchuk, Yu. P. & Karpiuk, M. M. (2021). Optimization of the hot stamping process of hydraulic cylinder eye forging in the QFORM software package. *Naukovi notatky*, 72, 80-87. https://doi.org/10.36910/775.24153966.2021.72.12
4. Chukhlib, V. L., Ashkelianets, A. V., Hubskyi, S. O., Petrov, O. V., Duvanskyi, O. M., Paliienko, V. O. & Okun, A. O. (2021). Development of a technological concept for designing forging processes, taking into account the influence of the deformation mode on the quality of forgings. *Bulletin of the National Technical University "KhPI". Series: Hydraulic machines and hydraulic units,* 1, 95-103. https://doi.org/10.20998/2411-3441.2021.1.12
5. Chukhlib, V. L. & Kolisnyk, K. D. (2024). Analysis and research of hook forging technology. *Visnyk Natsionalnoho tekhnichnoho universytetu "KhPI". Ser. : Tekhnolohii v mashynobuduvanni : zb. nauk. pr,* 2(10), 87-93. https://doi.org/10.20998/2079-004X.2024.2(10).09
6. Paliienko, V. O. & Chukhlib, V. L. (2025). Forging of a crankshaft taking into account the influence of deformation modes on the quality of forgings. *Naukovyi zhurnal Metinvest politekhniky. Ser.: Tekhnichni nauky,* 4, 246-253. https://doi.org/10.32782/3041-2080/2025-4-34
7. Duvanskyi, O. M. & Chukhlib, V. L. (2025). Research on the influence of forging parameters on the shape of the forging of the valve body [Doslidzhennia vplyvu parametriv kuvannia na formu pokovky korpusa zapirnoi armatury]. *Naukovyi zhurnal Metinvest politekhniky. Ser.: Tekhnichni nauky,* 4, 229-234. https://doi.org/10.32782/3041-2080/2025-4-31
8. Stebunov, S., Biba, N. (2004). QForm software created for technologists. *Kuzn.-Shtamp.Proizv.* 9, 38–42.
9. Kryukiv Railway Carriage Works. Available at: https://www.kvsz.com/index.php/ru/produktsiya/produktsiya-dlya-metropolitenov/zapasnye-chasti/item/313-rama-telezhki-vagonov-metropolitena-mod-81-717-714
10. Artemenko, A. V., Chepurnenko, Y. V. & Mazanko, D. H. (2012). Analysis of damage to bogie frames of metro cars. *Zbirnyk naukovykh prats DP "UkrNDIV",* 6, 29-33.
11. *Rules for the technical operation of subways in Ukraine*. (2015).
12. A training manual for studying the arrangement and operation of electrical, pneumatic and mechanical equipment of metro cars of series 81 - 717 and 81 – 714. (2005). KP "Kyivskyi metropoliten".
13. Dobrianskyi, S. S., Malafieiev, Yu. M. & Pukhovskyi, Ye. S. (2014). *Proektuvannia i vyrobnytstvo zahotovok / pidruchnyk.* NTUU "KPI".
14. Kukhar, V. V., Karhin, B. S., Anishchenko, O. S., Karhin, S. B. & Prysiazhnyi, A. H. (2017). *Tekhnolohichni protsesy za fakhom. Kuvannia i shtampuvannia : navchalnyi posibnyk.* PDTU.
15. Nosulenko, V. I. & Mirzak, V. Ya. (2019). *Kuvannia i hariache obiemne shtampuvannia : metod. rekomendatsii do vykonannia lab. robit : dlia stud. den. i zaochno-dystants. formy navch. spets. 131 "Prykladna mekhanika".* TsNTU.

Надіслано до редакції / Received: 06.01.2026
Прорецензовано / Peer-Reviewed: 25.02.2026
Прийнято до друку / Accepted: 16.03.2026
Опубліковано / Published: 30.03.2026

ISSN 3083-7219 (Print), ISSN 3083-7227 (Online)
Теорія і практика металургії, 2026, № 1
Theory and Practice of Metallurgy, 2026, No. 1

https://doi.org/10.15802/tpm.1.2026.04

UDC 621.928.2.001.2:621.928.2-192

Popolov D. V.[1,*]***, Shved S. V.***[2]***, Zaselskyi I. V.***[3]***, Velitchenko V. L.***[4]

Modeling of the deformed state of the screen box of a heavily loaded vibratory machine

[1] ORCID: 0000-0003-0347-8627. State University Economics and Technology, Ukraine
[2] ORCID: 0000-0003-2169-8893. State University Economics and Technology, Ukraine
[3] ORCID: 0000-0002-4834-4027. State University Economics and Technology, Ukraine
[4] ORCID: 0000-0003-3360-5332. State University Economics and Technology, Ukraine
*Email: popolov@duet.edu.ua

Пополов Д. В.[1,*]***, Швед С. В.***[2]***, Заселський І. В.***[3]***, Велитченко В. Л.***[4]

Моделювання деформованого стану грохотної коробки сильно навантаженої вібраційної машини

[1] ORCID: 0000-0003-0347-8627. Державний університет економіки і технологій, Україна
[2] ORCID: 0000-0003-2169-8893. Державний університет економіки і технологій, Україна
[3] ORCID: 0000-0002-4834-4027. Державний університет економіки і технологій, Україна
[4] ORCID: 0000-0003-3360-5332. Державний університет економіки і технологій, Україна
*Email: popolov@duet.edu.ua

Abstract. *The paper addresses the problem of improving the technical and economic efficiency of heavily loaded vibratory machines through optimization of the load-bearing frame of the screen box. The main elements providing the spatial stiffness of the box structure are tubular transverse tie-beams, which operate under conditions of intensive cyclic bending loads. Analysis of the available literature indicates that these elements belong to the most highly loaded and vulnerable structural components, for which fatigue failure is the dominant failure mechanism. The traditional approach to increasing the strength of structural elements, namely, enlarging the cross-sectional area, leads to an increase in the mass of the screen box and the associated inertial loads, which adversely affects the dynamic characteristics of the vibratory machine. The objective of this study was to improve the structural efficiency of the screen box of a vibratory machine by optimizing the geometry of the tie-beams using a rational material distribution along the length of the element. An approach is proposed that involves varying the outer diameter of the tubular tie-beam according to a parabolic law while maintaining a constant inner diameter. Such an approach makes it possible to reduce the beam mass in regions of low bending moments while simultaneously maintaining or increasing stiffness in the most heavily loaded sections. To evaluate the effectiveness of the proposed solution, a series of numerical experiments was carried out using the finite element method. The simulations included calculations of axial compression, bending under transverse inertial loading, determination of the first natural frequency, and estimation of the critical buckling load for tie-beams with both baseline and parabolic profiles. The obtained results demonstrate that the use of a parabolic profile makes it possible to reduce the mass of the tie-beam by 41%, while the transverse acceleration corresponding to the onset of yielding increases by 55%, and the first natural frequency increases by 18%. Stress distribution maps indicate a more uniform loading of the material in the tie-beam with the parabolic profile. The deformed state of the screen box was also modeled using both the baseline and the optimized tie-beams. The results show that the change in beam geometry has virtually no effect on the dynamic characteristics of the box. The first natural frequency of the structure changes only slightly, while the deformation pattern and the maximum displacement amplitude remain practically unchanged. The obtained results confirm the prospects of applying variable-section tie-beams for improving the energy efficiency and reliability of vibratory machines.*
Keywords: *vibratory machine, screen box, reliability, structural optimization, stress–strain state, natural frequencies, vibration resistance of structures.*

Анотація. *У статті розглядається проблема підвищення техніко-економічної ефективності важко навантажених вібраційних машин шляхом оптимізації несучої рами грохотної коробки. Основними елементами, що забезпечують просторову жорсткість конструкції коробки, є трубчасті поперечні балки, які працюють в умовах інтенсивних циклічних згинальних навантажень. Аналіз доступної літератури вказує на те, що ці елементи належать до найбільш навантажених та вразливих конструктивних елементів, для яких домінуючим механізмом руйнування є втомне руйнування. Традиційний підхід до підвищення міцності конструктивних елементів, а саме збільшення площі поперечного перерізу, призводить до збільшення маси грохотної коробки та пов'язаних з нею інерційних навантажень, що негативно впливає на динамічні характеристики вібраційної машини. Метою цього дослідження було підвищення конструктивної ефективності грохотної коробки вібраційної машини шляхом оптимізації геометрії балок з використанням раціонального розподілу матеріалу по*

© Popolov D. V., Shved S. V., Zaselskyi I. V., Velitchenko V. L., 2026
© Пополов Д. В., Швед С. В., Заселський І. В., Велитченко В. Л, 2026

This is an Open Access article under the CC BY 4.0 license https://creativecommons.org/licenses/by/4.0/

довжині елемента. Запропоновано підхід, що передбачає зміну зовнішнього діаметра трубчастої балки за параболічним законом при збереженні постійного внутрішнього діаметра. Такий підхід дозволяє зменшити масу балки в областях з низькими згинальними моментами, одночасно зберігаючи або збільшуючи жорсткість у найбільш навантажених перерізах. Для оцінки ефективності запропонованого рішення було проведено серію числових експериментів з використанням методу скінченних елементів. Моделювання включало розрахунки осьового стиску, згинання під поперечним інерційним навантаженням, визначення першої власної частоти та оцінку критичного навантаження на вигин для стяжних балок як з базовим, так і з параболічним профілями. Отримані результати показують, що використання параболічного профілю дозволяє зменшити масу стяжної балки на 41%, тоді як поперечне прискорення, що відповідатиме початку текучості, збільшується на 55%, а перша власна частота збільшується на 18%. Карти розподілу напружень вказують на більш рівномірне навантаження матеріалу в стяжній балці з параболічним профілем. Деформований стан ситового короба також було змодельовано з використанням як базового, так і оптимізованого стяжних балок. Результати показують, що зміна геометрії балки практично не впливає на динамічні характеристики короба. Перша власна частота конструкції змінюється незначно, тоді як картина деформації та максимальна амплітуда зміщення залишаються практично незмінними. Отримані результати підтверджують перспективність застосування анкерних балок змінного перерізу для підвищення енергоефективності та надійності вібраційних машин.
Ключові слова: *вібраційна машина, грохот, надійність, структурна оптимізація, напружено-деформований стан, власні частоти, вібростійкість конструкцій.*

Introduction

Vibratory machines are widely used in continuous technological processes for the processing of bulk materials in the mining, metallurgical, and construction industries. Such equipment belongs to the class of units with increased requirements for reliability, durability, and stability of technological performance indicators [1, 2]. At the same time, under modern conditions, improving their energy efficiency has become particularly important. This is associated both with the rising cost of energy resources and with the need to reduce the negative environmental impact of industrial activities. In particular, reducing the energy consumption of technological equipment directly contributes to lowering emissions of fuel combustion products during electricity generation, including carbon monoxide (CO), which is an important environmental factor [3, 4].

One of the promising directions for improving the energy efficiency of vibratory machines is the enhancement of the design of their load-bearing elements and the application of new approaches to component shape formation. Traditionally, the strength of structural elements is increased by enlarging their cross-sectional area. However, for vibratory machines this approach has significant limitations. An increase in the mass of components leads to higher inertial loads, which in turn adversely affects the dynamic characteristics of the system. Thus, a contradiction arises between the need to improve the strength and reliability of the structure and the requirement to reduce inertial loads. With increasing vibration frequency of the working body, this contradiction becomes even more pronounced.

Analysis of published data and problem statement

The main load-bearing elements of the screen box of a vibratory machine are the side plates and the tie-beams. The side plates are manufactured from steel sheet blanks reinforced with stiffening ribs. They serve as the supporting base for the installation of screen panels and transmit the inertial forces generated by rotating unbalanced exciters mounted on the box. The spatial stiffness of the structure is ensured by tubular transverse tie-beams with a circular cross-section that connect the side plates to each other. Since the side plates are located in the plane of vibration, the tie-beams are oriented perpendicular to it. As a result, they are subjected to significant periodic bending loads, the direction of which changes with the operating vibration frequency of the vibratory machine. Therefore, cyclic bending is the dominant loading mode for these elements, whereas axial tensile and compressive forces mainly arise due to deformation of the screen box and are not the governing loads [5].

In the study [6], performed using the ANSYS software package, it was established that the tie-beams of a vibratory machine are among the most heavily loaded and structurally vulnerable components of the machine. The authors of [7] determined that fatigue failure is the primary mechanism of their destruction. The results of modal and harmonic analyses made it possible to clearly identify the most critical zones of the structure that are prone to crack initiation and propagation.

In publication [8], an approach combining the analysis of vibratory machine dynamics with crack growth modeling was proposed. The dynamic behavior of the vibratory machine was described using a two-dimensional model developed based on the finite element method, in which the tie-beam was represented by an Euler beam element with a local defect. To estimate the crack growth rate, the Paris model was applied, allowing the variation of system stiffness during damage evolution to be taken into account. It was shown that the amplitude of the excitation force is the dominant factor determining the fatigue life of the tie-beam, while cracks located near the joints with the side plates propagate significantly faster due to increased stress concentration.

A number of studies address the problem of reduced durability of tie-beams associated with the tendency to increase both their dimensions and the dynamic intensity of vibratory machines. In particular, study [9] demonstrated that an increase in productivity and vibration frequency leads to a significant rise in

dynamic loads, which results in the formation of cracks in tie-beams. To improve structural reliability, the use of beams with redundant constraints was proposed, providing additional stiffness and the ability to sustain loads even in the case of partial damage to structural elements. Experimental investigations have shown that such a design contributes to efficient dissipation of vibration energy. It was found that in the improved beam the amplitude of the input power flow is manifested mainly in the low-frequency range and decays more rapidly at higher frequencies, which indicates an increase in the vibration resistance of the structure.

In [10], a mathematical model for calculating the dynamic stresses of tie-beams in a vibratory machine with linear oscillations was presented. The authors applied the finite element method integrated with the dynamic model of the vibratory machine, taking into account the influence of the material mass using the mass-flow method. It was demonstrated that traditional quasi-static calculation methods lead to significant errors because they do not account for high-frequency excitation components that may be close to the natural frequencies of the structure. It was established that the tie-beam experiences complex bending vibrations in both horizontal and vertical planes, while the maximum dynamic stresses occur mainly in the end sections of the tie-beams, where fatigue cracks are most likely to form.

The above considerations highlight the necessity of paying particular attention to the problem of fatigue failure of load-bearing elements in vibratory machine structures, especially tie-beams operating under long-term cyclic loading.

Considering the characteristics of spatially distributed inertial loads, improving the vibration resistance of the screen box of a vibratory machine can be achieved not by increasing the cross-sectional area of the transverse beams but, conversely, by rationally reducing their cross-section in the region of maximum deflection. Such an approach makes it possible to reduce the mass of the structure, decrease inertial loads, and improve the dynamic characteristics of the system.

The purpose and objectives of research

The objective of this study was to improve the technical and economic efficiency of vibratory machines through optimization of the load-bearing structure of their screen box by applying new approaches to the geometric design of tie-beams. This approach makes it possible to significantly reduce the mass of the structure while simultaneously improving its vibration and stiffness characteristics.

Materials and methods

The structure of the screen box of the vibratory screen GST-62.MF (Fig. 1) was selected as the object of the study. The box consists of side plates 1, interconnected by tie-beams 2 and two transverse beams 3, in which flange-mounted motor-vibrators 4 are installed and connected to the side plates of the box by flanges.

Considering their structural configuration, the tie-beams of the box can be regarded as statically indeterminate elements clamped at both ends by the elastic side plates. The most critical loading conditions occur when the operating frequency passes through their resonant frequencies. According to the analysis of the dynamic characteristics of vibratory screens [11], operating frequencies that significantly differ from the first natural frequencies of the structural elements of the screen box make it possible to avoid resonant excitation. Such resonant conditions can lead to large vibration amplitudes and significant destructive effects on the box structure and, consequently, reduce the durability and operational reliability of the machine.

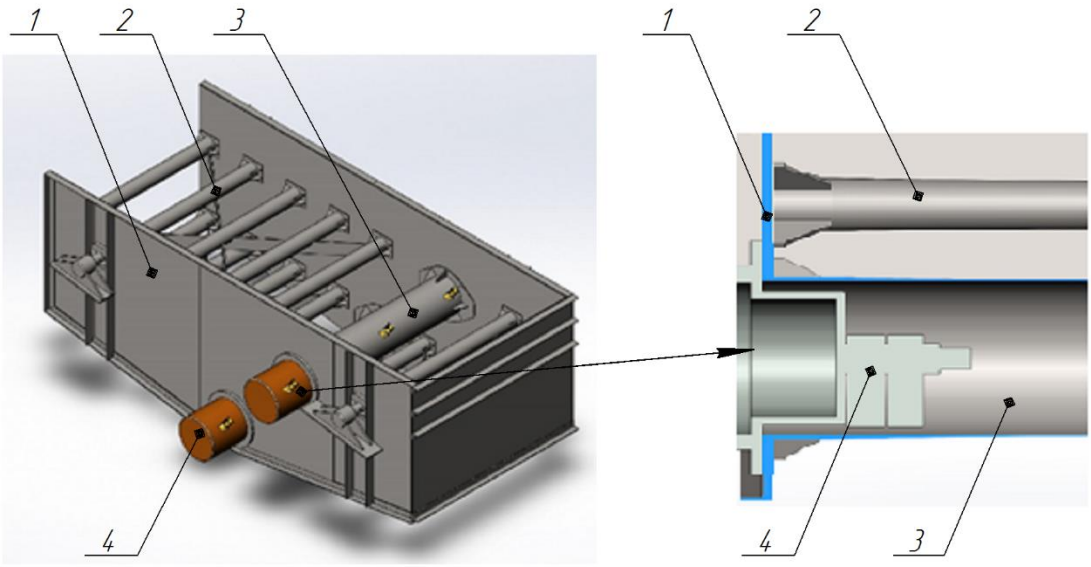

Figure 1 – Structure of the screen box of the vibratory screen GST-62.MF.

An increase in the operating frequency of the screen during the processing of metallurgical charge components generates additional dynamic loads, which necessitates the search for reserves to improve the structural stiffness of the working body and its components, primarily the tie-beams.

One of the possible approaches to reducing the influence of vibration loads is a rational modification of the cross-section of the tie-beam, taking into account the distribution of bending moments along its length. Such an approach involves reducing the mass in regions with small bending moments while maintaining or increasing stiffness in regions where the bending moments reach their maximum values. As a result, the mass of the beam can be reduced without a significant decrease in its bending stiffness, which contributes to an increase in the natural frequencies of the structure. One practical way to implement this approach is to reduce the cross-sectional area of the beam in its central part. Provided that technological manufacturing constraints and longitudinal strength requirements are satisfied, this makes it possible to reduce the amplitude of transverse vibrations of the beam.

Taking this into account, the geometric shape of the surface of a tie-beam with a circular cross-section and a constant inner diameter *d* can be described as a circular paraboloid, provided that the outer diameter of the section varies from the maximum value D_{max} at the junction with the side plate to the minimum value D_{min} in the plane coinciding with the axis of symmetry of the box, depending on the longitudinal coordinate according to a parabolic law

$$D(x) = 2 \cdot R(x) = 2 \cdot (a \cdot x^2 + b). \quad (1)$$

Considering the specified boundary conditions imposed on the shape of the generating curve of the tie-beam, the functional coefficients are determined by the following relationships:

$$\begin{cases} a = \dfrac{D_{\max} - D_{\min}}{0{,}5 \cdot L^2} \\ b = 0{,}5 \cdot D_{\min} \end{cases}, \quad (2)$$

where *L* – is the length of the tie-beam.

Fig. 2 shows the baseline profile of the tie-beam and the profile obtained according to the parabolic law of diameter variation.

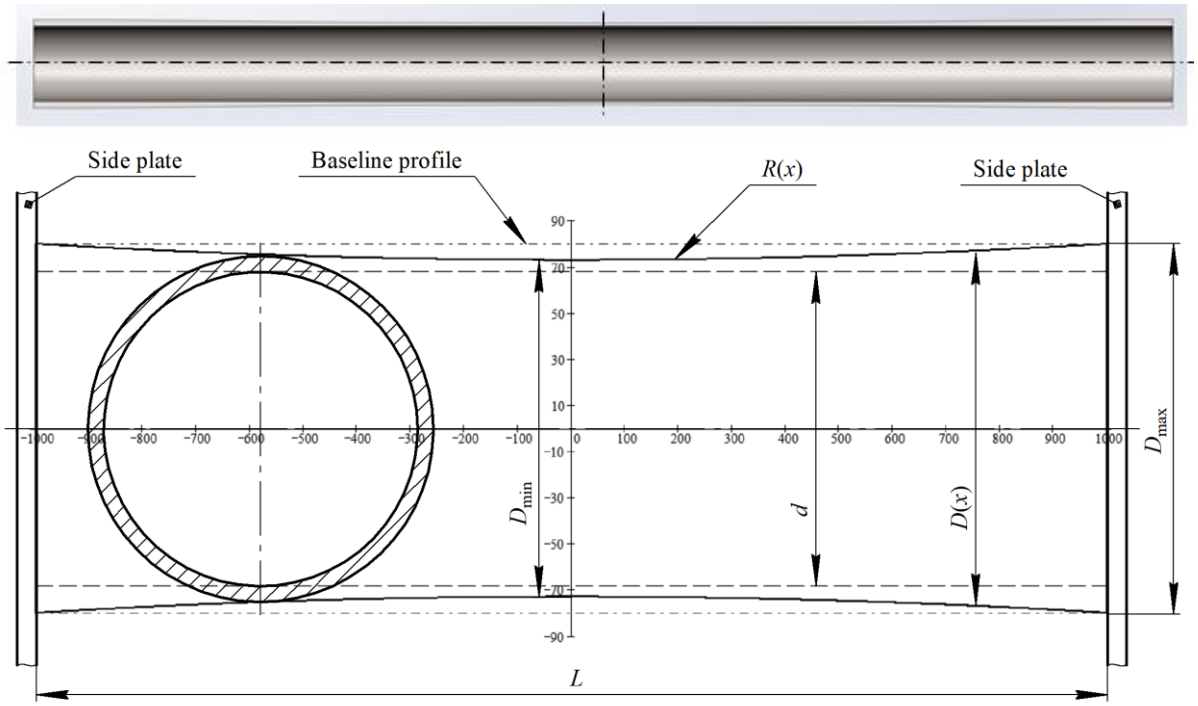

Figure 2 – Baseline profile of the tie-beam and the profile obtained according to the parabolic law of diameter variation (dimensions in mm).

Results of the Research and Their Discussion

To investigate the influence of static and dynamic loads on tie-beams with baseline and parabolic profiles, a series of comparative numerical experiments was carried out.

For each beam configuration, the following analyses were performed in the simulation environment:

axial compression until the stress corresponding to the yield strength of the material was reached at any point of the beam;

bending under transverse inertial loading (maximum transverse acceleration) with clamped ends until the yield strength of the material was reached;

determination of the first natural frequency of the beam with clamped ends;

determination of the critical compressive load corresponding to the buckling of the beam with clamped ends.

As a result of the numerical analysis, stress distribution maps were obtained (Fig. 3), while the corresponding quantitative characteristics are presented in Tab. 1.

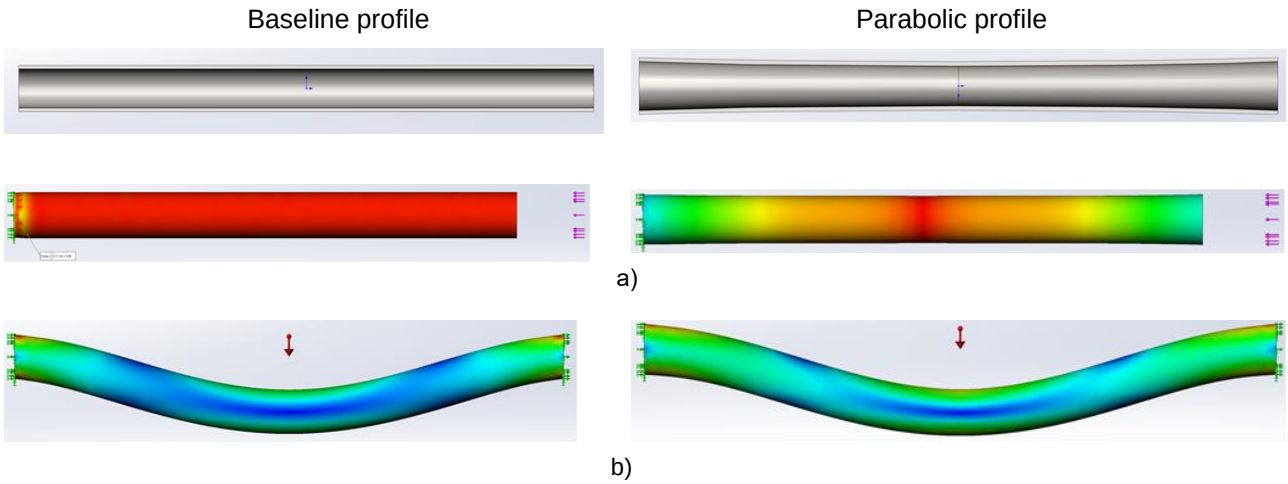

Figure 3 – Stress distribution maps: a – axial compression; b – bending at maximum acceleration.

Table 1 – Calculation results for tie-beams with different profiles.

Parameter	Profile		Deviation, %
	baseline	parabolic	
Axial compressive force at the yield limit, kN	1830	770	-58
Transverse acceleration at the yield limit, m/s²	4600	7110	+55
First natural frequency with clamped ends, Hz	218	258,06	+18
Resonant vibration amplitude, mm	0,17	0,226	+33
Critical buckling load for clamped supports, kN	1830	900	-51
Mass of the tie-beam, kg	88,16	52,39	-41

The stress distribution maps demonstrate a more uniform loading of the material in the tie-beam with a parabolic profile, reducing the extent of underloaded regions and increasing the vibration resistance of the structure. Such a distribution contributes to more efficient utilization of the material and improves the operational reliability of the structure.

The analysis of the calculated characteristics of tie-beams with different profiles shows that the tie-beam with a parabolic profile exhibits a significant mass reduction of 41% compared to the baseline design, which provides a potential reserve for reducing the overall mass of the working body. At the same time, the axial compressive force corresponding to the yield limit decreases by 58%, and the critical buckling load decreases by 51%.

The analysis of transverse dynamics indicates that the acceleration corresponding to the onset of yielding for the parabolic profile increases by 55%, while the first natural frequency of vibration increases by 18%. At the same time, the resonant vibration amplitude also increases by 33%.

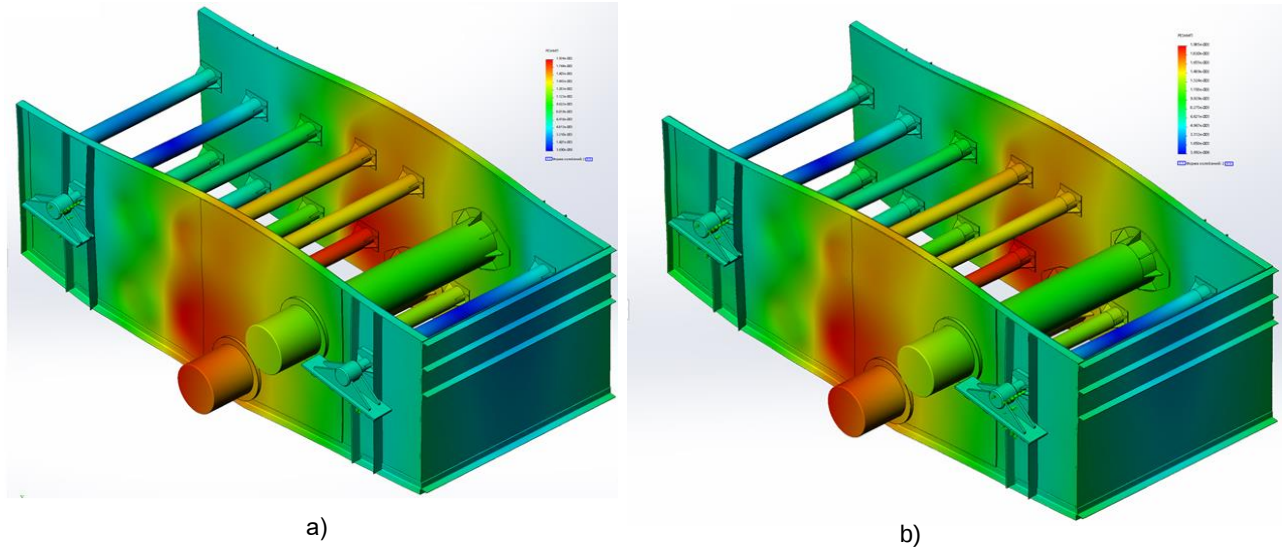

Figure 4 – Deformation distribution map of the screen box of the GST-62.MF vibratory screen:
a – baseline profile of tie-beams; b – parabolic profile of tie-beams.

In the real screen box structure, the boundary conditions of the tie-beams differ from those adopted in the simplified model. The elasticity of the side plates results in limited stiffness of the beam end restraints, while interaction with other beams through the side structural elements affects both the stress distribution and the dynamic characteristics of the system. This necessitates additional investigation of the frequency behavior of the tie-beams directly within the screen box structure.

Fig. 4 presents the deformation map of the screen box of the GST-62.MF vibratory screen.

The obtained results show that the first natural frequency of the screen box structure, compared with the baseline design, changes only slightly, increasing from 12.481 Hz to 12.662 Hz. The maximum resultant displacement amplitude of the box remains the same in both considered cases and equals $1.9 \cdot 10^{-2}$ mm. The configuration of the deformed state of the structure in both variants is practically identical. Analysis of the deformation distribution maps indicates that the character and spatial distribution pattern of the deformations for both screen box models are also essentially the same.

Conclusions

The conducted study has shown that tie-beams are important load-bearing elements of the screen boxes of vibratory machines and are subjected to significant cyclic loads. To improve their operational efficiency, the use of tubular beams with a variable outer diameter following a parabolic law while maintaining a constant inner diameter has been proposed. Such a geometry ensures a more rational distribution of material along the beam length in accordance with the distribution of bending moments.

The results of numerical modeling demonstrate that the use of a beam with a parabolic profile makes it possible to reduce its mass by 41%, while simultaneously increasing the allowable transverse acceleration and the first natural frequency of vibration. Analysis of the stress–strain state indicates a more uniform distribution of stresses within the beam material.It has been established that the use of such beams practically does not change the dynamic characteristics of the screen box of the vibratory machine. This confirms the feasibility of their application for reducing the structural mass and improving the energy efficiency and reliability of vibratory machines.

References

1. Zaselskyi, V. Y., Popolov, D. V., & Zaselskyi, I. V. (2018). Improving the reliability of agglomerate screens operating in the charge preparation lines of blast furnace shops. *Metallurgical and Mining Industry*, 7, 215–219.
2. Zaselskyi, V. Y., & Popolov, D. V. (2024). Identification of critical factors affecting energy consumption in the blast furnace production process. Theory and Practice of Metallurgy, (1), 13–20. https://doi.org/10.15802/tpm.1.2024.02
3. Fan, Z. (2021). Others. Low-carbon production of iron and steel: technology options, economic assessment, and policy. *Joule*. 5(4), 829–862. https://doi.org/10.1016/j.joule.2021.02.018
4. Patterson, S. R., Kozan, E., & Hyland, P. (2017). Energy efficient scheduling of open-pit coal mine trucks. *European journal of operational research*, 262(2), 759–770. https://doi.org/10.1016/j.ejor.2017.03.081
5. Uchytel, O. D. et al. (1998). Sorting of Mineral Raw Materials and Charge on Vibratory Screens: Monograph Porohy.
6. Ding, C. G. et al. (2011). The finite element analysis of vibrating screen. *Applied mechanics and materials*. 141, 134–138. https://doi.org/10.4028/www.scientific.net/amm.141.134
7. Li, C. L., He, F., Zhang, Y. Y., Gao, Y., & Gao, P. (2012). Failure Analysis and Structure Improvement of Beam of Liner Vibrating Screen. Advanced Materials Research, 619, 69–73. https://doi.org/10.4028/www.scientific.net/amr.619.69
8. Yan, F., Lu, H., & Xiao, L. (2024). Fatigue life prediction of cracked cross beam of mining linear vibrating screen under cyclic load. *Scientific reports*, 14(1). https://doi.org/10.1038/s41598-024-70671-5
9. Ou B., Yan J. (2015, 11–13 April). Experimental study of vibrating screen beam based on power flow method. *First international conference on information sciences, machinery, materials and energy*, Chongqing, China, Paris, France, 2015. https://doi.org/10.2991/icismme-15.2015.229
10. Long, H., Huang C.-Z., & Li D.-C. (2024). Dynamic analysis of beam structure of linear vibrating screen. *AIP advances*, 14(1). https://doi.org/10.1063/5.0182353
11. Yue-min Z. et al. (2009). Dynamic design theory and application of large vibrating screen. *Procedia earth and planetary science*, 1(1), 776–784. https://doi.org/10.1016/j.proeps.2009.09.123

Надіслано до редакції / Received: 12.01.2026
Прорецензовано / Peer-Reviewed: 24.02.2026
Прийнято до друку / Accepted: 16.03.2026
Опубліковано / Published: 30.03.2026

ISSN 3083-7219 (Print), ISSN 3083-7227 (Online)
Теорія і практика металургії, 2026, № 1
Theory and Practice of Metallurgy, 2026, No. 1

https://doi.org/10.15802/tpm.1.2026.05

UDC 621.774.38:669.245:536.2

***Medvedev M. I.*[1,*], *Bobukh O. S.*[2], *Kuzmina O. M.*[3], *Krasiuk A. D.*[4], *Ivanova L. K.*[5]**

Heat balance of billets during hot extrusion of nickel alloy pipes

[1] ORCID: 0000-0002-1230-420X. Ukrainian State University of Science and Technologies, Ukraine
[2] ORCID: 0000-0001-7254-3854. Ukrainian State University of Science and Technologies, Ukraine
[3] ORCID: 0000-0003-0794-0583. Ukrainian State University of Science and Technologies, Ukraine
[4] ORCID: 0009-0009-8354-687X. CENTRAVIS PRODUCTION UKRAINE PJSC Ukraine
[5] ORCID: 0000-0002-5997-610X. Ukrainian State University of Science and Technologies, Ukraine
*Email: medvedev4747@gmail.com

***Медведєв М. І.*[1], *Бобух О. С.*[2], *Кузьміна О. М.*[3], *Красюк А. В.*[4], *Іванова Л. Х.*[5]**

Тепловий баланс заготовок під час гарячої екструзії труб з нікелевого сплаву

[1] ORCID: 0000-0002-1230-420X. Український державний університет науки і технологій, Україна
[2] ORCID: 0000-0001-7254-3854. Український державний університет науки і технологій, Україна
[3] ORCID: 0000-0003-0794-0583. Український державний університет науки і технологій, Україна
[4] ORCID: 0009-0009-8354-687X. ПРАТ «СЕНТРАВІС ПРОДАКШН ЮКРЕЙН», Україна
[5] ORCID: 0000-0002-5997-610X. Український державний університет науки і технологій, Україна
*Email: medvedev4747@gmail.com

Abstract. *One of the main problems in the production of nickel-based alloy pipes by hot extrusion on horizontal hydraulic presses is the high level of surface defects. A key factor influencing defect formation is the temperature variation of the billet throughout the technological process. The aim of this work is to establish the regularities of temperature changes in nickel alloy pipe billets during the main stages of production on presses with forces of 16.0 MN and 31.5 MN using glass lubricants.* ***Methodology****. The study is based on a systematic analysis of the industrial process of hot extrusion of pipes from nickel alloy 602CA. The main stages considered include billet transportation, application of glass lubricant, transfer to the press, holding in the container, and extrusion. Temperature losses at each stage were determined using analytical and empirical equations based on thermographic measurements.* ***Results****. It was found that the total temperature drop of billets during auxiliary operations is inversely proportional to the wall thickness. Within the range of 40–120 mm and heating temperatures of 1050–1250 °C, this dependence is close to linear.* ***Scientific novelty****. A methodology for calculating billet temperature at the main stages of preparation for extrusion has been developed for the first time.* ***Practical utility.*** *The proposed approach enables a justified selection of glass lubricants according to actual temperature conditions, which improves the surface quality of pipes, reduces rejection rates, and decreases the amount of subsequent machining.*
Keywords. *hot extrusion, nickel-based alloys, pipe billets, heat balance, temperature field, cooling, glass lubricant, seamless pipes*

Анотація. *Однією з основних проблем при виробництві труб із нікелевих сплавів методом гарячого пресування на горизонтальних гідравлічних пресах є високий рівень поверхневих дефектів. Ключовим чинником їх утворення є зміна температури заготовки протягом усього технологічного процесу. Метою роботи є встановлення закономірностей зміни температури трубних заготовок із нікелевих сплавів на основних етапах виробництва труб на пресах із зусиллям 16,0 МН і 31,5 МН із використанням склозмазок.* ***Методика****. Дослідження базується на системному аналізі промислового процесу гарячого пресування труб зі сплаву 602CA. Розглянуто основні етапи: транспортування заготовки, нанесення склозмазки, подача до преса, витримка в контейнері та пресування. Поетапні втрати температури визначали з використанням аналітичних і емпіричних залежностей, отриманих за результатами термографування.* ***Результати****. Встановлено, що сумарне зниження температури заготовок під час допоміжних операцій обернено пропорційне товщині їх стінок. У діапазоні товщин 40–120 мм і температур нагріву 1050–1250 °C ця залежність є близькою до лінійної.* ***Наукова новизна.*** *Вперше розроблено методику розрахунку температури заготовок на основних етапах їх підготовки до процесу пресування.* ***Практична значущість****. Запропонований підхід дозволяє обґрунтовано обирати склозмазки з урахуванням реальних температурних умов процесу, що забезпечує підвищення якості поверхні труб, зниження рівня браку та скорочення обсягів подальшої механічної обробки.*
Ключові слова: *гаряче пресування, нікелеві сплави, трубні заготовки, тепловий баланс, температурне поле, охолодження, склозмазка, безшовні труби*

© Medvedev M. I., Bobukh O. S., Kuzmina O. M., Krasiuk A. D., Ivanova L. K., 2026
© Медведєв М. І., Бобух О. С., Кузьміна О. М., Красюк А. В., Іванова Л. Х., 2026

This is an Open Access article under the CC BY 4.0 license https://creativecommons.org/licenses/by/4.0/

Introduction. The rapid development of technology, the mining industry, and nuclear energy is inextricably linked to the use of pipes made of complex alloy steels and nickel- and iron-nickel-based alloys with enhanced operational properties (heat resistance, heat strength, fatigue strength, wear resistance, etc.) [1,2]. Today seamless pipes made of nickel alloys account for about 30% of the global market for such products.

In the cast state, billets from such alloys, according to the classification of the work [3], are classified as group B6. That is, in the cast state, these are extremely brittle alloys, the processing of which by pressure can be performed in one or two types only in the hot state, only under certain conditions - at an extremely low speed and a small degree of one-time deformation of the billet of limited dimensions and simple configuration.

This conclusion is confirmed by the results of many studies [4,5] and production practice of the product [6,7], from which it follows that with the improvement of technological and operational characteristics, high alloying of alloys contributes to an increase in their resistance to deformation and a decrease in technological plasticity. In turn, this contributes to a significant reduction in the temperature range of achieving maximum plasticity and high deformation heating [8,9], which leads to the impossibility of rolling these alloys. When producing pipes from such materials on roller pipe rolling plants, several technological problems arise, associated with the occurrence of violations of the continuity of the metal of the product [10,11].

Today, the only industrial method of manufacturing high-quality products from such alloys, in particular pipes, is the method of hot extrusion using glass lubricants. At the same time, for the successful implementation of the process of hot extruded pipes and minimizing the level of their defects, it is necessary to select the temperature of maximum plasticity of the deformed alloy and maintain the optimal temperature balance at all stages of its implementation [12, 13]. The temperature of maximum plasticity when extruded pipes with high accuracy for a number of nickel alloys can be selected according to the results of work [14, 15], which are shown in Fig. 1-3.

The alloys shown in Fig. 1-3 belong to the groups of nickel- and iron-nickel-based alloys according to GOST 5632-72 and standards DIN 2.4631, 2.4856, 2.4858; AISI/SAE N07080, N 06625, N06626 N08825.

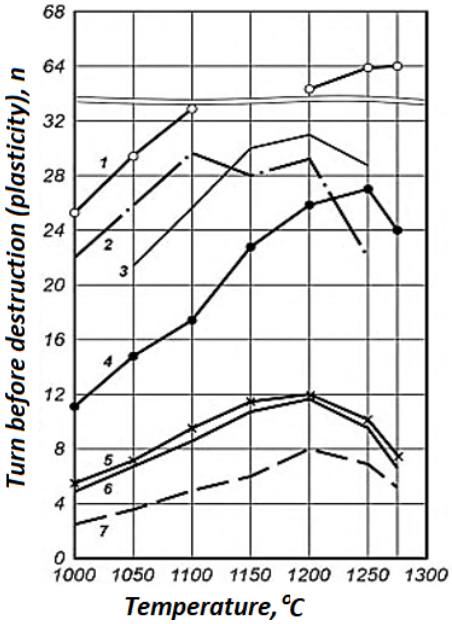

Figure 1 – Temperature ranges of maximum plasticity based on hot torsion test results for alloys: 1 – KhN78T (Ni–Cr alloy with Ti); 2 – KhN77TYuR; 3 – 12Kh18N10T (similar to AISI 321 / EN 1.4541); 4 – KhN70V; 5 – KhN70Yu; 6 – KhN60VT.

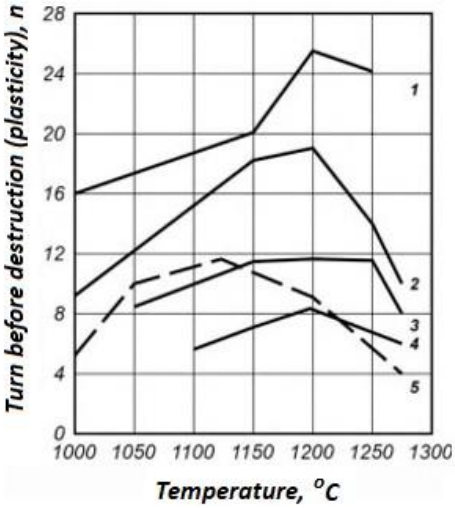

Figure 2 – Temperature ranges of maximum plasticity based on hot torsion test results for alloys: 1 – KhN45MKTYuB; 2 – 06Kh23N28MDT; 3 – KhN45MBTs; 4 – KhN40MDTYu; 5 – KhN55MBTs; 6 – 03Kh20N32M3B.

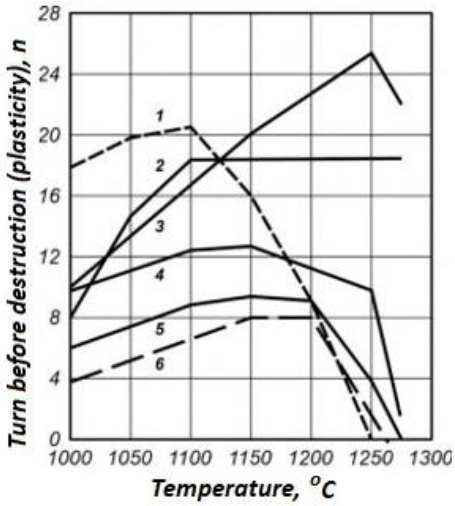

Figure 3 – Temperature ranges of maximum plasticity based on hot torsion test results for alloys: 1 – KhN45MKTYuB; 2 – 06Kh23N28MDT; 3 – KhN45MBTs; 4 – KhN40MDTYu; 5 – KhN55MBTs; 6 – 03Kh20N32M3B.

Solving the problem of frequent shortages of pipes made of such alloys in production is usually hindered by the lack of data on the magnitude and nature of the change in the temperature of the sleeves at the preparatory and transport stages of the deformation process on press installations. Such problematic issues arise on installations with presses with a force of 16.0 MN and 31.5 MN, for which there is currently no information on the rational choice of glass lubricants for the surfaces of the workpiece. The need for these data is explained by the fact that the glass lubricants currently available "work" well only in a limited temperature range (the temperature of heating the workpiece for extrusion), which is not constant at different stages of the technological process and places of their use, which, in particular, follows from the analysis of the data in Table 1 for glass lubricants "Pemco" [9].

Table 1 – Temperature conditions for Pemco glass lubricants.

Glass lubricant	Temperature of billet, °C	Use of glass lubricants in the technological process
VP68/1688	1060-1085	Rolling of billets and sleeves
VP68/1673	1135-1170	Rolling of billets and sleeves
VP68/1754	1100±20	Rolling of billets and sleeves
EG6800	1135-1170	Inside the sleeves, glass washers
EG6809	1085-1135	Inside the sleeves, glass washers (mix 6809 i 6800)
EG6826	1015-1085	Inside the sleeves, glass washers
VP68/2900	1080-1180	Into the cone of billet
	1080-1140	Inside the sleeves
EG6807	1080-1180	Into the cone of billet

As a result, unstable temperature conditions during the cooling of the billet at the stages of its preparation for pressing and the use of an irrationally selected glass lubricant for this purpose lead to defects in up to 80% or more of the pipes manufactured at the enterprises.

In this regard, work devoted to establishing the patterns of temperature change in nickel alloy pipe billets during the main stages of pipe production, which are manufactured by extrusion them on presses with a force of 16.0 MN and 31.5 MN, allowing the selection of a rational glass lubricant, is relevant.

State of the problem. Today, the only possible method of manufacturing pipes from hard-to-deform alloys, implemented in industrial conditions, is hot extrusion with glass lubricant, which is implemented according to the scheme of stress state of comprehensive uneven compression. This method allows for a sharp increase in the plasticity of the alloy, which makes it possible to apply large single-stage deformations of the material.

Currently, the hot extrusion method is the basis for installations with a horizontal hydraulic press, the working unit diagram of which is shown in Fig. 4.

Hot extrusion is mainly used to produce pipes from high-alloy steels and alloys; however, when the alloy lacks sufficient plasticity [6], defects appear on the pipe surfaces, the appearance of which is shown in Fig. 5.

An analysis of the quality of pipes manufactured in industrial conditions shows that the most common defects on the surface of pipes made from these alloys are transverse tears and cracks – typical defects on the outer and inner surfaces of pipes, which are localized breaks in the metal, oriented across the pipe axis along its entire perimeter and length. At the same time, the degree of development of these defects is greater on the inner surface than on the outer surface, which is due to the difference in deformation conditions [15].

Transverse tears and cracks are the result of reduced alloy plasticity due to its nature. To prevent this defect, the plasticity of the alloy is increased by:

- selecting and maintaining the temperature range of maximum plasticity, reducing its initial temperature for this purpose;
- limiting the degree of deformation; creating counterpressure in the matrix by performing an elongated or conical (with a small taper angle) calibrating belt in it or installing plastic shells on the surface of the workpiece.

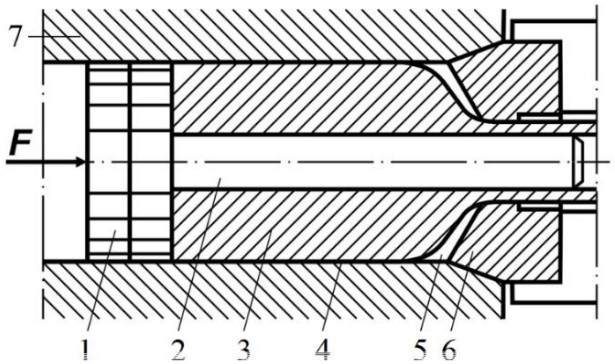

Figure 4. Diagram of the working unit of the installation with a horizontal hydraulic press: 1 – press washer; 2 – mandrel; 3 – sleeve; 4 – glass lubricant on the contact surface of the metal container; 5 – lubricating washer; 6 – die; 7 – container.

a b

Figure 5. Appearance of defects (breaches in integrity) on the inner surface of the pipe: a – longitudinal cracks; b – rough 'ripples'.

As a result, achieving a positive result in terms of improving the surface quality of pipes in these cases is accompanied by a sharp increase in labour intensity, time and financial costs of production.

Achieving high levels of performance characteristics of alloy 602CA after hot extrusion is only possible when it is deformed in a relatively 'narrow' temperature range (1080...1100 °C) [6]. Fulfilling this condition is crucial for ensuring the homogeneity of the alloy microstructure and preventing defects that could affect the performance characteristics of the products [9, 10]. In addition, maintaining the required temperature regime for hot extrusion minimizes the likelihood of surface defects such as cracks, porosity and local hardening, which improves the quality of the final product [11, 12].

Based on this, the rational temperature range for hot extrusion can be represented by the following inequality [16]:

$$T_{\min} \leq (T_0 \pm \Delta T) \leq T_{\max}, \quad (1)$$

where T_{min} is the minimum permissible temperature, which depends both on the load on the pipe extrusion equipment and on the susceptibility of the microstructure to dynamic recrystallisation, °C [13]; T_0 is the heating temperature in the heating device; ΔT is the resulting temperature change caused by both heat generation due to deformation (+) and heat loss during transportation of the sleeve from the heating device to the pipe press (-), °C; T_{max} – maximum sleeve temperature [14] at which grain boundaries in the alloy begin to melt, °C.

The known data on nickel alloy 602CA during its deformation, presented from the point of view of microstructural transformations [15], raise doubts about their reliability with regard to the value of ΔT in inequality (1). The development of finite element modelling of the extrusion process of nickel alloys is mainly focused on the deformation process from the moment the pipe begins to be pressed, which does not allow the value of ΔT in inequality (1) to be calculated [16,-18].

Currently, there is no method for calculating the temperature of the sleeve during the preparatory period of its extrusion on press installations with presses with a force of 16.0 MN and 31.5 MN. This circumstance does not allow determining rational thermotime parameters. That is, the solution to the problem of ensuring a consistently high quality of the surface of pressed pipes, while reducing labor, time and financial costs of production, is to maintain a rational temperature of the sleeves at all stages of their preparation for extrusion in order to select a rational glass lubricant for their surfaces.

One way to achieve this goal is a comprehensive analytical step-by-step solution to the problem, which is currently lacking in relation to the technology of extruded pipes on installations with presses with a force of 16.0 MN and 31.5 MN.

The aim of the work is to establish the patterns of temperature change in nickel alloy pipe billets at the main stages of pipe production, as well as how they are manufactured by extrusion them on presses with a force of 16.0 MN and 31.5 MN with glass lubricant.

Research methodology. The methodology included a systematic analysis of the existing technological process to produce hot-extruded pipes from nickel alloy 602CA on press units with horizontal hydraulic presses with a force of 16.0 MN and 31.5 MN. The main technological stages included:

1. transportation of the billet (sleeve) from the induction heater to the glass lubricant application table;
2. application of glass lubricant to the surface of the billet;
3. transporting the workpiece with glass lubricant to the press;
4. holding the workpiece in a container before pressing;
5. pressing in a container.

The duration of the above technological stages was determined by recording them with a stopwatch under real production conditions for hot-pressed pipes on the above-mentioned installations.

The chemical composition of the billets was determined using an Elvax plus spectrometer.

The thickness of the glass lubricant layer on the surface of the billet after completion of its expansion was determined after cooling the lubricant layer chips to room temperature using a vernier caliper with an accuracy of 0.01 mm.

The temperature of the outer surface of the billet was determined by thermography using chromel-alumel thermoelectrodes in combination with an electronic potentiometer.

The quality control of the manufactured pipes for compliance with regulatory and technical documentation was carried out visually.

For the analytical description of the process under consideration, both known and our own analytical and semi-empirical equations were used, which are given in [15].

Since the cooling of the billets in the technological chain under consideration occurs through heat transfer by thermal conductivity and radiation into an environment with a constant temperature, and the cooling time of the billets is relatively short, the heat transfer process does not have time to reach a steady state. In this regard, the change in the temperature of the workpiece during the preparatory stages of pressing can be calculated using the formula given in the work of Dzyuzer V. Ya. (2016):

$$m \cdot C_m \cdot \Delta T = A \cdot \bar{q} \cdot \tau \,, \qquad (2)$$

where m is the mass of the workpiece, kg; C_m is the specific heat capacity of the alloy, in J/(kg·K); ΔT is the change in the temperature of the workpiece, °C; A is the cooling area of the workpiece, m²; $\bar{q}$ is the average heat flux from the surfaces of the workpiece, W/m²; τ is the cooling time of the workpiece.

Transportation of the workpiece (sleeve) from the induction heater to the glass lubricant application table.

The temperature change at this stage during its duration τ_1 was calculated using the following converted equation:

$$\Delta T_1 = \frac{3{,}6 \cdot A \cdot \bar{q} \cdot \tau_1}{m \cdot C_m}. \qquad (3)$$

Analysis of equation (3) shows that the change in body temperature during cooling is directly proportional to the specific cooling surface area - A/m, which for a solid cylindrical body is inversely proportional to its radius. If cooling from the inner surface of a hollow cylinder can be neglected in this case, then to account for heat loss through its ends, the end radiation area (cross-sectional area of the cylinder opening) must be increased by 25%. In this case, equation (3) will look like this:

$$\Delta T_1 = \frac{7{,}2 \cdot k_G \, \bar{q} \cdot \tau}{C_m \cdot \gamma \cdot t}, \qquad (4)$$

$$k_G = \frac{1+0{,}625\frac{d}{D}\frac{d}{l}}{1+\frac{d}{D}},$$

where γ is the density of the alloy; t is the wall thickness of the billet D; d is the outer and inner diameters of the hollow billet, respectively; l is the length of the billet.

The average heat flux, which is the amount of heat released per unit of surface area per unit of time, and the heat transfer coefficient from the surface of the billet to the environment were calculated using the formulas of Gusovsky V.L. (2004):

$$\bar{q} = \alpha \cdot (T_0\text{-}20), \qquad (5)$$

$$\alpha = 145.1 \cdot \left(\frac{T_0}{1000}\right)^2. \qquad (6)$$

Based on the results of the measurements, it was established that the thickness of the glass lubricant layer on the billets is 0.1…0.2 mm. In this case, the heat transfer coefficient (α_{GL}) will be as follows:

$$\alpha_{GL} = \frac{1}{\frac{t_{GL}}{\lambda_{GL}} + \frac{1}{\alpha}}, \qquad (7)$$

where t_{GL} is the thickness of glass lubricant on the surface of the workpieces after processing, m; λ_{GL} is the specific thermal conductivity of glass lubricant, W/(m·K) (for calculations, λ_{GL}=930 W/(m·K) was assumed).

Equations (4)...(7) are applicable in the case of glass lubricant on the surface of the workpiece.

Application of glass paste to the surface of the workpiece.

The calculation of the temperature decrease (ΔT_2) during contact of the workpiece with cold glass paste with a density of 1500 kg/m³, specific heat capacity of 840 J/(kg K) and thickness of 0.5 mm was performed using the empirical equation:

$$T_2 = 0.24 \cdot \frac{T_0 - \Delta T_1}{t}. \qquad (8)$$

In equation (8), the value ΔT_1 is calculated using equation (4).

Transporting the billet with glass lubricant to the press.

At this stage, the temperature loss ΔT_3 was calculated using equation (4), considering the current thickness of the lubricant layer, calculated using equation (7).

Holding the billet in the container before pressing.

When the billet is placed in the container, air gaps are formed between the billet and the container, as well as the needle. In this case, the temperature loss ΔT_4 can be calculated using equation (4), considering the current thickness of the lubricant layer in equation (7), and representing equations (5) and (6) in the following form:

$$\bar{q} = \alpha \cdot (T_0 - \Delta T_1 - \Delta T_2 - \Delta T_3\text{-}400), \qquad (9)$$

$$\alpha = 203.5 \cdot \left(\frac{T_0 - \Delta T_1 - \Delta T_2 - \Delta T_3}{1000}\right)^{1.7}, \qquad (10)$$

where 400 is the container temperature, °C; 203.5 and 1.7 are empirical coefficients.

Pressing in a container.

During pressing, the air gaps between the outer surface of the workpiece and the inner sleeve of the container are filled with metal. Therefore, heat transfer from the workpiece to the container is carried out only by thermal conductivity through the glass lubricant layer. Assuming that under the action of normal contact stress during pressing, the thickness of the

glass lubricant layer will be 0.25 mm, the value of K_G in equation (4) can be calculated using the equation:

$$K_G = \frac{\lambda_{sm}}{l_{sm}} = \frac{0.93 \cdot 1000}{0,25} \approx 3720 \quad (11)$$

The mass of the container relative to the mass of the shells can be considered infinite, so the temperature of the container will not change significantly during pressing, which allows it to be taken as constant and equal to 400 °C. In this case, there will be a heat flow from the outer surface of the shells equal to:

$$q = K_G \cdot (T - 400) \quad (12)$$

To assess the effect of heat flow on the needle, we used the average calorimetric temperature of the system developed by A.I. Veynik (1975), which allows the heating and cooling of any bodies in the system to be considered independently of each other. In this case:

$$t_{kal} = \frac{T_g + w \cdot T_i}{1 + w} \quad (13)$$

where T_g is the weighted average temperature of the sleeve before pressing; w is a coefficient that takes into account the ratio of the masses and heat capacity coefficients of the sleeve and needle; T_i is the initial temperature of the needle, let's assume T_i = 400°C.

$$w = \frac{M_i \cdot C_{mg}}{M_g \cdot C_{my}}, \quad (14)$$

where M_g, M_i are the masses of the sleeve and needle, respectively; C_{mg}, C_{my} are the heat capacities of the sleeve and needle, respectively.

If we assume that $C_{mg}=C_{my}$, then

$$t_{\text{kal}} = T_g - \frac{d_i^2}{D_k^2} \cdot (T_g - 400). \quad (15)$$

The specific heat flux on the needle will be:

$$q_i = k \cdot (T_g - t_{\text{kal}}) = k \cdot \frac{d_i^2}{D_k^2} \cdot (T_g - 400). \quad (16)$$

Summing up the specific heat fluxes on the container and the needle, multiplying them by the cooling surface area and the time after the transformations, we obtain:

$$\Delta t = \frac{1.15 \cdot \tau}{S_p} \cdot (T_g - 400), \quad (17)$$

де τ – is the pressing time, s; S_p - is the wall thickness of the sleeve in the pressed state, mm.

For generally accepted clearances with the container and needle [9], the sleeve thickness is S_p=1.15 S. Then:

$$\Delta t = \frac{\tau}{S} \cdot (T_g - 400), \quad (18)$$

where T_g is the sleeve temperature, taking into account cooling during previous technological operations.

Research results.

The chemical composition of nickel alloy 602CA in the analyzed billets is given in Table 2.

Table 2 – Chemical composition of nickel alloy 602CA in billets.

Mass content of chemical elements, % (N and others)											
Cr	Fe	C	Mn	Si	Cu	Al	Ti	Y	Zr	P	S
25-26	9-10	0.20-0.23	0.10-0.12	0.4-0.5	0.05-0.10	2.0-2.2	0.10-0.15	≤0.05	≤0.05	≤0.01	≤0.01

According to the timing results, it was established that the duration of all stages of cooling the billet before the start of the pressing process is 30...37 seconds, in particular:

- the time of transporting the billet to the glass lubricant application table is 12...15 seconds;
- transportation of the billet coated with glass lubricant, 11...14 seconds;
- cooling in the container before pressing, 3...6 seconds;
- cooling during the pressing process, 1...2 seconds.

To estimate temperature losses at all stages of cooling, the average mass temperature of the sleeves was calculated. Changes in the specific heat capacity and thermal conductivity of nickel alloy 602CA in the temperature range of 1000... 1200 °C were assumed to be linear, which were within the range of 626...636 J/kg-K and 28.2...30.6 W/(m·K), respectively. For calculations, the specific density of 602CA alloys was assumed to be 8000 kg.

The results of calculations of the change in the temperature of the sleeves during cooling for 16.0 MN and 31.5 MN press installations are given in Table 3.

Analysis of the data in Table 3 shows that the total change in the temperature of the sleeves during their cooling while performing auxiliary technological operations on the press units at the same initial heating temperature is inversely proportional to the wall thickness of the sleeves. At the same time, this dependence in the range of accepted sleeve wall thicknesses is practically linear, as shown by the dependencies in Fig. 6.

The above dependencies make it possible to determine the values of temperature changes in billets (sleeves) with wall thicknesses of 40... 120 mm during their cooling at the stage of auxiliary technological operations on 16.0 MN and 31.5 MN press installations in the range of their initial temperatures 1050...1200 °C.

Table 3 – Change in the temperature of the sleeves during cooling on 16.0 MN and 31.5 MN presses.

T_0, °C	Stages of cooling the sleeves	Δt, °C						
		Wall thickness of the billet (t), mm						
		40	45	50	55	60	65	70
1200	1*	24.9	22.2	20.1	18.3	16.8	15.5	14.4
	2	7.1	6.0	5.4	4.9	4.3	4.2	3.9
	3	21.9	19.7	17.9	16.4	15.1	14.0	13.1
	4	6.0	5.4	4.9	4.5	4.2	3.9	3.6
	5	37.0	33.2	30.0	27.5	25.3	23.5	21.8
	ΣΔt	96.9	86.5	78.3	71.6	65.7	61.1	56.8
1150	1*	22.0	19.6	17.7	16.1	14.8	13.7	12.7
	2	6.2	6.0	5.4	4.9	4.3	4.2	3.9
	3	19.5	17.5	15.9	14.6	13.4	12.4	11.6
	4	5.3	4.8	4.4	4.0	3.7	3.4	3.2
	5	34.8	31.2	28.3	25.8	23.8	22.0	20.5
	ΣΔt	87.8	79.1	71.7	65.4	60.0	55.7	51.9
1100	1*	19.3	17.2	15.5	14.1	13.0	12.0	11.1
	2	6.5	5.8	5.2	4.7	4.3	4.0	3.7
	3	17.2	15.5	14.0	12.9	11.9	11.0	10.3
	4	4.7	4.2	3.8	3.5	3.2	3.0	2.8
	5	32.6	29.2	26.4	24.2	22.7	20.6	19.2
	ΣΔt	80.3	71.9	64.9	59.4	55.1	50.6	47.1
1050	1*	16.8	15.0	13.5	12.3	11.5	10.4	9.6
	2	6.2	5.5	5.0	4.5	4.2	3.8	3.6
	3	15.2	12.9	12.4	11.3	10.4	9.6	9.0
	4	4.0	3.6	3.3	3.0	2.8	2.6	2.4
	5	30.3	27.2	24.6	22.5	20.7	19.2	17.8
	ΣΔt	72.5	64.2	58.8	53.6	49.6	45.6	42.4

Note* 1 – transporting the billet (sleeve) from the induction heater to the glass lubricant application table; 2 – applying glass lubricant to the surface of the billet; 3 – transporting the billet with glass lubricant to the press; 4 – holding the billet in a container before pressing; 5 – pressing in the container.

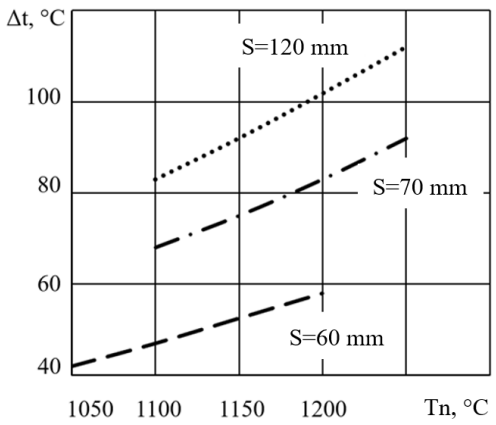

Figure 6. Dependence of the change in sleeve temperature Δt during cooling while performing auxiliary operations on the sleeve heating temperature Tn.

The obtained dependencies are recommended for use in the pipe extrusion shop to determine the rational values of the temperature-deformation parameters of extrusion from a heat-resistant nickel-based alloy 602CA. The use of these temperature-deformation parameters in the development and improvement of the technology for extruded pipes from heat-resistant nickel-based alloy 602CA in production conditions, based on the results of the work [19] made it possible to select glass lubricants with optimal viscosity in the range of 80-100 Pa s, thereby ensuring the production of pipes with high surface quality. Visual quality control of the pipes manufactured at the enterprise shows that out of 120 pipes manufactured using the results of calculations based on the proposed methodology, there were no pipes with surface defects. The quality of the outer and inner surfaces of the pipes is shown in Fig. 7.

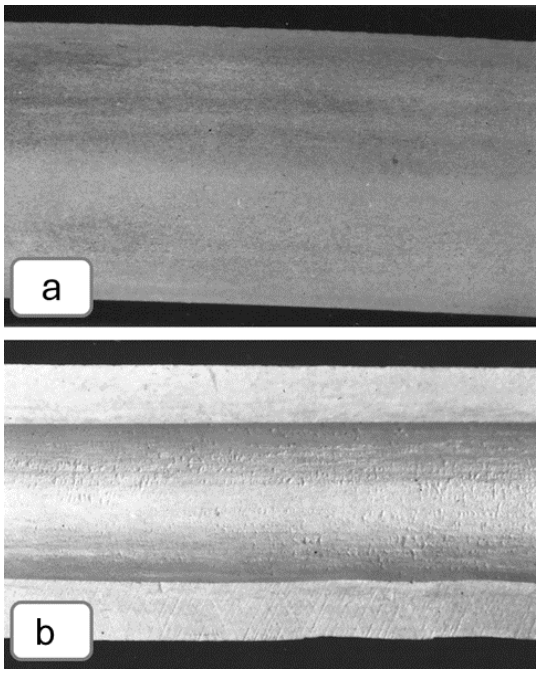

Figure 7. External and internal surfaces of extruded pipes: a) external, b) internal.

Conclusions

1. A method has been developed for calculating the temperatures of sleeves at different stages of their preparation for the extrusion process, the use of which allows the selection of a rational glass lubricant based on known dependencies of its viscosity on temperature.

2. The change in temperature of sleeves with the same initial temperature during auxiliary and transport operations is inversely proportional to the thickness of their walls.

3. For shells with wall thicknesses of 40...120 mm and initial temperatures of 1050...1250 °C, the decrease in temperature over the time spent on auxiliary and transport operations can be described by a linear relationship.

Acknowledgments. The research was conducted as part of the research project "Development of innovative technology for the production of heat-resistant pipes for the aviation industry of Ukraine" under the program "Scientific and scientific-technical activities of higher education institutions and scientific institutions" of the Ministry of Education and Science (Order of the Ministry of Education and Science No. 1572 of 27.12.2023).

References

1. Karimihaghighi, R., & Naghizadeh, M. (2023). Effect of alloying elements on aqueous corrosion of nickel-based alloys at high temperatures: A review. *Materials and Corrosion*. https://doi.org/10.1002/maco.202213705

2. Chyrkin, A., Sloof, W. G., Pillai, R., Galiullin, T., Grüner, D., Singheiser, L., & Quadakkers, W. J. (2015). Modelling csitional changes in nickel base alloy 602 CA during high temperature oxidation. *Materials at High Temperatures*, *32*(1-2), 102–112. https://doi.org/10.1179/0960340914z.00000000082

3. Kimstach, T. V., Uzlov, K. I., Repiakh, S. I., & Bilyi, O. P. (2025). Vyznachennia pryferentsiinoho sposobu vyhotovlennia vyrobiv z metaliv i splaviv. U Informatsiini tekhnolohii v metalurhii ta mashynobuduvanni. UDUNT. 56–60. https://doi.org/10.34185/1991-7848.itmm.2025.01.009

4. Wang, X., Liu, Z., Cheng, K., & Kong, Y. (2023). Chlorine-induced high-temperature corrosion characteristics of Ni-Cr alloy cladding layer and Ni-Cr-Mo alloy cladding layer. *Corrosion Science*, *216*, 111102. https://doi.org/10.1016/j.corsci.2023.111102

5. Schwing, R., Linn, S., Kontermann, C., Neubert, S., & Oechsner, M. (2021). Isothermal and anisothermal creep behavior of the nickel base Alloy 602 CA. *Materialwissenschaft und Werkstofftechnik*, *52*(2), 231–247. https://doi.org/10.1002/mawe.202000248

6. Qin, X., Huang, D., Yan, X., Zhang, X., Qi, M., & Yue, S. (2019). Hot deformation behaviors and optimization of processing parameters for Alloy 602 CA. *Journal of Alloys and Compounds*, *770*, 507–516. https://doi.org/10.1016/j.jallcom.2018.08.144

7. Karsten, E., Gerstein, G., Golovko, O., Dalinger, A., Lauhoff, C., Krooss, P., Niendorf, T., Samsonenko, A., & Maier, H. J. (2019). Tailoring the Microstructure in Polycrystalline Co–Ni–Ga High-Temperature Shape Memory Alloys by Hot Extrusion. *Shape Memory and Superelasticity*, *5*(1), 84–94. https://doi.org/10.1007/s40830-019-00208-7

8. Liu, Z., Deng, G., Wang, Z., Zhou, W., Yu, Y., & Zhou, J. (2023). Numerical simulation and experiment study on hot extrusion process of 18Ni (250) maraging steel large fan shaft for aero-engines. *The International Journal of Advanced Manufacturing Technology*. https://doi.org/10.1007/s00170-023-11301-8

9. Medvediev, M., Frolov, Ya., & Bobukh, O. (2023). *Presuvannia trub z nikelevykh i tytanovykh splaviv (pytannia teorii i tekhnolohii).* Zhurfond.

10**.** Lu, X., Díaz, A., Ma, J., Wang, D., He, J., Zhang, Z., & Johnsen, R. (2023). The effect of plastic deformation on hydrogen diffusion in nickel Alloy 625. *Scripta Materialia*, *226*, 115210. https://doi.org/10.1016/j.scriptamat.2022.115210

11. Amininejad, A., Jamaati, R., & Hosseinipour, S. J. (2021). Influence of Deformation and Post-Annealing Treatment on the Microstructure and Mechanical Properties of Austenitic Stainless Steel. *Transactions of the Indian Institute of Metals*. https://doi.org/10.1007/s12666-021-02277-8

12. Carrozza, A., Lorenzi, S., Carugo, F., Fest-Santini, S., Santini, M., Marchese, G., Barbieri, G., Cognini, F., Cabrini, M., & Pastore, T. (2023). A comparative analysis between material extrusion and other additive manufacturing techniques: Defects, microstructure and corrosion behavior in nickel alloy 625. *Materials & Design*, *225*, 111545. https://doi.org/10.1016/j.matdes.2022.111545

13. Mandal, M., Aashranth, B., Davinci, M. A., Samantaray, D., & Vasudevan, M. (2024). Mitigating manufacturing defects in seamless tubes: A failure analysis perspective. *Procedia Structural Integrity*, *60*, 510–516. https://doi.org/10.1016/j.prostr.2024.05.070

14. An, W., Liu, C.-z., Xiong, Q.-l., Li, Z., Huang, X., & Suo, T. (2023). Shear localization in polycrystalline metal at high-strain rates with dynamic recrystallization: Crystal plasticity modeling and texture effect. *International Journal of Plasticity*, *165*, 103616. https://doi.org/10.1016/j.ijplas.2023.103616

15. Medvedev, M. I., & Bobukh, O. S. (2024). Features of the technology of manufacturing pipes from heat-resistant steel and heat-resistant alloys. *Fundamental and applied problems of ferrous metallurgy*, 38, 415-430. https://doi.org/10.52150/2522-9117-2024-38-415-430

16. Medvediev, M. I., Bobukh, O. S., Boiarkin, V. V., Konovodov, D. V., Samsonenko A. A., (2022). Osoblyvosti hariachoho presuvannia trub z maloplastychnykh splaviv, lehovanykh nikelem. *Teoriia i praktyka metalurhii*, 6, 18-26. https://nmetau.edu.ua/file/zh_06_2022_vv2.pdf

17. Song, Y., Li, Y., Li, H., Zhao, G., Cai, Z., & Sun, M. (2022). Hot deformation and recrystallization behavior of a new nickel-base superalloy for ultra-supercritical applications. *Journal of Materials Research and Technology*. https://doi.org/10.1016/j.jmrt.2022.06.141

18. Jiang, H., Li, L., Dong, J., & Xie, X. (2018). Microstructure-based hot extrusion process control principles for nickel-base superalloy pipes. *Progress in Natural Science: Materials International*, *28*(3), 391–398. https://doi.org/10.1016/j.pnsc.2018.04.009

19. Medvedev, M., Shyfrin, Y., Frolov, Y., & Bobukh, O. (2022). Estimation of glass lubricant viscosity for hot extrusion of Cr-Ni steel and Ni alloy tubes. *Naukovyi Visnyk Natsionalnoho Hirnychoho Universytetu*, (1), 33–37. https://doi.org/10.33271/nvngu/2022-1/033

Надіслано до редакції / Received: 20.12.2025
Прорецензовано / Peer-Reviewed: 01.02.2026
Прийнято до друку / Accepted: 16.03.2026
Опубліковано / Published: 30.03.2026

ISSN 3083-7219 (Print), ISSN 3083-7227 (Online)
Теорія і практика металургії, 2026, № 1
Theory and Practice of Metallurgy, 2026, No. 1

https://doi.org/10.15802/tpm.1.2026.06

UDC 669.162.1.621.73.662.1/.5

Mishalkin A. P.[1]***, Ivashchenko V. P.***[2]***, Yaroshenko O. V.***[3]***,***
Petrenko V. O.[4,*]***, Chumak D. D.***[5]

Improvement of pig iron production technology by using the useful properties of the potential of secondary resources of raw materials and fuels

[1] ORCID: 0009-0002-7206-1809. Ukrainian State University of Science and Technologies, Ukraine
[2] ORCID: 0009-0007-3674-0181. Ukrainian State University of Science and Technologies, Ukraine
[3] ORCID: 0009-0002-6959-7725. Ukrainian State University of Science and Technologies, Ukraine
[4] ORCID: 0000-0001-5017-1674. Ukrainian State University of Science and Technologies, Ukraine
[5] ORCID: 0000-0001-7174-1824. Ukrainian State University of Science and Technologies, Ukraine
*Email: v.o.petrenko@ust.edu.ua

Мішалкін А. П. [1]***, Іващенко В. П.***[2]***, Ярошенко О. В.***[3]***,***
Петренко В. О.[4,*]***, Чумак Д. Д.*** [5]

Удосконалення технології виробництва чавуну шляхом використання корисних властивостей потенціалу вторинних ресурсів сировини та палива

[1] ORCID: 0009-0002-7206-1809. Український державний університет науки і технологій, Україна
[2] ORCID: 0009-0007-3674-0181. Український державний університет науки і технологій, Україна
[3] ORCID: 0009-0002-6959-7725. Український державний університет науки і технологій, Україна
[4] ORCID: 0000-0001-5017-1674. Український державний університет науки і технологій, Україна
[5] ORCID: 0000-0001-7174-1824. Український державний університет науки і технологій, Україна
*Email: v.o.petrenko@ust.edu.ua

Abstract. *The scientific and technical relevance of the study lies in determining the directions for improving the ways of using the useful properties of secondary resources in order to intensify the blast furnace process, increase its energy efficiency and reduce pollutant emissions. At the same time, economic efficiency is achieved by reducing the cost of purchasing primary raw materials and reducing waste generation, which corresponds to modern concepts of sustainable development on the way to "green" metallurgy.* ***Purpose of the study.*** *Scientific and practical substantiation of directions for improving the technology of pig iron production through the use of useful properties of secondary resources of raw materials and fuels that have a man-made origin. It is aimed at increasing the level of energy efficiency and improving the slag regime of the blast furnace process, reducing the man-made load on the environment of industrially developed regions of Ukraine. To achieve this goal, the following theoretical and practical tasks will be solved in the study: 1. The analysis of the current state of use of secondary resources of mineral raw materials and fuel in blast furnace production in the conditions of world and domestic metallurgical enterprises has been carried out; 2. The physicochemical properties of the most common types of secondary resources (man-made wastes of metallurgical origin: dust, sludge, scale, production of metallurgical lime: fractions from gas cleaning devices and heat treatment products of waste of plant origin, which are sources of pyrocarbon) have been investigated. Further - determination of the spectrum of their probable purpose, impact on the features and indicators of the blast furnace process, as well as justification of rational ways of their preparation and use; 3. Rational shares of substitution of traditional raw materials and fuels with secondary materials in the blast furnace process are substantiated, the use of which will not reduce the quality of pig iron and will not increase the specific consumption of coke. Their influence on physicochemical and heat-gas-dynamic processes, which is reflected in the characteristic zones of the blast furnace, has been studied; 4. The optimal technological schemes and recommendations for the methods of introduction and rational specific consumption of innovative materials based on man-made wastes have been determined, which will ensure the maximum level of use of their useful properties in the material and thermal balances of the blast furnace process; 5. The technological and environmental advantages of introducing into the blast furnace process a monomaterial, the composition, physicochemical features and spectrum of purpose of which are formed by heat treatment of a mixture of man-made industrial waste, are evaluat-*

© Mishalkin A. P., Ivashchenko V. P., Yaroshenko O. V., Petrenko V. O., Chumak D. D., 2026
© Мішалкін А. П., Іващенко В. П., Ярошенко О. В., Петренко В. О., Чумак Д. Д, 2026

This is an Open Access article under the CC BY 4.0 license https://creativecommons.org/licenses/by/4.0/

ed and their prospects as a substitute for the corresponding part of pulverized coal fuel (PCF) and fluxes are determined. ***Research methods.*** *When conducting a comprehensive study, the following methods will be used: analysis and generalization of materials of scientific and technical literature and patent sources, coordination of their results in accordance with modern trends and the best results of the practice of using secondary resources in blast furnace production; physicochemical methods of analysis chemical, thermogravimetric, to determine the composition, structure, metallurgical value, probable spectrum of purpose and reactivity of secondary resources of materials - substitutes for iron ore raw materials, coke and pulverized coal fuel (PCF); thermodynamic forecasting and kinetic modeling of the behavior of experimental materials of secondary origin under the conditions of their heat treatment to assess the influence of their properties on the course of physical and chemical processes and transformations to the thermal and gas-dynamic regime of the blast furnace. The expected results of the study should also include: development of scientifically grounded recommendations for the effective use of useful properties of the initial potentials of secondary resources of raw materials and fuel in blast furnace production; establishment of quantitative ratios regarding rational levels of substitution of traditional fuel and raw materials with secondary ones, without reducing the productivity of the furnace and the quality of pig iron while reducing the specific consumption of lime and PCF; development of a method for the implementation of a complex technological scheme for the preparation, heat treatment of experimental mixtures based on components of mineral raw materials and fuel, followed by the use of an innovative product in the conditions of blast furnace production of pig iron.* ***Scientific novelty of the work.*** *For the first time, systematically, on the basis of the results of an analytical and practical study, the energy efficiency of production and use in the blast furnace process of a two-component monomaterial based on dispersed waste from the production of lime and materials – waste of plant origin, obtained by implementing the effect of their pyrolysis under conditions of joint heat treatment of the initial mixture layer, was substantiated, tested on high-temperature models, poured thermal, in an inclined rotary drum-type furnace. For the first time, a resource-efficient and results-efficient approach has been used to assess the efficiency of the use of materials based on secondary resources of metallurgical and plant origin, based on an integrated combination of the results of thermodynamic forecasting, physical modeling and taking into account the provisions of the exergical methodology for assessing the energy efficiency of the objects of study. Methodological bases have been developed for the selection of rational schemes for the introduction of complex materials based on secondary materials into the blast furnace charge and in the air blast flow to stabilize gas-dynamic conditions in the charge layer, intensify recovery processes with a decrease in the specific consumption of coke per ton of liquid pig iron. The regularities of the influence of the composition and dispersion of secondary resources on the gas-dynamic and thermal parameters of blast furnace smelting have been revealed, which makes it possible to increase the accuracy of predicting the furnace course. It has been proved that the use of materials based on secondary resources of mineral raw materials and fuels can provide the effects of increasing the energy efficiency of pig iron production and reducing the environmental burden, which meets the requirements of sustainable development and the concept of "green metallurgy".*
Keywords: *pig iron, secondary materials, rational schemes, metallurgical lime, fuel, injection, pulverized coal, natural gas.*

Анотація. *Науково-технічна актуальність дослідження полягає у визначенні напрямів удосконалення способів використання корисних властивостей вторинних ресурсів з метою інтенсифікації доменного процесу, підвищення його енергоефективності та зниження викидів забруднювальних речовин. Водночас економічна ефективність досягається за рахунок зменшення витрат на закупівлю первинної сировини та скорочення обсягів утворення відходів, що відповідає сучасним концепціям сталого розвитку на шляху до «зеленої» металургії.* ***Мета дослідження.*** *Науково - практичне обґрунтування напрямків удосконалення технології виробництва чавуну шляхом застосування корисних властивостей вторинних ресурсів сировини та палива, які мають техногенне походження. Спрямована на підвищення рівню енергоефективності та поліпшення шлакового режиму доменного процесу, зниження техногенного навантаження на довкілля промислово розвинутих регіонів України. Для досягнення поставленої мети в дослідженні будуть вирішені наступні теоретико-практичні завдання: 1. Провести аналіз сучасного стану використання вторинних ресурсів мінеральної сировини та палива в доменному виробництві в умовах світових та вітчизняних металургійних підприємств. 2. Дослідити фізико-хімічні властивості найбільш поширених видів вторинних ресурсів (техногенних відходів металургійного походження: пилу, шламів, окалини, виробництва металургійного вапна: дріб'язок з апаратів газоочищення та продуктів теплової обробки відходів рослинного походження, що є джерелами піровуглецю). В подальшому – визначення спектру їх вірогідного призначення, впливу на особливості та показники доменного процесу, а також, обґрунтування раціональних способів їх підготовки та використання. 3. Обґрунтовати раціональні частки заміщення в доменному процесі традиційної сировини та палива вторинними матеріалами, використання яких не знизить якість чавуну та не підвищить питому витрату коксу. Досліджено їх вплив на фізико-хімічні та тепло-газодинамічні процеси, що відбивається в характерних зонах доменної печі. 4. Визначено оптимальні технологічні схеми та рекомендації щодо способів введення та раціональних питомих витрат інноваційних матеріалів на основі техногенних відходів що забезпечать максимальний рівень використання їх корисних властивостей в матеріальному та тепловому балансах доменного процесу. 5. Оцінити технологічні та екологічні переваги від впровадження в доменний процес мономатеріалу, склад, фізико-хімічні особливості та спектр призначення якого формуються шляхом термічної обробки суміші техногенних промислових відходів та визначено їх перспективність як замінника відповідної частини пиловугільного палива (ПВП) та флюсів.* ***Методи дослідження.*** *При проведенні комплексного дослідження будуть застосовані наступні методи: аналіз та узагальнення матеріалів науково-технічної літератури та патентних джерел, узгодження їх результатів у відповідності до сучасних тенденцій та кращих результатів практики використання вторинних ресурсів у доменному виробництві; фізико-хімічні методи аналізу - хімічний, термогравіметричний для визначення складу, структури, металургійної цінності, вірогідного спектру призначення та реакційної здатності вторинних ресурсів матеріалів – замінників залізорудної сировини, коксу та пиловугільного палива (ПВП); термодинамічне прогнозування і кінетичне моделювання особливостей поведінки дослідних матеріалів вторинного походження в умовах їх термічної обробки для оцінювання впливу їх властивостей на перебіг фізико-хімічних процесів і перетворень на тепловий та газодинамічний режим доменної печі. До очікуваних результатів виконання дослідження доцільно віднести, також: розробку науково обґрунтованих рекомендацій щодо ефективного використання в доменному виробництві корисних властивостей вихідних потенціалів вторинних ресурсів сировини та палива; встановлення кількісних співвідношень щодо раціональних рівнів заміщення традиційних матеріалів палива та сировини вторинними, без зниження продуктивності печі та якості чавуну при зменшені питомих витрат вапна та ПВП; розроблення способу впровадження комплексної технологіч-*

ної схеми підготовки, термічної обробки дослідних сумішей на основі компонентів мінеральної сировини та палива з наступним використанням інноваційного продукту умовах доменного виробництва чавуну. ***Наукова новизна роботи.*** *Вперше, системно, на основі результатів аналітико – практичного дослідження обґрунтовано, апробовано на високотемпературних моделях, в умовах наближених до реальних та підтверджено енергетично-сировинна ефективність виробництва та використання в доменному процесі двокомпонентного мономатеріалу на основі дисперсних відходів виробництва вапна та матеріалів – відходів рослинного походження, що отримується шляхом реалізації ефекту їх піролізу в умовах сумісної термічної обробки шару вихідної суміші, що пересипається термічної, в похилій обертовій печі барабанного типу. Використано вперше раціональний за витратою ресурсів та ефективний за результатами підхід для оцінювання ефективності застосування матеріалів на основі вторинних ресурсів металургійного та рослинного походження, що базується на інтегрованому поєднанні результатів термодинамічного прогнозу, фізичного моделювання та з урахуванням положень ексергійної методології оцінки енергоефективності об'єктів дослідження. Розроблено методичні основи для вибору раціональних схем введення комплексних матеріалів на основі вторинних матеріалів у доменну шихту та в потоці повітряного дуття для стабілізації газодинамічних умов в шарі шихти, інтенсифікації процесів відновлення при зниженні питомої витрати коксу на тонну рідкого чавуну. Виявлено закономірності впливу складу та дисперсності вторинних ресурсів на газодинамічні та теплові параметри доменної плавки, що дозволяє підвищити точність прогнозування ходу печі. Доведено, що застосування матеріалів на основі вторинних ресурсів мінеральної сировини та палива здатне забезпечити ефекти підвищення енергоефективності виробництва чавуну та зниження екологічного навантаження на довкілля, що відповідає вимогам сталого розвитку та концепції «зеленої металургії».*
Ключові слова: *чавун, вторинні матеріали, раціональні схеми, чорне вапно, паливо, вдування, пиловугільне паливо, природний газ.*

Introduction. The modern development of the metallurgical industry is characterized by increased requirements for the efficiency of the use of raw materials and fuel and energy resources, as well as for the environmental safety of production. One of the most energy-intensive processes is the production of pig iron in blast furnaces, which requires the consumption of significant volumes of natural raw materials and coke. Reducing the negative impact on the environment leads to the search for new ways of development and innovative solutions to improve the technology of the domain process.

One of its promising directions is the complex and rational use of the properties of the potential of secondary resources of raw materials and fuels. Such resources include metallurgical waste (sinter and blast furnace dust, sludge, scale), carbon-containing waste from coke oven and coal production, dispersed waste from limestone preparation and lime production, as well as alternative reducing agents and energy materials. Their rational use allows not only to partially replace traditional types of raw materials and fuel, but also to increase the complexity of the use of mineral and fuel and energy resources on the scale of the enterprise.

Thus, improving the technology of pig iron production through the use of secondary resources of raw materials and fuel is an important task for both scientists and industrial enterprises, because it combines economic feasibility, environmental responsibility and technological progress.

Keywords: cast iron, secondary materials, rational schemes, black lime, fuel, injection, pulverized coal fuel, natural gas.

Analysis of the results of the influence of external factors on the physical and chemical features of processes in the characteristic zones of the furnace and the main indicators of the blast furnace process. Establishing the influence of component and chemical composition, granulometry and ratio of components of the initial charge on physical and chemical processes in the characteristic zones of the furnace; determination of the rational composition of blast, specific costs and rational ratio of PCF and natural gas (NG) in it, as factors affecting the stability of the blast furnace operation, are relevant areas of research aimed at improving the technology of iron smelting.

The energy efficiency of pig iron production, in the context of changes in the ratio of PCF and NG costs as components of the fuel and recovery potential of the process, is influenced by the consistency between the theoretical basis and the results of practical verification of its main provisions: the rationality of the costs of the components of the initial potential and the efficiency of the results of the actual use of their useful properties.

Changes in the conditions of heat and gas-dynamic processes, which is reflected in the increase in thermal loads on the air lances and the shaft, on their service life, the stability of the gas-dynamic melting mode, the evenness of the furnace and its technical and economic indicators, caused the need to adjust the physical properties of the charge. The latter affect the indicators of the slag regime, which requires, in turn, neutralization of the negative impact of PCF ash, namely, its chemical composition on the course of blast furnace smelting.

Therefore, in the conditions of blowing PCF into the blast furnace, ensuring cost-efficient production of mineral raw materials and energy is an urgent task. Its solution requires research aimed at determining the patterns and methods of controlling processes in the blast furnace furnace, which are characterized by a high level of uncertainty. Thus, according to the results of the study [1], when using the PCF injection technology, the volume of gases emitted during the combustion of its combustible components differs from similar conditions during the combustion of GHG by more than 150 times, and the density of PCF in the transport system before their introduction into the furnace in air blast jets can vary by 2 or more times. In

the conditions of injection of pulverized coal fuel, it is obvious that it is becoming relevant to continue research aimed at:

1. To determine, for the conditions of variability of physical characteristics and chemical composition of the components of the blast furnace charge, the most rational ratios in the blast of PCF and NG. At the same time, it is necessary to take into account the change in gas-dynamic conditions in the blast furnace column and compare the contributions of thermal effects from their combustion to the energy balance of the smelting.

2. Study of the influence of dispersion, moisture and chemical composition of PCF on combustion processes and features of the formation of reducing gases (CO, H_2) in the mure zone.

3. Clarification of the gas dynamics of the blast furnace in case of changes in the volume of PCF injection, the ratio of PCF and NG, including the distribution of temperatures and concentrations of reducing gases in different areas of the mine.

4. Study of the conditions for the formation and ensuring the stability of the interaction of hot blast with PCF, NG, coke and their carbon-containing substitutes of plant origin with the prediction of the rational level of oxygen enrichment of the blast and the heating temperature.

5. Clarification of the influence of PCF on the formation, composition and properties of blast furnace slag and pig iron, especially on the results of its desulfurization.

6. Reduction of specific energy consumption and CO_2 emissions by replacing part of the coke with pulverized coal fuel without reducing the level of useful use of the properties of gases: their reducing capacity and physical heat of gaseous iron reduction products.

7. Development of complex physical and chemical models of the thermal and material balance of the blast furnace, taking into account the injection of PCF and its alternative substitutes, to predict changes in the quality, efficiency and cost of pig iron.

As a logical conclusion of the stages of research aimed at improving the domain process, a concise structured scheme has been developed in the format of a scientific and technical task, the use of the components of which determines the expected effects of the implementation of the main areas of research (Table 1).

Table 1 - Structured scheme in the format "main areas of research - expected technical and economic effects.

No.	Research areas	Expected effect
1	Optimization of the coke-PCF ratio in the domain process.	Reducing coke consumption, saving fuel, reducing the cost of pig iron.
2	Study of the thermal balance of the blast furnace during the introduction of PCF in the air blast flow.	Stabilization of the temperature regime, increasing the thermal efficiency of the process.
3	Determination of gas-dynamic conditions in the characteristic zones of the furnace (gas flow distribution, pressure, gas permeability of the charge, etc.).	Rational in terms of costs and efficient in terms of the results of using the components of the energy potential of gases (CO, H2): their chemical and physical heat as a condition for increasing the productivity of the process.
4	Analysis of the influence of chemical composition and granulometry of the components of the base charge (iron ore components and fuel).	Improving the gas permeability of the base charge layer, reducing energy costs for its purging, reducing the level of dust removal.
5	Improvement of the technology of preparation and supply of PCF (drying, grinding, dosing, introduction of oxygen into the blast.	Improving the gas permeability of the base charge layer, reducing energy costs for its purging, reducing the level of dust removal.
6	Comprehensive environmental assessment of the level of CO_2, SO_x, NO_x emissions with/without the use of PCF and its replacement with pyrolyzed biomass.	Reduction of harmful emissions, increase of environmental safety of production.

In our opinion, the consequences of the use of secondary iron-containing materials and pyrolyzed biomass (pyro-biocarbon – hereinafter referred to as PBC) in the blast furnace process should be considered to establish their impact on the process, by implementing the following step-by-step research algorithm: improving the technology using these materials → determining specific technical requirements for their granulometry, physical properties, chemical composition → establishing particles and their rational ratio. The introduction of which will not increase/decrease the specific consumption of coke, will not worsen the gas permeability of the charge, the quality of pig iron and will not reduce the productivity of the blast furnace.

According to the scheme of the previously developed algorithm, we will focus on the analysis of the probable consequences of the use of secondary iron-containing resources, pyrolyzed biomass and materials obtained by joint heat treatment of components of their mineral base and waste of plant origin containing carbon.

1. Impact on the consumption of reducing agent (coke). Partial replacement of a certain proportion of PCF and PBC coke injected into the furnace in the blast stream by implementing PCI-like technology can reduce coke consumption. In this case, the real replacement factor depends on the origin of the material containing carbon, its composition and, especially, on the method of production, during the implementation of which the physical and chemical properties and functional spectrum of the purpose of the substitute

material are formed. And a change in gas composition, which provides a change in the growth of the value of the H_2/CO indicator, can, in turn, cause a change in the intensity and features of the reduction of the components of iron ore components of the blast furnace charge.

Regarding the question of the essence and expediency of using the terms "biochar" and "pyrucarbon". It refers precisely to the terminological distinction in modern thermochemical technology of carbon materials.

Pyrolysis is the thermal decomposition of organic raw materials without access or with limited access to oxygen (αO2 < 1). That is, regardless of the temperature or type of furnace, this process is the basis of both biochar and pyrocarbon.

Biochar is a solid product formed by the pyrolysis of biomass, usually at low or medium temperatures (300÷700 °C) [2]. The main characteristics of its production process include the following:

- preserves the structure of the initial biomass (porosity, carbon matrix);
- has a high content of fixed carbon (60÷90%), but still contains volatile substances;
- it is used in metallurgical processes, in particular as a substitute for coke or anthracite, as well as energy as a fuel, ecology as a sorbent, CO_2 absorber;
- in the future, the beneficial properties of carbon can significantly expand the range of its functional purpose in combination with other elements.

As for pyrocarbon, according to [3], it is more temperature-forming, which is formed during deeper pyrolysis or carbonization, when volatile components are almost completely removed. Its important properties include: almost pure amorphous or graphite-like carbon; high electrical and thermal resistance; lower reactivity than biochar; used in composites, anodes, electrodes, metallurgical processes as a reactionally stable material. reducing agent. The temperature range for obtaining pyrucarbon according to the data [3] is 800 -1300°C, the coefficient of excess oxygen ensures the production of volatile content ≤5 % in it, and together these parameters provide a compact, graphite-like structure of carbon and complete carbonization.

Based on the analysis of the features of the relevant technologies, the temperature criterion and their other differences, Table 2 was created, the data of which allow determining the limit in this issue

Table 2 – Characteristic features and parameters of biochar and pyro-biocarbon production processes.

No.	Parameter	Biochar	Pyro-biocarbon
1	Pyrolysis temperature	300÷700°C	At 300 ÷ 450°C - low-, and in the range of 800÷1200°C - high-temperature biomass pyrolysis
2	Degree of carbonation	Partial	Partial/full
3	Volatile content, %	10÷40	min - ≤5, max ~40
4	Structure	Porous, organic	Compact, porous/graphite
5	Application	Sorbent, energy (fuel/reducing agent)	Reducing Agent/Fuel, Synthetic Materials for Metallurgy
7	Process atmosphere	α_{o2}= 0,7÷0,9 (insufficient oxygen supply)	α_{o2} = 0,3 ÷0,85- regulated by the type, conditions of the thermal unit and factors of external influence on them

In the studies, the results of which are given in [4], a two-level technological scheme for the production of metallurgical materials - slag-forming materials for the purpose of production has been developed: protection against secondary oxidation and cooling of steel, protective for the crystallizer of continuous caster and ladle, refining, deoxidation, as well as the production of an effective reducing agent. The use of experimental batches of materials, products of compatible pyrolysis of the initial mixture of components, in industrial conditions confirmed their effectiveness.

The characteristic features that determine the advantages of the technology of combined heat treatment of mixtures based on materials - waste of plant origin as a source of pyrocarbon, and their mineral part, the properties of the components of which form the composition, physical properties and spectrum of their purpose, include the following:

- technological flexibility and peculiarities of the behavior of the initial mixture in the conditions of an inclined rotary furnace ensure the production of pyrolyzed materials with a content of 5÷ 95% pyrocarbon in them by its heat treatment; up to 40% of pyrogases (CO, CH4, H2);
- parameters that are regulators of heat treatment conditions, namely the coefficient of excess oxygen (αO2), the temperature of the furnace working space, the speed of rotation of the furnace, the angle of its inclination, the specific consumption of charge, fuel and cooling conditions ensure the receipt of materials of the expected quality and the required purpose.
- the use of the secondary energy potential of pyrolysis products (their physical and chemical components) provided a reduction in the specific consumption of fuel (natural gas) by 50-75%, depending on the ratio in the initial charge of waste materials of plant origin (lignin) and components that form the mineral base of the product, usually from several oxides.

Therefore, in the future, in the study, pyrocarbon obtained under the conditions of a rotary inclined furnace, by implementing the technology created by DMetI scientists, will be defined as pyro-biocarbon.

Regarding the effect on the gas permeability of the charge layer [5].

In blast furnace production, gas permeability (permeability [5]) is often expressed in conventional

units according to empirical dependencies of the type: $K=a(d_p)^2/f$, where: dp is the average diameter of the charge particles; f is the resistance factor (depends on the shape of the grains, humidity and their bulk density); a is the proportionality factor. The value of the permeability coefficient depends on the particle size distribution (small fractions reduce permeability; increased moisture reduces gas permeability;— particles that are heterogeneous in geometry cause "channel formation"; embankment pressure - when compacted, the pores are compressed; The position of the melting zone of the melting zone of small particles sharply impairs the permeability. As for the practical significance of the coefficient: high permeability contributes to the stable movement of gases (CO, CO_2, H2, H2O), uniform reduction of $Fe_2O_3 \rightarrow Fe$. Low - leads to the formation of "hanging" zones, an increase in pressure, overconsumption of coke and can cause disruption of the furnace. Therefore, ensuring optimal permeability is an important task in the formation of charge, granulation of agglomerate, preparation of pellets and coke and its substitutes (PCF, NG, PBC).

The introduction of a large number of finely dispersed PCF fractions (<5–10 mm) according to data from [5] leads to clogging of the pore space: the gas permeability of the layer decreases, the pressure drop increases, and local zones of "suffocation" of the gas flow appear. The identified negative effects will lead to an increase in specific fuel consumption and instability of recovery coefficients. Therefore, a prerequisite before feeding into the furnace is the operation of agglomeration / handling of substitute materials, which form a secondary reserve resource base of raw materials and fuel [6]. They, for the most part, are dispersed materials that have, for the most part, a man-made origin

3. To get a more complete picture of the likely consequences of the use of secondary resources, it is necessary to determine their impact on the behavior of the sintering zone. Their introduction into the charge will change its physical properties (temperature interval that determines the softening and melting temperatures, thickness of softening and melting zones in the characteristic zones of the blast furnace

4. Chemical risks. Secondary materials often contain an increased content of S, P, Cl, $R_{,2O}$, Zn, which, accordingly, increases the content of harmful impurities and their negative impact on the quality of the metal (S and P); leads to the accumulation of R2O in the slag/gas circuit, refractory furnace lining. and their substitutes. The total content of R2O (Na_2O+K_2O) should be, according to [7], limited to 2–3 kg/t of pig iron, depending on the characteristics of the blast furnace.

5. Effects of mechanical and physical origin. If secondary materials have low strength, they are able to form large amounts of fines and dust during the transportation of bulk materials, which makes it difficult to evenly distribute materials on the blast furnace when they are loaded. In the study [6], it was found that pelletized (pellets), pre-sintered (agglomerate) or cold-bonded briquettes, which have additionally passed the stage of stabilization of their properties, work much better under the conditions of the blast furnace process.

Thus, taking into account the consequences of the possible impact of the use of secondary materials in the form of the above effects and the occurrence of risks for the stability of the process, we can state the following. The creation and implementation of an algorithm for improved blast furnace smelting technology with their use is a step-by-step process, the successful implementation of which requires control of external risks, the source of which is the physical and chemical properties of substitute materials. It is advisable to define the scheme of its implementation using an integrated approach as: (A) preparation of secondary raw materials → (B) laboratory experiments/pilot tests → (C) phased introduction of experimental materials in a real furnace with constant monitoring and control of the main indicators of the process → (D) correction of technology parameters / specific consumption of coke, fluxes, etc., which will be determined by the test results as important.

Regarding specific technical requirements and recommendations regarding the "safety" of boundaries and quantitative ranges of parameters of secondary substitute materials. On the basis of the generalized and agreed upon the results of theoretical studies and the results of industrial practice adaptation of substitute materials to the conditions of blast furnace smelting (specific furnaces, technologies, coke consumption, agglomeration properties of iron ore components of secondary origin), the authors [7] define the following requirements-recommendations as important.

Granulometry of substitute materials for iron ore components:

- the target size of pellets/agglomerate is Ø 8÷16 mm with a probable optimum of 9÷13 mm) for pellets [8];
- the content of fractions <5÷10 mm should be ≤ 2–5 wt% of the total mass of iron ore materials. For "risky" stoves - aim for ≤2%. Fractions <1–3 mm should be minimized at the stages of control in the warehouse, when sorting materials) [9];
- the fraction of large pieces, depending on the characteristics of the furnace, can be 20–40 mm, but changes in the size in the direction of their increase negatively affect the gas permeability of the layer of charge materials. Therefore, it is necessary to control the ratio of fractions (large/medium/small) to avoid local "failures" in the course of the domain process.

Physical characteristics, according to [10], are determined by such indicators as:

- strength (pellets) - (+6.3 mm) ≥ 90–92%;
- abrasiveness - abrasiveness index ≤ 5–8% for typical classes;
- porosity/impact strength of the pellet: must ensure the preservation of shape during transportation before loading and in the furnace to a temperature of

1250–1350 °C.

Regarding the chemical composition of iron ore materials (pellets/agglomerate), the study [10] determines their rational chemical composition. For iron ore raw materials, it is desirable to have a Fe content of ≥ 60–65%. A lower iron content increases the amount of slag, which reduces iron yield [11].

Regarding (SiO_2), (S) and (P). For high-performance smelting modes, according to studies[10], it is necessary to strive to ensure the total content of + and raw materials in the fuel: SiO_2 ≤ 3–5%; sulfur (S) ≤ 0.02–0.06%, since most of it turns into liquid cast iron; phosphorus (P) ≤ 0.03–0.05%

For pyrolyzed biomass and biochar, the authors [12] requirements:

- total carbon: the higher and more stable its content, the better the replacement of coke;
- moisture - ≤ 5–10% (higher humidity worsens the quality of its introduction with blowing into the furnace, reducing the efficiency of coke replacement);
- ash, which may include harmful impurities (Cl, S, P, Zn) - their content must be minimized, because an increase in Zn, Cl provokes problems when they condense on furnace fires, corrosion, etc.

In addition to the requirements for the physical and chemical properties of ferroraw materials, an important issue is to determine its rational share, which should replace traditional agglomerate and pellets. Based on the analysis, it can be argued that their values depend on the specific furnace, specific consumption of coke, equipment, technology of their pelleting and other factors that have a theoretical basis and practical confirmation.

Thus, the total share of the introduction of iron ore substitutes that have not passed the agglomeration stage, which meet the basic requirements given above, can probably be ≤ 5% of the total mass of iron ore components. In the future, when implementing a step-by-step algorithm, it is advisable to increase it to 10–15%, which is confirmed by the results of the study [6].

It is advisable to increase the specific consumption of PBC (pyro-biocarbon) as a substitute for the coke fraction introduced into the furnace in blowing jets using PCI technology, replacing the corresponding share of PCF in it: initially from 10% of the coke equivalent; After successful tests, it is possible to increase up to ~15–20% of the equivalent, depending on the reactivity capacity, mechanical resistance, and other important properties of pyro-pyrucarbon. It can also be expected that the implementation of the combined method with the supply of PCF, PBC and NG in the air blast stream can become a factor that will contribute to reducing the specific consumption of coke, stabilizing the thermal balance of smelting and reducing the level of CO2 emissions, as indicated by the authors [12].

Generalized according to the results of the research and industrial practice, "safe" ranges of specific consumption of materials, substitutes for traditional components of blast furnace charge and blasting, it is necessary to adapt to the conditions of a particular furnace, which is noted in [13], only after pilot tests. In the future, based on the results obtained and after adjusting the main process parameters for new materials, the process is examined in real conditions on a blast furnace.

To create safe conditions for the introduction of the technology of introducing materials, which are defined as substitutes for the VFR part, which are introduced in the flow of air blast enriched with oxygen, the following practical measures have been defined. Achieving a significant level of energy efficiency of the combined heat treatment of the mixture of starting materials – waste in the conditions of pyrolysis of waste of plant origin is possible when monitoring the parameters of the current batches of raw materials and fuels: their chemical composition, humidity and granulometry, as well as compliance with the mass ratio of the components of the initial mixture.

When implementing biomass pyrolysis in the conditions of an inclined furnace [4], rotating, creates a spilling layer of charge, constantly updating the surface of interaction of volatile (CO, CH4, H2) with oxygen of the working atmosphere of a thermal reactor, - to control the temperature indicators, the duration of the initial mixture in the characteristic zones of change in its state: evaporation of moisture, drying, pyrolysis, and stabilization of the final product in terms of the content of pyrocarbon, C, volatile components, sulfur, phosphorus, SiO2. These indicators, together with its particle size distribution, determine the further spectrum of functional purpose of materials for heat treatment of the initial mixture.

A promising method of heat treatment of dispersed materials of substitutes based on waste materials of plant origin (biomass), based on the results of high-temperature experiments and practical use of the material [4], it is necessary to recognize the combined heat treatment of a number of materials of secondary mineral origin as its oxide part and waste of plant origin as a source of pyrocarbon. At the same time, the physical and chemical properties of the metallurgical product, which is based on secondary materials, were formed by transforming their initial properties under the influence of appropriate heat treatment conditions into an innovative material with the expected spectrum of functional purpose.

In the conditions of blast furnace production, when using innovative materials based on materials that form its secondary resource and fuel base, it is recommended to gradually increase them when introduced into the initial blast furnace charge or air-blasted feeding, starting, according to [14], with 5–10% of the coke equivalent, or the proportion of PCF, lime or iron ore component removed from the blast furnace before its sintering. The requirements, the fulfillment of which will ensure the effective use of materials of the secondary base of raw materials and fuel/reducing agent resources in the blast furnace process, are constant monitoring of the main parameters of the process: conditions of their loading and

distribution, pressure drop, gas permeability of the charge material layer, coke consumption, changes in the composition of liquid pig iron and its productivity when introducing substitute materials into the charge (iron ore components) or into blasting.

The transition of blast furnaces from blowing natural gas (BNG) to the use of pulverized coal fuel (PCF) changes the conditions for the flow of heat and gas dynamic processes (physical chemistry of the furnace as a whole). The implementation of this technological solution can have a number of consequences that will affect the following parameters that are important for the stability of the process in the blast furnace.

1. Thermal balance of the process: decrease in the calorific value of the gaseous medium: PCF has a lower specific calorific value compared to BNG, which requires compensation due to increased oxygen consumption when the blast parameters change; increased thermal load on the tuture zone: PCF combustion is more localized, which creates high temperature gradients.

2. Gas-dynamic state in the furnace: increase in the volume of gases from combustion: PCF gives more CO and N_2, which changes the distribution of gas flow in the mine; deterioration of the gas permeability of the charge: small particles of coal and ash can accumulate in the intergranular space, increasing the hydraulic resistance of the layer; change in the nature of iron reduction: the ratio of CO/CO_2 and H_2/H_2O in gases on the furnace changes, which affects the kinetics of iron, manganese, silicon reduction reactions.

3. Chemical composition of products of chemical reactions and physicochemical transformations: an increase in the proportion of solid carbon in the reducing medium of the initial charge layer → enhances the carbonization of iron, affecting the composition of cast iron (an increase in carbon, sulfur is possible); increase in ash removal, PCF impurities (SiO_2, Al_2O_3, Fe_2O_3, S) pass into slag, changing its composition, basicity and viscosity.

4. Stability of the furnace running and controllability of the iron smelting process: ensuring an increase in sensitivity to fluctuations in blow parameters requires a more precise regulation of oxygen consumption, pressure, temperature and humidity; minimization of the likelihood of local "clogging" of the charge due to insufficient gas distribution; increased requirements for automated systems for control and regulation of the main process parameters, including loading and distribution of charge components.

5. Economic and environmental aspects: reduction of the cost of pig iron due to cheaper fuel (PCF) compared to coke and GHG; increase in specific emissions of CO_2 and dust compared to the use of natural gas; substantiation of the feasibility of combined injection (PCF + NG + H_2) for further optimization of the blast furnace process in terms of its energy and environmental indicators.

Thus, the transition of blast furnaces from natural gas injection to the use of pulverized coal fuel (PCF) leads to changes in heat-gas-dynamic (physicochemical) conditions in the furnace working space. This leads to certain consequences for the course of processes, the stability of pig iron smelting and the efficiency of its results. Table. 3 for the system "change - consequence - expected result" shows possible consequences and physicochemical effects, the source of which can be the replacement of natural gas with PCF (Pulverized coal fuel).

On the basis of analytical-theoretical analysis and scientific forecasting of the expected, when replacing the main components of the material and thermal balances of the blast furnace process (iron ore components of the blast furnace charge and natural gas), the results summarized in (Table 1-2), it is advisable to make a scientifically - practically grounded and generalized conclusion on the expediency of using combined blasting (PCF + NG + H_2) in the form of recommendations on their rational ratios, conditions, features mechanism and analysis of restrictions on the use of hydrogen in blast.

Regarding the mechanism of action and factors affecting the level of application in the production of hydrogen pig iron:

1. According to the data given in [15], which are consistent with the thermodynamic forecast, hydrogen (H_2) contributes to the shift in the development of iron reduction reactions to the upper part of the furnace, increasing the proportion of indirect reduction. This reduces the specific consumption of coke and CO_2 yield, but becomes a source of the cooling effect of the charge. The thermal level of the process decreases: RAFT (raceway adiabatic flame temperature) falls, which requires compensation for heat losses by increasing the temperature and enriching the blast with oxygen and preheating the gases - components of the blast) [16].

RAFT (Raceway Adiabatic Flame Temperature) is the adiabatic flame temperature in the combustion zone near the blast furnace lances, i.e. the maximum temperature that is theoretically reached during the combustion of fuel (coke, PCI, gases) without taking into account heat loss. RAFT determines:

heat dissipation intensity in the lance zone;

FeO → Fe reduction conditions;

combustion stability and thermal balance of the blast furnace process.

The unit of measurement is degrees Celsius (°C) or Kelvin (K).

Typical values: 2000–2300 °C (for coke), 1900–2200 °C (at PCI).

2. The use of NG (methane) gives a high reducing capacity and, according to data [17], has a significant potential for coke substitution, but its dissociation is an endothermic physicochemical transformation that requires heating of NG before its introduction into the blast or additional oxygen, which will ensure the leveling of the effect of "cooling" the endothermic reaction of methane decay and retains RAFT [16].

Table 3 – Generalized table of the impact of the use of PCF as a substitute for natural gas on the results of the blast furnace process.

No.	Changing smelting conditions	Consequence	Expected result
1	Replacing natural gas with PCF	Increase in specific oxygen consumption, change in the composition of the gas flow	Accelerating iron recovery, reducing natural gas consumption
2	Change in the ratio of gas volumes in the furnace	Increase in the proportion of CO, decrease in the content of H_2 in the gas phase	Increasing the regenerative capacity of the gas flow
3	Increase in the temperature of the torch in the combustion zone	Growth of temperature gradients in the lance zone	Intensification of heat exchange, improvement of charge melting
4	Increase in slag mass from PVP	Change in the composition and viscosity of slag	Improvement of cast iron desulfurization conditions in slag optimization
5	Reducing the gas permeability of the blast furnace with an excess of PCF	Complication of the course of gases, increase in hydraulic resistance	The need to optimize the granulometry of the charge and the flow rate of PCF
6	Increasing the proportion of carbon potential in the furnace	Intensification of FeO Reduction in Slag and Iron Ore Material	Reduction of specific consumption of coke, fuel economy
7	Increasing the amount of solid carbon in the combustion zone	Intensification of CO generation, increase in combustion temperature	Increasing the recovery capacity of the gas flow, improving the reduction of FeO
8	Reducing the volume of gases entering the furnace	Change in gas dynamics, decrease in N_2 volumes in blast furnace gas	Reduction of heat loss, increase in the concentration of reducing gases
9	Increase in the proportion of oxygen in the tuar's blow	Improving the combustion conditions of PCF, stabilizing the temperature regime	Increasing process stability and blast furnace performance
10	Change in the structure of the slag (introduction of additional sulfur and ash from coal)	Complications of the cast iron desulfurization regime	The need to optimize the chemical composition of slag and the slag mode of smelting
11	Increased heat load on the combustion zone	Risk of overheating of the lances, uneven heat distribution in the charge layer	Implementation of measures for cooling and control of the distribution of PCF

Pulverized coal fuel (PCF) contributes to the provision of carbon "support" due to the positive effects of slag formation from PCF ash components and the preservation of the structure of the coke bed; high PCF consumption is possible only at RAFT ≈ 2150 – 2300 °C when enriching blast O_2. ≈1200 °C and enrichment O_2. Marginal modes of use of H_2 were determined by the authors by the minimum permissible RAFT and the temperature of the furnace gases. The rational specific consumption of hydrogen injected into the furnace in the stream of carrier gas together with PCF, theoretically justified, modeled and experimentally confirmed by the authors in the study [19] in the absence of radical reconstructions of the furnace, is approximately 7÷20 kg of H_2/t of pig iron (~ 80 ÷ 220 nm³/t of pig iron). The equivalent of coke substitution is approximately 1.9 kg of PCF per 1 kg of H_2. From an industrial perspective, the injection of heated H_2 in the test blast furnaces demonstrated a 33–43% reduction in CO_2 when carefully balanced with the thermal balance of the smelting. This indicator, obviously, corresponds to the level of development of science, technology and equipment, the technical limit of which in the conditions of pig iron production is not typical for modern process modes.

As a summary based on the analysis of the results of the studies discussed above, it is necessary to give the following recommendations for the use of secondary materials - substitutes for iron ore components and coke in the blast furnace process:

As for the introduction of secondary components, it should be noted that the exact values of rational particles will depend on a specific blast furnace, technological features of the process, physical and chemical characteristics of coke, when operating them - from technologies and equipment for agglomeration and its other methods. Therefore, the recommendations below relate to the rational in terms of "starting" particles of substitute components, their chemistry and granulometry, the conditions of preparation for use at the stage of practical tests:

- keep the content of <5–10 mm fraction in the initial charge of ferroraw materials ≤ 2–5%;
- Fe content in pellets/agglomerate/pellets - ≥60–65%; the content of S, P – minimize (S ≤0.02–0.06%);
- $\Sigma(Na_2O+K_2O)$ – to control their total content at the level of 2–3 kg/t of liquid pig iron;
- biomass/materials of plant origin - must be prepyrolyzed and mechanically stable;
- pellets from secondary concentrates - 10-30% with optimization of the content of fluxes, coke, or other carbon source material.

We believe that for the appropriate level of development of blast furnace production technology, it is important to search for substitutes for traditional materials of its resource base, which will improve the process in the direction of increasing its energy efficiency in accordance with the social and environmental requirements of our time. And the rational use of the components of their physical and chemical potential

should become a benchmark of efficiency for researchers when improving the process in the blast furnace.

Scientific and technological forecasting of the practical application of materials of the secondary base of resources of raw materials, fuels in the conditions of blast furnace production. The main requirements that will contribute to their effective use include the following parameters and characteristics: granulometry, physical characteristics, chemical composition of iron ore materials and pyro-biocarbon, as well as determination of approximate shares of substitute materials and practicalmeasures to ensure their safe implementation in blast furnace production.

In the conditions of blast furnace production, when using innovative materials based on production waste, which form its secondary resource and fuel base, it is advisable to gradually introduce them into the initial blast furnace charge or air-blasted feed, starting according to [12], with 5–10% of the coke equivalent, or lime as a particle removed from the blast furnace before its sintering. The requirements, the fulfillment of which will ensure the effective use in the blast furnace process of materials of secondary, with signs of man-made origin, the base of raw materials and reducing fuel, are constant monitoring of the main parameters of the process: conditions of their loading and distribution, pressure drop, gas permeability of the charge materials layer, coke consumption, changes in the composition of liquid cast iron and its productivity when introducing substitutes into the charge (iron ore components) or feeding into a blast furnace (PBV, dispersed CaO, etc.).

The operation of PCI blast furnaces can cause changes in the conditions of physicochemical and heat-gas-dynamic processes occurring in the reaction zone, which affect similar processes in other characteristic zones of the furnace [1] during the transition to PCI technology. Therefore, in order to determine the peculiarities of pulverized coal injection and its impact on the processes implemented in the blast furnace, we will consider the essence, goals and probable results of the impact on the main indicators of the blast furnace process. The process of modern technology is based on replacing part of the coke with a cheaper and more energy-efficient type of fuel.

Regarding the technological essence, goals and outcome of PCI. Dispersed coal dust (0÷75 μm) is supplied through the lances along with air directly to the coke carbon combustion zone of the blast furnace. As a result, part of the coke in the charge is replaced by PVP, which is supplied by jets of gas to the carrier gas into the zone of interaction of air oxygen with coke carbon of the blast furnace charge. The main goals of the introduction of PCI technology are: reducing the consumption of coke, which is a source of economic effect, because coke is the most expensive element of the charge - in the cost of pig iron it is ~ 40%; providing flexibility in the choice of fuel through the use of anthracite and other types of coal) and, as a result, reducing total CO_2 emissions

It is more expedient under the condition of heat treatment/preparation of dispersed materials - waste, which is proven by the results of high-temperature experiments and practice [4], is the implementation of combined heat treatment of a number of materials of secondary origin - mineral origin (oxide part) and waste of plant origin (sources of pyrolysis carbon). At the same time, the properties of materials based on secondary materials, the common feature of which is man-made origin, and their physical and chemical properties of the initial properties and composition of components, which, during combined heat treatment under the conditions of biomass pyrolysis, are transformed into the properties of an innovative material. The latter determine the spectrum of functional purpose of the material. The two-level closed circuit of regeneration of initial and secondary energy resources of the process developed by the authors allowed: to use the fuel and chemical energy of pyrogases in the thermal unit of the first level as much as possible; physical heat of gases generated during the combustion of pyrogas for pyrolysis of biomass in the second-level unit; chemical energy of pyrogas generated in the unit of the second level – as an additional source of fuel and chemical energy in the unit of the first level. A promising direction for improving the RSI technology is the replacement of a fraction of coke or PVP with materials based on pyro-biocarbon, which have undergone joint heat treatment [20].

A modern method of replacing part of the coke with a cheaper and more energy-efficient type of fuel, which is currently PVP, is implemented by implementing PCI technology) - injection of pulverized coal fuel into a blast furnace. The main goals of the implementation of the RSI are defined: reducing the consumption of coke, the most expensive element of the charge, by using fine coal dust (0–75 microns), which is supplied through the lances along with air directly to the combustion zone; achieving a higher level of energy efficiency of the blast furnace process; the possibility of using less scarce types of coal.

Regarding the reduction of CO_2 emissions, since less coke is burned (1 kg of PCI ≈ 0.85 kg of coke), according to [21], the coke replacement factor is not a direct indicator of the change in CO_2 emissions. The reduction in emissions is achieved by reducing the production of coke. In total, this gives a noticeable reduction in CO_2/t of pig iron [22]. The results of the study [23] also state that the coke replacement rate is not a direct indicator of changes in total CO_2 emissions.

The authors [21] refer to the optimal parameters of PCI technology that ensure the effectiveness of the use of VFR:

- consumption of pulverized coal fuel 120÷200 kg/t of pig iron (the optimal value according to their definition is 150÷180 kg/t);
- particle size: 0÷75 μm (average diameter 30-40 μm);
- humidity: ≤ 1.0 %;
- ash content: ≤ 10 %;

- volatile substance content: 18–25%;
- blast temperature: ≥ 1100 °C.

The study also determined that when inflating 150 kg/t, the coke savings are about 130 kg/t of pig iron.

In our opinion, the determination of the coefficient of replacement of coke with pulverized coal fuel, which is introduced into the zone of interaction of oxygen of air blast with the components of the charge, with the involvement of coke production and taking into account its CO2 emissions, is not scientifically, technologically and economically justified. This approach neutralizes the individual contributions of coke production and its use in the blast furnace process, generalizing them, which calms and distracts from the search for more advanced schemes and innovative materials, the introduction of which will meet the challenges of our time and are aimed at improving blast furnace production.

It is advisable to determine the following as components of the overall integral effect of partial replacement of coke with materials such as PCF, NG, H_2, pyro-biocarbon by using PCI technology (Pulverized Coal Injection):

1. Reduction of coke oven consumption in kg of coke/t of pig iron as a direct positive effect created by the partial replacement of coke, PCFNG, H_2 / pyro-biocarbon. It is determined by the substitution coefficient of each material introduced into the furnace [21].

2. Reduction of specific CO_2 emissions (kg CO_2 / t pig iron % of baseline values) as the total result of the reduction of carbon burned due to its replacement with H_2 or pyro-biocarbon [24]. At the same time, part of the hydrogen → H_2O, which reduces specific CO_2 emissions.

3. The introduction of H_2 into the blast changes the kinetics of the reduction reactions and the temperature regime, which contributes to a moderate increase in the productivity of the furnace, but in order to obtain the effect, according to [25], thermal compensation of the thermal balance of the process is necessary.

4. To guarantee the positive effects of the introduction of H_2, it is necessary to reduce technological and operational risks due to the preliminary heating of H_2/NG before the introduction of H_2/NG into the blast, modernization of lances, control systems, ensuring stable properties of PVP, pyro-biocarbon, as well as ensuring appropriate levels of logistics and their cost, especially H_2 [26].

Based on the generalization, systematization and coordination of the results of these works in a similar direction, an analysis of indicators for the system "Coke – PCI → PCF" for the conditions of the domain process was carried out (Table 4). Its use allows you to determine the difference in the use of materials (coke, PCF) according to the main energy, technological, environmental and economic criteria, which, based on the achieved process indicators, will make it possible to predict the prospects of their application. In Table. Figure 4 presents the results of the influence of PCI technology on the indicators of the domain process, systematized according to the data from [21-23, 27].

Table 4 – Impact of VFR use on coke consumption and main parameters of the blast furnace process.

No.	Parameter	Impact PCI
1	Coke consumption	It decreases (for every 1 kg of pulverized coal injected with the blast, approximately 0.8–0.9 kg of coke is saved).
2	Combustion zone temperature	It decreases, by about 80-100°C, so you need to increase the oxygen supply
3	Reducing capacity of gases (CO, H_2)	Increases, which has a positive effect on the level and time of metallization
4	Gas permeability of the charge	It does not change, it deteriorates slightly if you increase the consumption of PVP >200 kg/t of pig iron
5	Cast iron quality	Does not change at optimal melting mode
6	Blow consumption	Increases due to additional oxygen supply
7	Total heat of the process	It can decrease — partially compensated by an increase in the O_2 content in the blast

Based on the coordination of the research data analyzed in the work, the following are established as the most probable, rational parameters of the PSI technology:

- PCF consumption: 150–180 kg/t;
- particle size: the average diameter is 20–80 microns;
- humidity: ≤ 1.0 %;
- ash content: ≤ 10% using PCF, for pyro-biocarbon (PBC) - ≤ 5%;
- volatile substance content: 18–25%; for PBC – regulated by pyrolysis conditions (time, temperature, αO2);
- blast temperature: ≥ 1100 °C.

The interchange of coke with PCF, according to data [21], is approximately:1 kg of pulverized coal fuel can replace ≈ 0.75 - 0.90 kg of coke. With an injection of 150 kg/t PCI, the coke savings are about 130 kg/t of pig iron.

Coordination of the results obtained in the study, their systematization and generalization according to the main features, made it possible to coordinate them with the data of the analyzed works and on their basis to develop a comparative table. 5 the data of which, in our opinion, give an objective characterization of the reducing agents of the blast furnace pro-

cess: coke, PCF and pyro-biochar of plant origin. The choice of indicators in it is focused on the energy, environmental and technological aspects of the blast furnace process, which makes it possible to predict the prospects for their use in the conditions of modern pig iron production.

Table 5 – Comparative data of indicators of carbon-containing materials and their impact on the parameters of the domain process.

Indicator	Coke	PCI - pulverized coal fuel	Pyro-biochar of plant origin
Origin	Primary product of coal coking	Crushed coal (anthracite or other types of thermal coal	Secondary resource with fuel and reducing agent properties obtained by biomass pyrolysis (wood, agricultural waste, lignin)
Filing form	Solid lumpy particles of 25÷80 mm, introduced into the furnace from above as a component of the charge, according to the algorithm of the current technology of its loading	Dusty, blown through the lance of the device in the flow of carrier gas (air blast)	The device is blown through the lance by analogy with the introduction of PCF into the blast furnace
Upper calorific value (HHV), MJ/kg	28÷30	25÷28	20–25 MJ/kg (depending on biomass origin and pyrolysis conditions)
Fixed carbon content, %	85÷90	60÷75	60 ÷ 70; 90÷96 (depending on the conditions of pyrolysis, the type of biomass, and the purpose of the pyrolyzed material
Ash content, %	10÷12	8÷10	1–5
Volatile content, %	1÷2	15÷25	20÷35 (at a humidity of ≤ 1.0, which is obtained in the process of drying biomass without the implementation of the pyrolysis stage, ~ 60)
Humidity, %	1÷3	≤1	initial for waste of plant origin 5÷10; lignin, which is a product of hydrolysis treatment of waste of plant origin 48÷60
Reactivity to CO_2 (CRI) / reactivity as a reducing agent	Low (slow combustion) / significant, implemented in the blast furnace process in the form of C and CO	High – burns quickly in the reaction zone when it is injected with heated air blast	Very high due to the porous structure of pyro-biocarbon/ higher than coke and PCF
Mechanical strength	High, which is necessary to maintain gas permeability to the blast furnace charge layer)	No requirements - it is introduced into the furnace with a heated air blast through lances, used mainly as fuel	There are no requirements for using PVP or GHG as a substitute. Medium – low strength requires agglomeration of pyrocarbon with iron ore material
CO_2 emissions from combustion, kg/GJ	94÷96	92÷94	15–20 (neutral balance, because CO_2 is of biogenic origin)
Coke substitution effect, kg/t of pig iron	—	0,8÷0,9 kg of coke per 1kg PCI	0,6–0,8 kg of coke per 1 kg of pyro-biocarbon
Optimal consumption, kg/t of pig iron	350÷450	120÷200	According to some data, 40÷120; clarified by further research
Effect on the temperature of the combustion zone	Basic level (2200÷2300 °C)	Decrease (by 50÷100 °C)	Decrease (by 50 - 100°C) - requires an increase in O_2
Gas permeability of the charge	High	Virtually unchanged	May decrease with excess specific flow rate
Impact on the quality of cast iron	Stable	Stable or slightly higher due to purity	Improves due to less sulfur and ash
Ash content	10÷12 %	8÷10 %	1÷5 % (depending on the type and raw material)
Sulfur content, %	0,5÷0,7	0,3÷0,6	≤0,1
Phosphorus content (P)	0,05÷0.1 %	0,03÷0,08 %	< 0.02 %
Impact on the quality of cast iron (S, P, Si)	Basic level	Slight decrease S i P	Significant decrease S i P
Equivalent of replacing coke	-	1 кг PCI ≈ 0,85 kg of coke (as fuel)	1 kg of pyro-biocarbon: as fuel ≈ 0.60÷0.85 kg of coke (depending on the carbon content); as a reducing agent - 0,90÷1, 1 кг

Table 5 (continued)

Indicator	Coke	PCI - pulverized coal fuel	Pyro-biochar of plant origin
Cost, % of coke	100	50÷70	40÷50 - due to the use of the heat of combustion of volatile and the use of physical heat of gaseous combustion products of volatile biomass under the conditions of its pyrolysis (CO2, H2O, NO2) and higher reactivity as a reducing agent
Environmental assessment	High values of CO_2 emissions and environmentally harmful gases	Less CO_2. With partial substitution with biocarbon, a decrease in CO_2 by 10÷20%	Minimal CO_2 emissions, renewable resource. Reduction of CO_2 by 40÷60%; SO_x < 0, 07.
Основна перевага	Стабільність властивостей і міцність	Reduced coke consumption, cost-effective	Environmental friendliness, higher reactivity as a reducing agent, renewability, low S and P content
Main disadvantage	High price, CO_2 emissions, exhaustive source	Requires blowing system, combustion control	Lower heat of combustion, dependence of chemical composition on the type of biomass
The best application	Base blast furnace charge (also agglomerated)	120÷180 kg/t of pig iron through lances	5–15% equivalent to coke; 20–30% replacement of PCF when implementing PCI.
Overall score	Traditional and reliable reducing agent	Cost-effective and flexible, requires further research and adaptation to the process conditions in the blast furnace	A promising substitute for the useful properties of PCF and NG (fuel, reducing agent), and in the future coke Requires further research on adaptation to existing technologies

Based on the generalization of the data obtained in the work, it is necessary to determine the following:

1. Coke is a basic, structural component of the charge, provides sufficient, regulated by external factors gas permeability and thermomechanical stability of the layer of components of the blast furnace charge.

2. PCI as a technological solution is an optimal, under the conditions of the development of science and technology, an intermediate option that reduces coke consumption without losing process stability.

3. Pyro-biocarbon is environmentally friendly, requires minor thermal correction of blowing (increase in oxygen, temperature increase and their control). An effective substitute for the share of coke can be effective when it is administered in an amount of up to 20–30% of the mass of coke.

Thus, with a high probability, it can be stated that the integrated-integrated direction of blast furnace production improvement, which combines the technologies of pulverized coal injection with the introduction of pyro-biocarbon, the use of hydrogen reduction agents, as well as the involvement of secondary iron-containing materials and fuel and energy resources of man-made origin, is a promising and strategically justified way of development of modern blast furnace metallurgy.

Regarding the requirements for metallurgical quality indicators of components and basic blast furnace charge, as well as for the optimality of combined blast parameters, based on the coordination of the research results analyzed above, the following was determined. The components of the expected and most real integral effect from the use of hydrogen technologies on operating furnaces should be the following:

- reduction of specific CO_2 emissions: approximately **−10 – 15%** in mode B, **−20 – 30%** in mode C (subject to careful thermal compensation of certain heat losses; 33–43% is currently confirmed in test furnaces with **heated** H_2 and special heat balance measures)..

- **coke oven consumption**: up to **≤ 280–310 kg/t** in modes B–C (actually recorded range of values) with high PCF/NG; H_2 injection allows you to reduce the carbon fraction, but requires optimization of O_2/Tsuv for RAFT).

- performance: +2÷8% depending on gas permeability limits and maintaining a rational thermal level - O_2 blast enrichment stabilizes the flame and the reaction zone of combustion of fuel components.

Theoretical analysis of the relevant sources and scientifically grounded forecasting of the physical and chemical features of the process in the blast furnace indicates the following.

Combined injection of **PVP + GHG + H_2** is **an effective** way to increase energy efficiency and "greening" of the blast furnace process, **provided that the heat balance is controlled** (RAFT, TCG) through **the enrichment of O_2, a sufficiently high TDV. and heating of gases injected into the blast furnace** . . with a consistent, phased increase in the flow rate H_2 and a corresponding correction of PVP/O÷$_2$ **coke ≤ 280 ÷ 310 kg/t**. With such indicators, the stability of the blast furnace process is also maintained.

Determining the prospects of technological solutions for the efficiency of the use of VFR and GHG as substitutes for coke, increasing the level of use of useful properties of the initial potential of traditional

raw materials and fuels is a reserve for improving the blast furnace process.

The reserves of the blast furnace process as a set of hidden or not fully realized technical and technological capabilities of blast furnace smelting, allow, when they are involved in the process of iron smelting, to determine specific technical directions for its improvement by:

- reduction of specific fuel consumption (coke, VFR, PCI, pyro-biofuel energy);
- increasing the productivity and duration of the furnace campaign;
- improving the quality of cast iron;
- reduction of CO_2, CO, NO_x, SO_x and dust emissions;
- rational use of the properties of secondary and alternative resources of raw materials and fuel, which contributes to ensuring the stable operation of the furnace.

Regarding the forecast for the development of blast furnace production in Ukraine, taking into account the resource base, the level of technology development, the state of the environment and economy during the war.

After a sharp decline in 2022 (due to the destruction of factories, changes in the quality of mineral raw materials, fuel, their sources and logistics supply routes), the recovery in 2024-2025 was partial, but the metallurgy sector as a component of the state's economic potential is still well below the pre-war level, and the total capacity remains reduced due to the failure of a significant part of the plants.

Raw material and energy constraints (especially coking coal, ultra-high electricity prices) are a key bottleneck for the sustainable recovery and further development of carbon metallurgy. To compensate for them, manufacturers increase coke imports, which can cause risks in logistics and pricing. And the growing level of exports of iron ore intermediate products (enriched concentrate, pellets) significantly reduces the possible added value - the profit of the enterprise, industry, state.

The resumption of exports remains dependent on the operation of ports and railways; Logistics tariffs and safety of transportation of metallurgical products affect their competitiveness.

Environmental commitments and the global decarbonization trend are driving the transition from large blast furnaces to a steel production scheme using EAF/DRI solutions (direct reduced chipboard/iron) and the use of hydrogen technologies in the medium term.

The combination of the technology of injection of pulverized coal fuel with the introduction of pyro-biocarbon, the use of hydrogen, as well as with the involvement of secondary iron-containing materials and fuel and energy resources of man-made origin will make it possible to:

- reduce specific coke consumption and CO_2 emissions due to partial substitution, artificially created from fossil coal, coke for renewable bio-pyrocarbon materials of plant origin;
- to increase the resource and energy efficiency of the process through the utilization of by-products and secondary products of the metallurgical cycle;
- provide flexibility in managing the material, thermal and recovery balance of the furnace due to the combination of iron, carbon and hydrogen sources;
- to bring the blast furnace process technology closer to the requirements of low-carbon ironmaking.

Thus, the direction of further development indicated in the study is of high scientific and practical importance, corresponds to modern trends in circular metallurgy, energy efficiency and decarbonization, and also creates the basis for a gradual transition to hydrogen-oriented processes of direct and partially restored pig iron production.

The analysis of unused reserves of blast furnace production, and the development of innovative materials, including those based on man-made materials of metallurgical origin, made it possible to develop a method for the production and use of "black lime" as a monomaterial, which is advisable to introduce into the blast furnace in combination with other air blast components (PVP, NG), as a substitute for part of their specific costs.

Fig. 1 shows the form of "black lime -CHV", which was obtained under the conditions of a pilot installation - a laboratory inclined drum-type furnace with a rotating drum at αo2 = 0.85; Tmax = 1150°C. Material composition in % wt.: CaO = 88.2; C = 10.7.

The results of the research, which were obtained when determining the features of the combined pyrolysis of dispersed lime and lignin - the waste of agricultural waste processing, indicate that the degree of fixation of pyrocarbon on the particles of the mineral base (CaO) is 20 times higher than the similar indicator of mechanical mixing of two dispersed materials.

Fig. 1 – The appearance of "black lime" after carrying out compatible pyrolysis of components in the conditions of the spilled layer at temperature T_{max} =1150°C, α_{O2} = 0,85.

Pyrucarbon is firmly fixed on the surface of lime particles, significantly increasing the size of monomaterial particles (2.5 ÷ 4.5 mm).

Regarding the fractional and chemical composition of dispersed lime accumulated in gas cleaning cyclones during the production of metallurgical metastable lime, it is necessary to determine the following. The typical fractional structure of pulverized lime is very variable and depends on the type of dust collector (cyclone/bag filter), combustion / calcination and grinding conditions. In the practice of metallurgical lime production, lime dust has the following fractional composition <10 μm-5–30 %; 10–63 μm - 30–60 %; 63–125 μm-10–30 %; 125–250 μm-5–15 %; >250 μm - 0–5%. The given ranges of lime dust are often fixed in practice.

Under the conditions of high-temperature pyrolysis of the initial charge based on a mixture of CaO and a material of plant origin containing carbon, at its initial moisture content ~ 17.8% and temperature of ~ 1200°C, the following physicochemical processes and transformations are carried out:

- at the stage of preparation - mixing of components - primary enlargement of dispersed particles of the original mixture, which led to the hydration of lime (CaO → CaCO3);

- under the conditions of heat treatment with the implementation of compatible pyrolysis of the mixture - final enlargement with the formation of a product - monomaterial CaO-C_{pyro}; dehydration of lime (CaCO3 → CaO); stabilization of fractional, chemical composition and properties of monomaterial;

- cooling of "black lime", its accumulation, transportation, quality control, functional purpose.

In addition to pulverized lime, it is advisable to use a fraction of CaCO3, which is formed in sufficient for industrial use (recycling) as a component in the CaO-C mixture.

As for the methods of production of Ch. For the first time, on the basis of theoretical justification after experimental testing in laboratory conditions, the method of black lime production was implemented under the conditions of an inclined rotary kiln using the initial mixture of lignin (humidity ≈ 48%) + fineness CaO (dry). The result of the next stage of the study was the development of a method for obtaining HF without the use of external sources of thermal energy [28].

The implementation of the process in the temperature range, which is 1150 ÷ 1200°C, made it possible to dehydrate lime using the thermal effect of the reaction to heat the initial mixture before loading it into the furnace, as well as to exclude the development of the FexOy reduction reaction with pyrocarbon. The content of iron oxide in an innovative material - a product of heat treatment of the components of the initial mixture, determining the level of its oxidation potential, expanded the range of functional purpose and physicochemical capabilities of the pyrolyzed monomaterial (CaO + C + FeO) as a slag-forming material [4].

The calculation method established the optimum replacement of PVP in the composition of PVP blasting with black lime, which is 10÷13 % of the specific consumption or energy contribution of PVP. At the same time, there is an objective possibility of reducing the modulus of the basicity of the agglomerate (and, accordingly, the basicity of blast furnace slag), which in the modern blast furnace process is the main iron ore component of the charge, to B ≈ 1.15, which reduces the melting point and viscosity of the blast furnace slag. At the same time, we should expect an acceleration of the dissolution of CaO in the furnace slag, which intensifies the desulfurization of cast iron.

Thus, an additional advantage of the use of monomaterial (FR) is the improvement of the agglomeration process, the properties of the sintered material, the reduction of the specific consumption of limestone and fuel for sintering of the initial charge, and in the future, in the blast furnace process: increasing the stability of tuyere devices (coating CaO with pyrocarbon reduces abrasiveness/corrosion), reducing the specific consumption of PCF, coke and CO2 emissions.

The calculations determined that for the initial conditions (current PCF supply = 120 kg/t of pig iron; carbon content 85%; black lime: C content ≈ 25%, free CaO ≈ 75%) when replacing 10% of PCF with black lime by mass of PCF, approximately 30.6 kg of CaO/t of pig iron will be introduced into the reaction zone of interaction with the components of the charge. With the optimum replacement of PCF with black lime, which is 10–13%, the introduction of such an amount of CaO into the furnace is sufficient to significantly affect the local balance of slag basicity in the lance zone. However, it is necessary to adjust the amount of fluxes to obtain the recommended limits of the basicity of furnace slag by reducing the corresponding indicator of iron ore agglomerate to ≈ 1.15. That is why, when implementing this technological solution, the optimal combination of adding CaO, which contains pyrolyzed monomaterial "from below" and reducing part of the fluxes included in the agglomerate fed from above, is achieved.

Let us turn to the analysis of physicochemical mechanisms explaining the above data.

1. Microcontact (CaO–C): Carbon is on the surface of CaO. The result of the reaction of carbon with CO_2 is a local intense formation of CO near the surface of CaO. This increases the partial pressure of CO, which contributes to rapid gasification, reduction of iron, that is, increases the efficiency of the fuel fraction, which reduces the specific losses of coke.

2. Faster dissolution of CaO in slag: dispersed CaO particles with a large reaction surface dissolve in the furnace slag faster, compared to the flux of agglomerate fed from above. Therefore, at an early stage of the formation of furnace slag, a rapid local correction of its basicity occurs, which increases the effect of refining liquid drops of iron-carbon melt from sulfur.

3. Lowering the melting point of agglomerate at B ≈ 1.15: reducing the viscosity and melting point of the slag phase improves the conditions for its formation, removal and facilitates the contact of metal with slag as a condition favorable for creating kinetic advantages of desulfurization.

4. Protective coating of CaO - dust with pyrovchar: the layer of carbon on the surface of CaO reduces the abrasiveness and aggressiveness of materials supplied through the lances, helps to prolong the operation of blowing lances.

5. Improving the agglomeration conditions and strength of the agglomerate by reducing its modulus of basicity, which has a positive effect on the thermal balance of the process, reducing fuel consumption.

It is advisable to implement the practical use of innovative material based on man-made materials – waste from relevant industries that have passed a joint stage of high-temperature or low-temperature pyrolysis, according to two technological schemes. According to the first, the main goal is to improve the slag mode of smelting with a certain reduction of the modulus of the basicity of the agglomerate to B ≈ 1.15÷1.10, with obtaining an additional effect due to the use of the fuel component of the potential of pyro-biocarbon as a substitute of the corresponding share of PCF. For such a scheme, the rational range of the composition, which will provide the necessary properties and purpose of the CF, is defined: C = 10 ÷12%; CaO = 88 ÷90%. The second scheme is implemented in order to replace the maximum possible proportion of PVP with pyro-biocarbon (C_{pyro} → CO2 + Skox → CO), the reactivity of which as a fuel and reducing agent exceeds similar characteristics of graphite, coke and is on a par with charcoal. For this version of the technological solution, the content of PBC in the monomaterial is ≥ 85, and the effect of the presence of CaO in it is minimized. The possibility of its increase has been experimentally determined due to the introduction of 5÷7 % of dispersed waste of fine iron ore or metallurgical waste containing iron oxides into the initial mixture of components that are sources of C and CaO. In this case, in the tuyere zone of the furnace, the formation of the slag phase with the participation of CaO, which is part of the monomaterial, proceeds along the ferritic path, which accelerates the creation of furnace slag with increased reactivity.

Conclusions & recommendations

The integrated-integrated direction of blast furnace production improvement, which combines the technologies of pulverized coal injection with the introduction of pyro-biocarbon, the use of hydrogen reduction agents, as well as the involvement of secondary iron-containing materials and fuel and energy resources of man-made origin, is a promising and strategically justified way of development of modern blast furnace metallurgy.

Replacement of PVPCF (full or its parts) with a monomaterial - "black lime", in comparison with the supply of a mechanical mixture (PCF+CaO), subject to segregation during transportation, should provide a technological advantage - a better microcontact combination (CaO↔C) and less segregation in the supply path. The use of waste materials in the production of "black lime" also provides an economic advantage - a reduction in the cost of material and has an environmental orientation - the disposal of man-made waste. When using it as a blast component, it is necessary to exclude the possibility of bringing the basicity of furnace slag beyond the values recommended according to the current technological instructions.

The components of the direction of improvement of the blast furnace process, having a scientific justification, correspond to modern trends in circular metallurgy, energy efficiency and decarbonization, and their implementation contributes to the creation of a basis and conditions for a gradual transition to hydrogen-oriented processes of direct reduction of iron and, partially, carbon, recovered through the use of innovative solutions for the production of pig iron.

References

1. Shostak, V. Iu., Chaika, A. L., Sokhatckii, A. A., Tciupa, K. S.,. Kornilov, B. V, & Moskalina, A. A. (2017). Osobennosti vduvaniia pyleugolnogo topliva i teplovoi raboty furmennoi zony domennoi pechi. *Theory and Practice of Metallurgy*, 3-4, 21-26.

2. Yaashikaa, P. R., Senthil Kumar, P., Varjani S., Saravanan, A. (2020). A critical review on the biochar production techniques, characterization, stability and applications for circular bioeconomy Biotechnology Reports, 28. https://doi.org/10.1016/j.btre.2020.e00570

3. Santos, D. C. B. D., Evaristo, R. B. W., Dutra, R. C., Suarez, P. A. Z., Silveira, E. A., & Ghesti, G. F. (2025). Advancing biochar applications: a review of production processes, analytical methods, decision criteria, and pathways for scalability and certification. Sustainability, 17(6), 2685. https://doi.org/10.3390/su17062685

4. Meshalkin, A. P., Sokur, Iu. I., Kamkina, L. V, Meshalkin, V. A. (2014). Ispolzovanie vtorichnykh energoresursov pri vos-stanovitelno-teplovoi obrabotke riada tekhnogennikh otkhodov. “Sistemnye tekhnologii” *Regionalnyi mezhvuzovskii sbornik nauchnykh trudov*, 3(68), 156-162.

5. Yang, H., Xiwei, Q., Wei W. (2023). Research and application of coupled mechanism and data-driven prediction of blast furnace permeability index. *Appl. Sci.*, 13(17), 9556. https://doi.org/10.3390/app13179556

6. Gavel, D. J., Ademab, Al., van der Stelb, J., Peetersb, T. et. al. (2021). A comparative study of pellets, sinter and mixed ferrous burden behaviour under simulated blast furnace conditions. *Ironmaking @ Steelmaking*, 48(4), 359–369. https://doi.org/10.1080/03019233.2020.1786644

7. Warren, P.,& Geerdes, M. Spotlight on Na_2O and K_2O Behavior in Blast Furnace Operation. AISTech 2024 — Proceedings of the Iron & Steel Technology Conference 6–9 May 2024, Columbus, Ohio., USA.. P. 135. https://doi.org/10.33313/388/017

8. Iljana, M., Paananen, T., Mattila, O. et. al. 2022. Effect of iron ore pellet size on metallurgical properties. *Metals*, 12(2), 302; https://doi.org/10.3390/met12020302

9. Bhagyaraj, D., Kalidhasan, S. K., Satalgoan, H. S., Srinivasan, M., et. al. (2023). Blast Furnace process optimization for sustainable Iron making. J*ETIR* 10(10), 602–617 https://www.jetir.org/papers/JETIR2310070.pdf?utm_source=chatgpt.com.

10. Iron ore pellets for blast furnace – a technical guide. https://maxtonco.com/iron-ore-pellets-for-blast-furnace-a-technical-guide/

11. S&P Global. Specifications Guide Global Iron Ore. 2024 by S&P Global Inc. All rights reserved. pp. 1-19. https://www.spglobal.com/commodityinsights/PlattsContent/_assets/_files/en/our-methodology/methodology-specifications/global_iron_ore.pdf?utm_source=chatgpt.com.

12. Orre, J., Ökvist, L. S., Bodén, A., & Björkman, B. (2021). Understanding of blast furnace performance with biomass introduction. *Minerals*, 11(2), 157. https://doi.org/10.3390/min11020157

13. Gavela, Dh. J., Ademab, C, A., van der Stelb, J. et. al, (2020). A comparative study of pellets, sinter and mixed ferrous burden behaviour undersimulated blast furnace conditions ironmaking & Steelmaking. https://doi.org/10.1080/03019233.2020.1786644

14. Dang, H., Wang, G., Wang, C., Ning, X., Zhang, J., Mao, X., Zhang, N., & Wang, C. (2021). Comprehensive study on the feasibility of pyrolysis biomass char applied to blast furnace injection and tuyere simulation combustion. ACS Omega, 6(31), 20166–20180. https://doi.org/10.1021/acsomega.1c01677

15. Barrett, N., Mitra, S., Doostmohammadi, H., O'dea, D., Zulli, P., Chew, S., & Honeyands, T. (2022). Assessment of Blast Furnace Operational Constraints in the Presence of Hydrogen Injection. ISIJ International, 62(6), 1168–1177. https://doi.org/10.2355/isijinternational.isijint-2021-574

16. Gao, X., Zhang, R., You, Z., Yu, W., Dang, J., & Bai, C. (2022). Use of hydrogen–rich gas in blast furnace ironmaking of v–bearing titanomagnetite: mass and energy balance calculations. *Materials*, 15(17), 6078. https://doi.org/10.3390/ma15176078

17. Tang, Ju., Chu, M., Li,.Zedong, F. Z., et. al. (2021). Mathematical simulation and life cycle assessment of blast furnace operation with hydrogen injection under constant pulverized coal injection. *Journal of Cleaner Production*, 278, 123191. https://doi.org/10.1016/j.jclepro.2020.123191

18. Zhang, W., Dai, J., Li, C., et. al. (2021). A review on explorations of the oxygen blast. furnace process. *Steel Research International*, 92(1). https://doi.org/10.1002/srin.202000326

19. de Castro, J. A., de Medeiros, G. A., da Silva, L. M., Ferreira, I. L., de Campos, M. F., & de Oliveira, E. M. (2023). A numerical study of scenarios for the substitution of pulverized coal injection by blast furnace gas enriched by hydrogen and oxygen aiming at a reduction in co2 emissions in the blast furnace process. *Metals*, 13(5), 927. https://doi.org/10.3390/met13050927

20. Mishalkin, A. P., Kamkina, L. V., Kovalov, D. A., Kamkin, V. Iu., Synytsyn, Ya. S., Kolbin, M. (2018). Rozrobka umov poperednoi pidhotovky parametriv teplovoi obrobky sumishei tekhnohennykh vidkhodiv na osnovi oksydiv kaltsiiu, zaliza i vuhletsiu. *Theory and Practice of Metallurgy*, 3-4, 37-42.

21. Babich, A. (2021). Blast furnace injection for minimizing the coke rate and CO2 emissions. Ironmaking & Steelmaking, 48(6), 728–741. https://doi.org/10.1080/03019233.2021.1900037

22. Carpenter, A. M. (2006). Use of PCI in blast furnaces. *Copyright IEA Clean Coal Centre*. 1-66. https://www.sustainable-carbon.org/wp-content/uploads/dlm_uploads/reports/Combustion/use-of-pci-in-blast-furnaces-ccc-116.pdf?utm_source=chatgpt.com.

23. Babich, A., Senk, D., & Fernandez, M. (2010). Charcoal behaviour by its injection into the modern blast furnace. ISIJ International, 50(1), 81–88. https://doi.org/10.2355/isijinternational.50.81

24.Lan, C., Hao, Y., Shao, J., Zhang, S., Liu, R., & Lyu, Q. (2022). Effect of H2 on blast furnace ironmaking: a review. *Metals*, 12(11), 1864. https://doi.org/10.3390/met12111864

25. Nogami, H., Kashiwaya, Y., & Yamada, D. (2012). Simulation of blast furnace operation with intensive hydrogen injection. *ISIJ International*, 52(8), 1523–1527. https://doi.org/10.2355/isijinternational.52.1523

26. Yilmaz, C., Wendelstorf, J., & Turek, T. (2017). Modeling and simulation of hydrogen injection into a blast furnace to reduce carbon dioxide emissions. *Journal of Cleaner Production*, 154, 488–501. https://doi.org/10.1016/j.jclepro.2017.03.162

27. Feliciano-Bruzual, C. (2014). Charcoal injection in blast furnaces (Bio-PCI): CO2 reduction potential and economic prospects. Journal of Materials Research and Technology, 3(3), 233–243. https://doi.org/10.1016/j.jmrt.2014.06.001

28. Mishalkin, A. P., Kolbin, M. O, Kamkina, L. V. at al. UA. Patent na vynakhid №86714. Sposib oderzhannia teploizoliuiuchoi sumishi, shcho samoobpaliuietsia. Biul. №9, 2009.

Надіслано до редакції / Received: 15.12.2025
Прорецензовано / Peer-Reviewed: 17.02.2026
Прийнято до друку / Accepted: 16.03.2026
Опубліковано / Published: 30.03.2026

ISSN 3083-7219 (Print), ISSN 3083-7227 (Online)
Теорія і практика металургії, 2026, № 1
Theory and Practice of Metallurgy, 2026, No. 1

https://doi.org/10.15802/tpm.1.2026.07

UDC 669.15'782'24'26'28:620.193.41

***Siharov Ye. M.*[1,*], *Smirnov O. M.*[2], *Pokhvalityi A. A.*[3], *Orlov D. V.*[4], *Skorobagatko Yu. P.*[5]**

Increasing the corrosion resistance of ferrosilide in hot sulfuric acid by alloying with chromium, nickel and molybdenum

[1] ORCID: 0000-0002-8229-7877. Дніпровський державний технічний університет, Україна
[2] ORCID: 0000-0001-5247-3908. Фізико-технологічний інститут металів та сплавів НАН України, Україна
[3] ORCID: 0000-0002-9652-767X. Дніпровський державний технічний університет, Україна
[4] ORCID: 0009-0002-4464-3561. ТОВ «Турбогаз Ужгород», Україна
[5] ORCID: 0000-0002-1724-9895. Фізико-технологічний інститут металів та сплавів НАН України, Україна
*Email: siharovyevgen@gmail.com

***Сігарьов Є. М.*[1,*], *Смірнов О. М.*[2], *Похвалітий А. А.*[3], *Орлов Д. В.*[4], *Скоробагатько Ю. П.*[5]**

Підвищення корозійної стійкості феросиліду у гарячій сірчаній кислоті при легуванні хромом, нікелем та молібденом

[1] ORCID: 0000-0002-8229-7877. Dniprovsky State Technical University, Ukraine
[2] ORCID: 0000-0001-5247-3908. Physico-Technological Institute of Metals and Alloys of the National Academy of Sciences of Ukraine, Ukraine
[3] ORCID: 0000-0002-9652-767X. Dniprovsky State Technical University, Ukraine
[4] ORCID: 0009-0002-4464-3561. “Turbogaz Uzhgorod” LLC, Ukraine
[5] ORCID: 0000-0002-1724-9895. Physico-Technological Institute of Metals and Alloys of the National Academy of Sciences of Ukraine, Ukraine
*Email: siharovyevgen@gmail.com

Abstract. *The corrosion resistance of ferrosilides of the Fe-Si-Cr-Ni-Mo-Mn system in concentrated sulfuric acid in the temperature range of 25-200°C was investigated. The corrosion rate was calculated based on electrochemical parameters using passivation and temperature dependence models of the Arrhenius type. It was confirmed that the main factor determining corrosion resistance is the silicon content. The existence of a critical Si content threshold was shown, upon reaching which a continuous passive SiO_2 film is formed, which provides a reduction in the corrosion rate by 1-2 orders of magnitude. Characteristic temperature ranges of the corrosion process were identified: stable passivation (25-80°C), transitional regime (80-150°C) and degradation of the passive state (150-200°C). It has been shown that Cr and Mo in Fe-Si alloys enhance the stability of the passivated state, particularly at high sulfuric acid temperatures, whereas Ni primarily affects the electrochemical characteristics, and Mn reduces the effectiveness of passivation. The effectiveness of adding chromium to Fe-Si alloys increases proportionally with the Si content; molybdenum stabilizes passivation at acid temperatures above 150°C and reduces the rate of localized corrosion; nickel is not a determining factor at high acid temperatures. The influence of operational factors (turbulence, erosion, impurities) on the corrosion rate has been determined. The expected corrosion rates for the studied alloys in sulfuric acid have been calculated, taking into account industrial operating conditions. The experimental data obtained can be used to develop new corrosion-resistant materials and optimize the composition of Fe-Si alloys for operation in high-temperature aggressive environments of concentrated sulfuric acid.*
Keywords: *Fe-Si alloys; corrosion resistance; sulfuric acid; passivation; silicon dioxide; electrochemical corrosion; high-temperature corrosion; alloying elements.*

Анотація. *Досліджено корозійну стійкість феросилідів системи Fe-Si-Cr-Ni-Mo-Mn у концентрованій сірчаній кислоті в діапазоні температур 25-200°C. Виконано розрахунок швидкості корозії на основі електрохімічних параметрів із використанням моделей пасивації та температурної залежності типу Арреніуса. Підтверджено, що основним фактором, який визначає корозійну стійкість, є вміст кремнію. Показано існування критичного порогу вмісту Si, при досягненні якого формується суцільна пасивна плівка SiO_2, що забезпечує зниження швидкості корозії на 1-2 порядки. Виділено характерні температурні області корозійного процесу: стабільна пасивація (25-80°C), перехідний режим (80-150°C) та деградація пасивного стану (150-200°C). Показано, що Cr і Mo у складі феросиліду підвищують стабільність пасивного стану, особливо при високих температурах сірчаної кислоти, тоді як Ni впливає переважно на електрохімічні характеристики, а Mn знижує ефективність пасивації. Ефективність введення хрому до складу феросиліду зростає пропорційно вмісту Si, молібден стабілізує пасивацію при температурах кислоти вище 150°C і знижує швидкість локальної корозії, нікель не є*

© Siharov Ye. M., Smirnov O. M., Pokhvalityi A. A., Orlov D. V., Skorobagatko Yu. P., 2026
© Сігарьов Є. М., Смірнов О. М., Похвалітий А. А., Орлов Д. В., Скоробагатько Ю. П., 2026

This is an Open Access article under the CC BY 4.0 license https://creativecommons.org/licenses/by/4.0/

визначальним фактором при високих температурах кислоти. Визначено вплив експлуатаційних факторів (турбулентність, ерозія, домішки) на швидкість корозії. Розраховані очікувані швидкості корозії для досліджуваних сплавів у сірчаній кислоті з врахуванням умов промислової експлуатації. Отримані експериментальні дані можуть бути використані для розробки нових корозійностійких матеріалів і оптимізації складу феросиліцидів для роботи у високотемпературних агресивних середовищах концентрованої сірчаної кислоти.
Ключові слова: *феросиліди; корозійна стійкість; сірчана кислота; пасивація; діоксид кремнію; електрохімічна корозія; високотемпературна корозія; легувальні елементи.*

Introduction

Corrosion of alloys in acidic environments remains one of the key challenges in modern metallurgy and chemical engineering [1, 2]. Operating conditions are particularly challenging at elevated temperatures in concentrated sulfuric acid, where traditional corrosion-resistant materials, notably stainless steels and nickel-based alloys, demonstrate limited suitability due to the intense destruction of passive protective films and the development of localized corrosion processes [3, 4].

In this regard, there is growing interest in ferrosilicides as promising materials with enhanced corrosion resistance. Fe-Si alloys demonstrate enhanced corrosion resistance in sulfuric acid; they are capable of forming a dense passive silicon dioxide film on the surface, characterized by high chemical inertness in strong acids [4, 5]. At the same time, the effectiveness of the passivation film's preservation significantly depends on the silicon content, the acid temperature, and the presence of alloying elements in the alloy, such as chromium, molybdenum, nickel, and manganese [6, 7]. The issue of determining the critical silicon content and the effect of complex alloying of ferrosilicide on the kinetics of corrosion processes and the stability of the passive film, at which a stable passive state is ensured over a wide operating temperature range, remains insufficiently studied.

It is also important to take into account not only laboratory conditions but also real-world operating conditions, including flow turbulence, erosion wear, and the presence of impurities, which can significantly alter corrosion mechanisms and lead to an increase in the rate of material degradation [8].

Classical studies [1, 4] have shown that even at silicon contents in the range of 14-16%, ferrosilicides undergo a transition from Fe-oxide to SiO_2-controlled passivation, which is accompanied by a sharp decrease in corrosion current density and explains the high corrosion resistance of high-silicon cast irons and intermetallides. According to the phase diagram [9], at a Si content >14.37% Si, the Fe_3Si intermetallic phase forms, and a Si content in the alloy exceeding 15% defines a region where a mixture of iron and Fe_3Si predominates; in this region, upon cooling of the melt, the formation of ordered intermetallics and a significant decrease in ductility are expected.

During crystallization, the main final phases in an alloy containing >15% Si up to 99% of the total mass will be FeSi, Fe_3Si, and Fe_5Si_3 (Fig. 1), with only up to 1% of unbound Si (in the form of fine crystals and/or inclusions). The brittleness of such an alloy is explained by the virtually complete absence of ferrite and the acquisition of ceramic properties. At the same time, such an alloy acquires properties of thermal-oxidative stability and corrosion resistance due to the formation, under appropriate heat treatment conditions, of a protective layer of SiO_2.

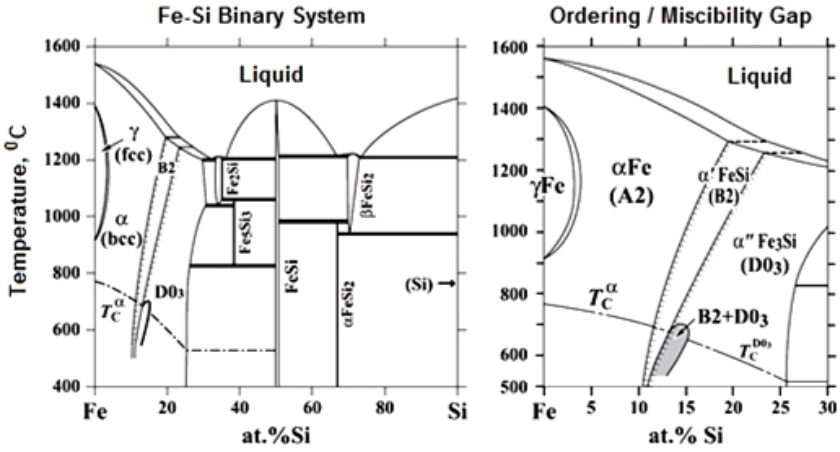

Fig. 1. Fe-Si phase diagram at 1 atm from Numakura and Tsugawa (1972).

A mixture of FeSi, Fe_3Si, and Fe_5Si_3 in sulfuric acid performs better than the individual phases, ensuring a long-lasting passive state of ferrosilicide [9-11]. The synergistic effect of resistance to H_2SO_4 is achieved through the following mechanism: Fe_3Si (with an optimal Fe/Si ratio) promotes the formation of a passivation film (SiO_2 + Fe oxides), Fe_5Si_3 promotes the formation of amorphous SiO_2, and FeSi promotes less stable passivation. The formation of SiO_2, which is poorly soluble in H_2SO_4, prevents ion diffusion.

The interaction of Fe-Si with sulfuric acid over time is accompanied by active corrosion in the initial period

due to the anodic dissolution of iron:

$$Fe \rightarrow Fe^{2+} + 2e^- \quad (1)$$

followed by oxidation

$$Fe^{2+} \rightarrow Fe^{3+} + 2e^- \quad (2)$$

cathodic reactions in acidic media

$$2H^+ + 2e^- \rightarrow H_2\uparrow \quad (3)$$

Corrosion reaction upon contact with acid

$$Fe + H_2SO_4 \rightarrow FeSO_4 + H_2\uparrow \quad (4)$$

this, in turn, is accompanied by the enrichment of the ferrosilicon surface with silicon (Si) and the formation of a passivation film of silicon dioxide (SiO_2) during its oxidation

$$Si + 2H_2O \rightarrow SiO_2 + 4H^+ + 4e^- \quad (5)$$

or films of hydrated silicon dioxide

$$Si + 2H_2O \rightarrow SiO_2 \cdot nH_2O + 2H_2\uparrow \quad (6)$$

chemically inert in H_2SO_4, followed by a transition to a passive state.

When casting products from such Fe-Si alloys, it is necessary to cool them slowly along with the mold. Rapid cooling can cause metastable states to "freeze," and the formation of the Fe_3Si intermetallic compound may be partially suppressed. In this case, part of the Si will remain in the solid solution (in α-Fe) or nanometric intermetallic precipitates will form. An excessive metastable structure can affect phase distribution, and there is a risk of hot or cold cracks forming in cast parts due to internal stresses. Conditions for machining are created by thermal tempering or controlled recrystallization, which in turn can lead to the formation of brittle intermetallides and an increase in brittleness over time or under the influence of temperature.

The presence of impurities (Al, Mn, C, P, S, etc.) in Fe-Si alloys promotes the formation of secondary phases and the incorporation of some Si into complex complexes, which alters the phase distribution and structure of the alloy. At the same time, low S and P content (< 0.05%) prevents brittleness and intergranular corrosion of the alloy.

Recent studies [1-7, 9, 11] have confirmed that ferrosilicides are one of the most promising classes of materials for use in aggressive acidic environments. However, the lack of comprehensive studies comparing the corrosion resistance of pure and economically alloyed ferrosilides under high-temperature operating conditions in concentrated H_2SO_4 underscores the relevance of further research in this area.

The purpose of the work.

The aim of this study is to investigate the corrosion resistance of Fe-Si-Cr-Ni-Mo-Mn ferrosilicides in concentrated sulfuric acid over a temperature range of 25-200°C, to determine the effect of silicon content and alloying elements on the corrosion rate, and to examine the characteristics of passive film degradation.

Analysis of recent studies and publications.

The optimal composition of an Fe-Si alloy, in terms of casting properties, is as follows: 12-16% Si, up to 2.5% C (S, P < 0.05%), with the remainder being Fe. The typical structure of such an alloy consists of a ferritic matrix (Fe + Si solid solutions), free graphite inclusions (fine plates or globules), and a minimum of cementite. Due to the silicon content of up to 16%, hardness increases (~250-350 HB and higher), with a simultaneous decrease in ductility, and corrosion resistance in acids (especially in H_2SO_4) increases due to the formation of a SiO_2 film during heat treatment [12].

Obtaining more ductile alloys is possible by reducing the silicon content to 6-10% Si or by alloying with elements that increase ductility. This approach is based on addressing the fundamental issue - the presence of an intermetallic, brittle Fe_3Si matrix. The improvement in ductility is also partially achieved through process modifications or changes in the alloy's chemical composition and structure.

In the Fe-Si-C system, silicon sharply reduces the solubility of carbon in liquid and solid iron. For example, at a silicon content of >15%, the solubility of carbon in liquid Fe decreases to 0.1-0.2% at 1500°C. Excess carbon from the melt is converted into graphite (silicon "displaces" carbon from the metal into the graphite phase). When the alloy contains more than 12–13% Si, the carbon activity a_C increases, and the activity coefficient f_C at 15% Si will be >10 (carbon becomes energetically "excessive"); the system's attempt to minimize energy leads to the formation of a solid phase - graphite. The primary graphitizer in Fe-Si alloys is silicon itself. Already at >4% Si, silicon stimulates graphitization - it reduces the stability of cementite Fe_3C and promotes the precipitation of carbon as graphite. An excess of graphite reduces acid resistance but improves casting properties.

To prevent graphite precipitation, it is advisable to reduce the carbon content in the charge (< 0.05% C), use $CaO\text{-}SiO_2$ slag, and raise the melting temperature to 1580-1620°C, which temporarily increases the solubility of C, and deoxidize with Al. The effects of high S content on graphitization are mitigated by preliminary desulfurization of the melt.

The addition of Ni, Mo, Co, and Cr to the ferrosilicide composition in limited quantities (1-5% Ni, 1-2% Mo, 3-6% Cr) helps reduce brittleness [4], but does not ensure full ductility of the alloy.

Nickel has high solubility in ferrite (α-Fe) and in Fe_3Si intermetallic compounds, contributing to the stabilization of the solid solution, which in turn ensures the presence of Si in supersaturated α-Fe during cooling. In addition, Ni slows down the ordering of Fe_3Si, resulting in the formation of finer intermetallic compounds and a reduction in brittleness.

Molybdenum has limited solubility in solid Fe-Si alloys, but even a small amount of Mo significantly slows down diffusion. Mo tends to form carbides and silicides ($MoSi_2$ and $FeMoSi_2$, respectively), but at concentrations up to 1% Mo in alloys with <15% Si, these compounds will promote the formation of fine

precipitates. Overall, molybdenum acts as a solid solution hardener and promotes the formation of a fine-grained alloy structure and a reduction in brittle intergranular fracture. The impact toughness of such low-alloyed Fe-Si alloys can increase by ~10-20% from the base level.

The presence of chromium in Fe-Si alloys will promote the formation and stabilization [13] of a passive oxide film, but in sulfuric acid, its stability will depend on concentration and temperature. It is known [1, 2, 5, 12] that an alloy containing 20-35% Ni, 15-20% Cr, 2-5% Mo (analogous to Alloy 20) (Table 1). For high resistance in hot concentrated (90-98% H_2SO_4) acid, it is considered advisable to use high-nickel alloys with a content of ≥50-60% Ni, 12-17% Mo, and 14-16% Cr (equivalent to Hastelloy C-276 / Alloy C-276) (Table 1).

Table 1 - Chemical composition of selected H_2SO_4-resistant alloys, wt. %.

Alloys	Ni	Cr	Mo	Fe	Cu	Si	Mn	W	Co	Other / Notes
Hastelloy C-276	55-57	15-16	15-17	≤5	-	≤0.08	≤1	3-4.5	≤2.5	C≤0.01%, others Ni
Hastelloy C-22	56	20-22.5	12.5-14.5	2-6	-	≤0.08	≤0.5	2.5-3.5	≤2.5	Improved Cr/W balance
Hastelloy B-2	bal	-	26-30	≤2	-	≤0.1	≤1	-	-	Cr-free, for reducing acids
Alloy 20	32-38	19-21	2-3	35-45	3-4	≤1	≤2	-	-	Ti=0.6-1.0%, Nb≈0.1%
904L	23-25	19-23	4-5	bal	1-2	≤1	≤2	-	-	N≈0.1%, S low
Monel 400	63-70	-	-	2-3	28-34	≤0.5	≤2	-	-	High plasticity
Inconel 718*	50-55	17-21	2.8-3.3	bal	-	≤0.35	≤0.35	-	≤1	Al 0.2-0.8, Ti 0.6-1.15
Iron alloy with ~14%Si (ferrosilide)	≤1	≤0.5	-	bal	-	13–15	≤0.5	-	-	Hard Fe–Si phases, brittle

* contains additionally 4.75-5.5% Nb

It should be noted that Alloy 20 is significantly more resistant than 316L stainless steel in sulfuric acid, but this is true only for moderate concentrations of H_2SO_4; at high temperatures, degradation occurs and the corrosion rate increases significantly (M. Bazgir, K. Rahmanik, 2021).

When using Hastelloy (C-276, C-22) in concentrated sulfuric acid, corrosion is higher than in HCl, and for C-276 it can reach 0.5-2 mm/year (S. Hastuty, A. Widiatmoko, T. Sudiro et al., 2023).

Ferrosilicides (Duriron - Fe-Si alloys with 14-18% Si) have demonstrated high resistance in H_2SO_4 due to the SiO_2 surface passivation effect, and according to [9], the corrosion rate does not exceed 0.01 mm/year. At the same time, in industrial applications, hydrodynamic factors (flow velocity, destruction of the passivation film, etc.) have a negative impact on the corrosion rate.

In a study of the stability of Fe-Si (containing 6% Si) in boiling concentrated H_2SO_4, the authors [14] demonstrated a decrease in the corrosion rate (≈0.056 mm/year) over time (passivation of the alloy).

The corrosion resistance of Fe-Si alloys with 8-20% Si content in H_2SO_4 at 250°C was investigated in [15] using potentiometric polarization and potential decay analysis. It was shown that the passivity of alloys with 14% Si is controlled by the formation of a SiO_2 film with low electrical conductivity. At Si contents below 14%, the alloy's behavior is determined by a passive iron oxide film. A restoration of passivity was observed at Si contents of 14% and 16% following a potential drop, which was explained by self-passivation after the dissolution of the iron oxide film and the saturation of the surface with Si.

A comparison of the corrosion resistance in 10% and 20% H_2SO_4 solutions of an alloyed intermetallic coating composed of Fe_3Si, applied to the surfaces of AISI420 and AISI304 stainless steels containing Cr and Ni, and to the surface of A3 carbon steel, was conducted in the study [16] using an electrochemical method and static immersion tests. It was confirmed that, due to the presence of Cr and Ni alloying elements, the Fe_3Si coating was dense, relatively thick, and had only a few defects, which helped ensure the protection of stainless steel against surface corrosion. The pronounced passivation of Fe_3Si in sulfuric acid was confirmed.

Changes in the phase composition, microstructure, and pore structure of porous pressed Fe-Si samples obtained by the synthesis of elemental powders, as well as corrosion resistance to a sulfuric acid solution (at a concentration of 160 g/l), were investigated in [17]. The following sequence of phase formation was established: α-Fe, Fe_3Si, η-Fe_5Si_3, and ε-FeSi during sintering. A two-phase nature of the corrosion kinetics of the Fe-Si alloy was revealed, with average corrosion rates of 0.00211 %/year and 0.00118 %/year, respectively.

The authors of a study on the corrosion resistance of Fe-Si alloys in boiling solutions of 95% and 50% sulfuric acid [18] found that the critical Si content for passivation lies in the range of 9-10% Si and 12-15% Si in 95% and 50% acid, respectively. The oxide film formed on the surface of passivated Fe-Si alloys was investigated using X-ray diffraction and scanning microscopy. It was found that the passivation film

consisted of an amorphous oxide with an Si/O atomic ratio of approximately 0.5, and its growth rate depended on the alloy composition and acid concentration.

The feasibility of using Fe-Si alloy in boiling sulfuric acid and hydrogen iodide in the thermochemical hydrogen production process was investigated in [19]. It was confirmed that although the corrosion resistance of the Fe-Si alloy increases with increasing Si content, the material becomes brittle. Using the chemical vapor deposition method, a Fe-Si alloy with a graded composition (CG Fe-Si) was preliminarily prepared, containing 14% Si on the surface and 3% Si on the substrate. The resulting CG Fe-Si alloy exhibited corrosion resistance in boiling H_2SO_4 (at a concentration of 17.7 kmol/m³) equivalent to that of a Fe-Si alloy with 12% Si; however, after 300 hours of immersion in the acid, the SiO_2 film on the surface became prone to delamination around areas with microcracks caused by cooling during chemical deposition.

Research results and discussion. The smelting of experimental Fe-Si alloys was carried out in an IST-016 induction furnace at the laboratory of the Department of Metallurgy at DSTU according to the following procedure.

In the first stage, in accordance with the theoretical rationale outlined above, the charge was properly prepared by refining the cast iron to remove sulfur to the specified levels (less than 0.05% S). Desulfurization of the molten cast iron was achieved by blowing dispersed magnesium (99.9% Mg, manufactured in China) through a submerged tuyere according to the method described in [20]. The resulting molten refined cast iron was poured into cast iron molds. In the next stage, by remelting the steel billet and refining the melt in the furnace, steel castings with the specified chemical composition were obtained.

After forming a single charge from refined ingots of cast iron, steel, and ferroalloy (FeSi45) -used to produce a molten metal with a silicon content of 6-15% Si - the charge was loaded into the crucible of the induction furnace. During the smelting process, slag was skimmed off the surface of the metal bath. A portion of the Fe-Si metal melt was left in the furnace crucible to form a “slurry” and increase the degree of incorporation of the alloying elements added in subsequent stages.

In the second stage of melting, the calculated amount of refined cast iron was added to the resulting Fe-Si melt, and after its incorporation, FeSi45 and alloying elements (FeCr, Mo, Ni) were added. During the absorption of the alloying elements, the melt was protected from the effects of atmospheric oxygen by blowing argon (at a flow rate of 0.05 m³/min) onto the surface of the bath through a tube located under a graphite plug at the furnace throat.

During the melting process and prior to pouring, the bath temperature was measured. A “Smotrich-5P” partial-emission pyrometer and TS360309 immersion thermocouple blocks with a “Heraeus” Digitemp DTK 01-T-II digital temperature meter were used. The pouring temperature of the resulting melts was determined relative to the liquidus temperature of the expected composition; an excess temperature gradient of 83-96 degrees was maintained, taking into account heat losses during transfer to the ladle and during pouring into preheated (600-620°C) sand-clay molds.

Table 2 – Results of elemental analysis of experimental Fe-Si alloys.

№ alloy	Conditional marking	Contents, %					
		Fe	Mn	Si	Cr	Ni	Mo
1	FS17Cr4	75.78	1.82	17.7	3.9	0.21	0.04
2	FS19Cr3NM	72.01	2.57	18.97	3.69	1.47	1.08
3	FS24Cr6N2M	64.94	1.46	23.99	6.37	1.74	1.23
4	FS27Cr6NM	49.45	6.67	27.67	6.16	1.11	0.6
5	FS12Cr8N2	74.26	1.43	12.38	7.85	2.15	0.05
6	FS25Cr6NM	66.1	1.32	24.3	6.1	1.62	1.1
7	FS16Cr6N2M	77.2	1.2	15.9	6.2	1.9	1.05

Data on the fluidity, linear shrinkage, shrinkage cavity volume, and porosity of the alloys were obtained using standard methods. To determine the casting properties of the experimental alloys, a standardized casting test with a constant cross-section and central metal feed was used. The hardness of the alloys was determined using the Brinell method on a TSh-2M device.

Prior to testing the obtained experimental alloys for corrosion resistance [10], a SiO_2 passivation film was formed on their surfaces. According to the theory, film formation proceeds as follows: Si → SiO_2 (dense film); Fe → Fe_2O_3 (outer layer); Ni → NiO (in the presence of Ni, it reacts with Fe_2O_3); Cr → Cr_2O_3; carbon-oxidizes locally but burns off rapidly from the surface layer at 800-900°C.

In this process, Si forms a dense layer of SiO_2 that inhibits further oxidation, causing the surface to passivate rapidly, while the deeper alloy layers remain virtually unaffected by oxidation. To create a protective oxide film of SiO_2 on the surface of the castings, controlled surface oxidation was ensured rather than oxidation of the entire volume, taking into account the following conditions:

- the temperature during heat treatment in the furnace was maintained at 850-1000°C for 3-4 hours, with the castings held in the dry air atmosphere of the working space;

- a moderate heating rate (up to 5 °C/min) and cooling of the castings in the furnace to <200°C were intended to prevent cracking and destruction of the SiO_2 passivation film.

To calculate the thickness (x) of the SiO_2 film on Fe-Si alloys (including those doped with Cr, Ni, and Mo) for a heat treatment duration (t), the parabolic oxidation law was used, in μm:

$x^2 = k_P \cdot t$, where k_P is the parabolic rate constant (μm²/h). This is due to the fact that at high heat treatment temperatures of ferrosilicide, the film growth rate is limited by the diffusion of ions through the already formed oxide layer.

Figure 2 shows a graph of the increase in the thickness of the oxide passivation film during heat treatment for the studied alloys No. 1, 2, 3, and 7 at holding temperatures of 800°C (a) and 1100°C (b), respectively.

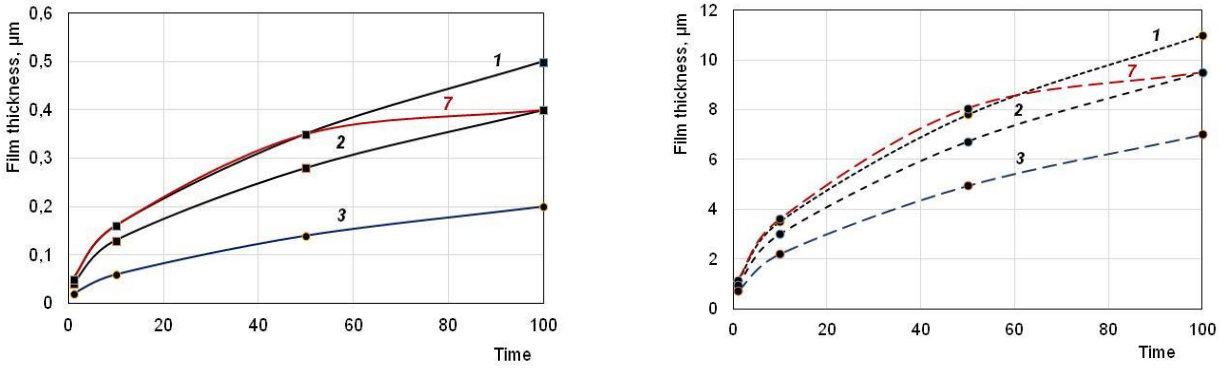

a b

Fig. 2. The kinetics of the growth in thickness of the oxide passivation film during heat treatment for alloys No. 1, 2, 3, and 7 at holding temperatures of 800°C (a) and 1100°C (b), respectively.

Annealing alloy No. 1 at 1100°C for 5 to 10 hours (Fig. 2, b) results in the formation of a film thick enough to protect the ferrosilicide surface. With longer aging, the film thickness reaches 11 μm, which can lead to cracking due to internal stresses in the oxide and the formation of microcracks. At temperatures of 1000-1100°C, SiO_2 begins to crystallize into α-cristobalite, which may contribute to the formation of micropores at the oxide grain boundaries.

The film growth rate slows down over time due to a diffusion barrier formed by the SiO_2 layer, which blocks the influx of oxygen atoms into the metal. The critical film thickness, at which it retains plasticity, high strength, and does not delaminate, is 5-7 μm. If the thickness exceeds 10 μm, the accumulated stress energy can lead to spontaneous delamination of the film.

The film's density is determined by its ability to block oxygen from reaching the metal and is calculated using the Pilling-Bedworth ratio (PBR) [10], which is approximately 1.88 for SiO_2. Under conditions where PBR < 2.5, the film is continuous and completely covers the metal surface without breaking away from its own volume. At heat treatment temperatures of 800-900°C, the film remains amorphous, ensuring ideal density.

A positive effect of Fe-Si alloying elements on the formation of the passivation film has been observed. Thus, Ni improves the plasticity of the metal beneath the film, partially compensating for the brittleness of the high-silicon matrix, and enhances the film's adhesion (creating an "anchor effect" at the metal-oxide in

\]terface), preventing its delamination during cooling, mechanical loading, or vibrations. Mo increases the strength of the metal substrate itself at 800-900 °C and resistance to pitting corrosion, which can occur if the acid contains chloride impurities. Cr strengthens the film itself by partially dissolving in it, which increases its fracture toughness. As a result, a multilayer structure forms instead of pure SiO_2. Directly on the metal is a dense SiO_2 film, and on the outside is a thin layer of iron chromites ($FeCr_2O_4$) or chromium oxide (Cr_2O_3), which makes the film less brittle.

However, it is not the thickness but the chemical stability of the passivation film in an acidic liquid medium that plays the key role. Upon contact with sulfuric acid, the iron on the surface begins to dissolve, but the silicon remains. It reacts with water to form hydrated silicon dioxide (6). This layer becomes extremely dense, chemically inert, and insoluble in acid.

To assess the tendency to form a stable passivation effect in Cr-, Ni-, and Mo-alloyed ferrosilicides (Table 2), the equivalent silicon content Si_{eq} was calculated, which accounts for the influence of the alloying elements:

$$Si_{eq} = Si + k_{Cr} \cdot Cr + k_{Mo} \cdot Mo + k_{Ni} \cdot Ni \quad (7)$$

k_{Cr}, k_{Mo} та k_{Ni} - empirical equivalents adapted for SiO_2 passivation (Olssand and Landolf, 2023), which are 0.4, 0.6, and 0.2, respectively.

For example, for alloy No. 2 (Table 2), the calculated Sieq value is ≈ 22.85%, indicating a 1.2-fold "increase" in the equivalent Si content upon alloying. In general, the oxidation of 3–6% Cr introduced into Fe-Si with 15-19% Si ensures the formation of a combined protective layer of SiO_2 + Cr_2O_3 in concentrated H_2SO_4, but one that is less continuous than at >24% Si.

The corrosion rate of such complex multicomponent alloys in hot sulfuric acid depends heavily not only on its temperature but also on the acid concentration (diluted or concentrated), the presence of oxidizing agents, the formation of Fe_3Si and Fe_5Si_3 phases, and the Fe-Si structure of the products, which depends on the manufacturing method and heat treatment, as well as the flow velocity of the medium (turbulence, erosion development, etc.).

According to [9], when ferrosilicide is exposed to sulfuric acid, active corrosion is observed at Si_{eq} < 16%; at 16-20% Si_{eq}, partial passivation occurs; at 20-24% Si_{eq}, an unstable passivation film forms; and as Si_{eq} increases beyond 24%, stable passivation occurs.

The characteristic temperature ranges of the corrosion process can be identified as follows: stable passivation (25-80°C), a transitional regime (80-150°C), and degradation of the passive state (150-200°C). At temperatures > 150°C, degradation of the passivation film is observed, with the corrosion rate of the Fe-Si alloy increasing by an order of magnitude compared to when Si content is > 24% and when Si < 15%.

At a concentration of 98%, sulfuric acid acts as a passivator; it is a strong oxidizing agent that instantly forms a protective layer of SiO_2 enriched with chromium oxides on the surface of the high-silicon alloy. At the same time, while the passivation film is stable at an acid temperature of 25°C, at 200°C the acid is extremely aggressive, actively dissociates, and the kinetic energy of the molecules allows them to penetrate through the SiO_2 film layer. The film undergoes “chemical erosion.” The introduced dopants (Mo, Cr) stabilize the passive state and prevent catastrophic destruction of the passivation film.

For X-ray diffraction analysis of the experimental alloys, a DRON-4M diffractometer with digital data acquisition and a Cu-Kα X-ray tube was used. The “Match! 4.2” software was used for the interpretation and calculation of the diffractogram.

The phase and elemental compositions of the surfaces of experimental alloy samples No. 1, 2, 4, and 5 are shown in Fig. 3.

Electrochemical corrosion tests were performed on samples of the experimental alloys (Table 2). Classical potential range from $E_{(ref)}$ to E_1, where $E_{(ref)}$ = -2.00 V; E_1 = 2.00 V. V = 0.74 mV/s - scan rate; current range ±45 mA.

Using the results of the electrochemical corrosion test (corrosion current icorr, mA/cm²) and the Arrhenius equation

$$i_{corr(T)} = i_{corr} \cdot \exp(-E_a/(RT)) \quad (8)$$

to account for the effect of changes in acid temperature in the range of 25-200°C, as given by [9]

$$V_{corr} = (3{,}27 \cdot 10^{-3} \cdot i_{corr} \cdot EW)/\rho \quad (9)$$

calculated the corrosion rate, mm/year, of the experimental alloys (Table 2) taking into account operation in “passive” (immersion in 98% H_2SO_4) and “industrial” (turbulent flows of 98% H_2SO_4, erosion) modes, with consideration of the stabilizing effect of Cr and Mo. In equation (9): *EW* - equivalent weight of the alloy, g/eq; ρ - density of the alloy, g/cm³.

The dependence of the corrosion rate (material loss) on the acid temperature during operation of the alloys (Table 2) in the “industrial” mode is shown in Fig. 4.

Alloys No. 4, 3, and 6 (Table 2) exhibit the best expected corrosion resistance (Fig. 4) within the studied temperature range (25-200°C). At the same time, an increase in the Si content in ferrosilicide to >15%, as shown above, is accompanied by increased brittleness, the development of microcracks, and a disruption in the density of the passivation film, and requires the development of a special casting technology and imposes limitations on operating conditions.

Taking into account the results obtained, the following composition can be considered optimal for an economically alloyed ferrosilicon with increased resistance in H_2SO_4, suitability for machining, and “industrial” operating conditions, in %: 15.5-17.5 Si; 4.5-6.0% Cr; 1.5-2.0% Ni; 1.2-1.5% Mo; 0.1-0.4% C.

The experimental data obtained can be used to develop new corrosion-resistant materials and optimize the composition of ferrosilides for use in high-temperature, aggressive environments containing concentrated sulfuric acid.

Conclusions

(1) The casting and selected mechanical properties of experimental Fe-Si alloys containing 12-27% Si and alloyed with Cr, Ni, and Mo were investigated.

(2) It was confirmed that the silicon content in Fe-Si alloys is the primary factor determining the corrosion resistance of ferrosilicides in concentrated sulfuric acid. At Si contents below 15%, partial formation of a passivation film was observed; at 16-20% Si, a partially stable SiO_2 film layer forms; and when the Si content increases to 24% or higher, a continuous protective SiO_2 film forms, which reduces the alloy’s corrosion rate by 1-2 orders of magnitude.

(3) The following characteristic temperature regions of the corrosion process have been identified: stable passivation (25-80°C), a transitional regime (80-150°C), and degradation of the passive state (160-200°C). At temperatures >150°C, degradation of the passivation film is observed, with the corrosion rate of the Fe-Si alloy increasing by an order of magnitude when the Si content is > 24% compared to when Si < 15%. The corrosion rate was calculated based on electrochemical parameters using passivation models and Arrhenius-type temperature dependence. It was confirmed that the main factor determining corrosion resistance is the silicon content. The existence of a critical threshold for Si content was demonstrated; upon reaching this threshold, a continuous SiO_2 passive film forms, which reduces the corrosion rate by 1-2 orders of magnitude.

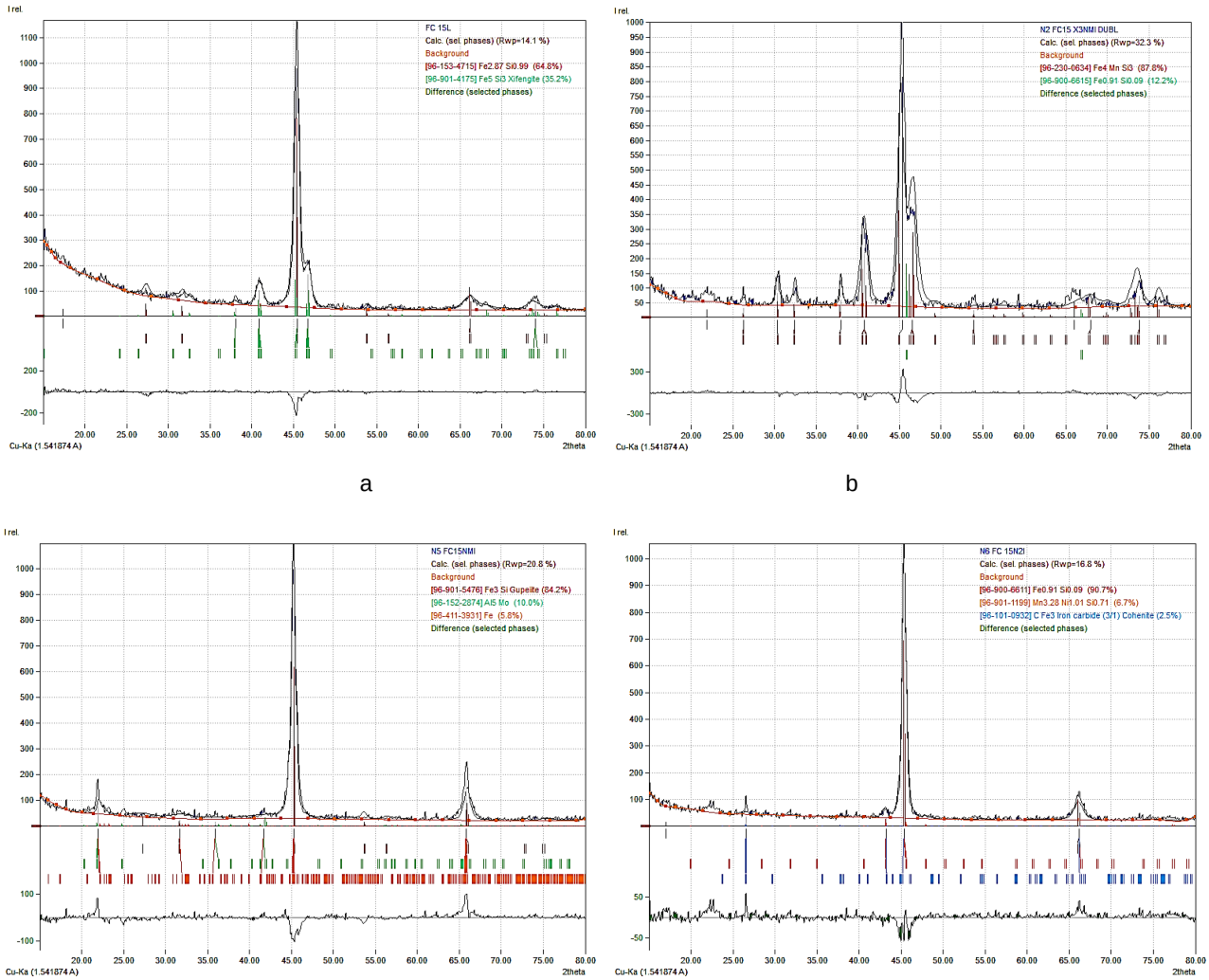

Fig. 3. Phase and elemental compositions of the surfaces of alloy samples No. 1 (a), No. 2 (b), No. 4 (c), and No. 5 (d) (Table 2): a) 64.8% $Fe_{2.87}Si_{0.99}$; 35.2% Fe_5Si_3 and Fe 82.3%; Si 17.7%; b) 87.8% $Fe4MnSi_3$; 12.2% $Fe_{0.91}Si_{0.09}$ and Fe 65.7%; Si 21.0%; Mn 13.3%; c) 84.2% Fe_3Si; 10.0% Al5Mo; 5.8% Fe and Fe 77.9%; Si 12.1%; Al 5.9%; Mo 4.2%; d) 90.7% $Fe_{0.91}Si_{0.09}$; 6.7% $Mn_{3.28}Ni_{1.01}Si_{0.71}$; 2.5% Fe_3C and Fe 88.8%; Si 4.8%; Mn 4.7%; Ni 1.5%; C 0.2%, respectively.

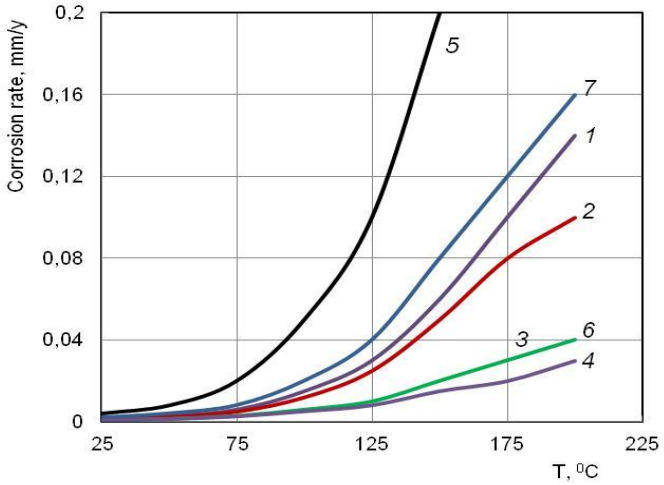

Fig. 4.. Calculated expected corrosion rates of the experimental Fe-Si alloys (Table 2) in concentrated acid (98% H_2SO_4) as a function of acid temperature. The curve for alloy No. 6 practically coincides with the curve for alloy No. 3.

(4) It has been shown that the actual corrosion rate of ferrosilicide is determined not only by composition but also by the operating conditions of the alloys, namely, medium turbulence, erosion development, and the presence of H_2O and Fe^{3+}; the difference in material mass loss between laboratory and industrial conditions can be 10-20 times.

(5) It has been established that the formation of a continuous passive SiO_2 film, as well as the formation of Fe_3Si and Fe_5Si_3, are key factors in ensuring the enhanced corrosion resistance of ferrosilicides in hot concentrated H_2SO_4. A critical silicon content of >24% Si can be identified, at which the transition to a stable passive state of the alloy occurs even when the acid temperature rises to 200°C in systems with aggressive hydrodynamics. At the same time, increasing the Si content in ferrosilicides beyond 15% is accompanied by increased brittleness, the development of microcracks with acid penetration, and a disruption of the passivation film density, and requires the development of special casting technologies and operating conditions.

(6) Obtaining more ductile ferrosilides is possible through alloying with elements that enhance ductility by addressing the underlying issue - the presence of an intermetallic brittle matrix (Fe_3Si). It is advisable to introduce Ni, Mo, and Cr into the Fe-Si alloy in limited quantities, which reduces brittleness but still does not make the alloy fully ductile.

(7) The addition of chromium to an Fe-Si alloy enhances surface passivation through the formation of Cr_2O_3, but is effective only with sufficient Si content; molybdenum stabilizes the passive state at acid temperatures above 150°C and reduces the rate of localized corrosion; nickel has a partial effect on electrochemical parameters but is not a determining factor at high acid temperatures. Oxidation of 3-6% Cr added to a Fe-Si alloy with 15–19% Si ensures the formation of a combined protective layer of SiO_2 + Cr_2O_3 in concentrated H_2SO_4, but one that is less continuous than at >24% Si

(8) Based on the experimental results, the following composition can be considered optimal for an economically alloyed ferrosilicon with increased resistance in H_2SO_4, suitability for machining, and “industrial” operating conditions: 15.5-17.5% Si; 4.5-6.0% Cr; 1.5-2.0% Ni; 1.2-1.5% Mo; 0.1-0.4% C.

References

1. Fontana, M. G. Corrosion Engineering. (1986). 3rd ed. *New York: McGraw-Hill*.
2. Uhlig, H. H., Revie, R. W. (2008). Corrosion and Corrosion Control. 4th ed. *Hoboken: Wiley*. https://doi.org/10.1002/9780470872864
3. Davis J.R. Corrosion of Nickel and Nickel Alloys. *ASM International*. 2000. https://doi.org/10.31399/asm.tb.cnia.t59290001.
4. Wranglén, G. (1985). An Introduction to Corrosion and Protection of Metals. *Chapman & Hall.*
5. Marcus, P. (Ed.). (2011). Corrosion Mechanisms in Theory and Practice. https://doi.org/10.1201/b11020
6. Olsson, C.-O.A., Landolt, D. (2003). Passive films on stainless steels-chemistry, structure and growth. *Electrochimica Acta*, 48, 1093-1104. https://doi.org/10.1016/S0013-4686(02)00841-1.
7. Frankel, G. S. (1998). Pitting corrosion of metals: A review. *Journal of The Electrochemical Society,* 145(6), 2186-2198. https://doi.org/10.1149/1.1838615
8. ASTM G31-21. Standard Practice for Laboratory Immersion Corrosion Testing of Metals. *ASTM International*. 2021.
9. Jennings, H. S. (2006). ASM Handbook, Corrosion - Environments and Industries. *ASM International,* 13C, 690-703.
10. Standard Practice for Calculation of Corrosion Rates and Related Information from Electrochemical Measurements (ASTM 102-89). https://doi.org/10.1520/G0102-89R15E01
11. Stawarz M. (2023). Crystallization of Fe_2Si and Fe_5Si_3 phases in high-alloy cast irons. *Crystals*. https://doi.org/10.3390/cryst13071033
12. Srivastava, S. K. & Crook, P. (2016). Unpublished Work. *Haynes International*.
13. Li, W., Xu,, C., Chen K., et al. (2022). Corrosion of Fe-Cr-Si alloys in oxidizing and sulphidizing environments coatings. *Coatings*. https://doi.org/10.3390/coatings12101588
14. Kwon, H.-C., Kim, D.-J., et al. (2011). Corrosion characteristics of Fe–Si, Ni–Ti and Ni alloys in sulfuric acid environments. *Korean Journal of Materials Research*.
15. Omurtag, Y., & Doruk, M. (). Some investigations on the corrosion characteristics of Fe-Si alloys. *Corrosion Science*, 10(4), 225-231.
16. Tang, C., Wen, F., Chen, H., Liu, J., Tao, G., Xu, N., & Xue, J. (2019). Corrosion characteristics of Fe3Si intermetallic coatings prepared by molten salt infiltration in sulfuric acid solution. Journal of Alloys and Compounds, 778, 972–981. https://doi.org/10.1016/j.jallcom.2018.11.198
17.Shen, B., He, Y., Wang, Z., Yu, L., Jiang, Y., & Gao, H. (2020). Reactive synthesis of porous FeSi intermetallic compound. Journal of Alloys and Compounds, 826, 154227. https://doi.org/10.1016/j.jallcom.2020.154227
18. Onuki, I., Futakawa, M., Tayama, I. Corrosion resistance of Fe-Si alloys in boiling sulfuric acid. *Materials for thermochemical processes*. https://doi.org/10.2472/JSMS.46.1041
19. Ioka, I., Mori, J., Kato, C. et al. (1999). The characterization of passive films on Fe-Si alloy in boiling sulfuric acid. *Journal of Materials Science Letters*, 18, 1497-1499.
20. Sigarev, E. N., Chernyatevich, A. G., Chubin, K. I. et al. (2011). Desulfurization of hot metal by the injection of disperse magnesium through a submerged rotating tuyere. *Steel Transl*, 41, 487-491. https://doi.org/10.3103/S0967091211060155

Надіслано до редакції / Received: 03.12.2025
Прорецензовано / Peer-Reviewed: 12.02.2026
Прийнято до друку / Accepted: 16.03.2026
Опубліковано / Published: 30.03.2026

ISSN 3083-7219 (Print), ISSN 3083-7227 (Online)
Теорія і практика металургії, 2026, № 1
Theory and Practice of Metallurgy, 2026, No. 1

https://doi.org/10.15802/tpm.1.2026.08

UDC 669.15'26-198:628.477.6:544.3

***Stepanenko D. O.*[1], *Togobytska D. M.*[2,*], *Semiryagin S. V.*[3], *Povorotnya I. R.*[4], *Belkova A. I.*[5]**

Prospects for recycling leather industry waste as a source of chromium-containing raw materials: physicochemical analysis of the Fe–Cr–P–O system

[1] ORCID: 0000-0001-5913-2284. Інститут чорної металургії ім. З. І. Некрасова НАН України, Україна
[2] ORCID: 0000-0001-6413-4823. Інститут чорної металургії ім. З. І. Некрасова НАН України, Україна
[3] ORCID: 0000-0002-8733-3216. ДП «НПІ» ДНІПРОЕНЕРГОСТАЛЬ», Україна
[4] ORCID: 0000-0001-5872-7403. Інститут чорної металургії ім. З. І. Некрасова НАН України, Україна
[5] ORCID: 0000-0001-8519-9351. Інститут чорної металургії ім. З. І. Некрасова НАН України, Україна
*Email: dntog@ukr.net

***Степаненко Д. О.*[1], *Тогобицька Д. М.*[2,*], *Семірягін С. В.*[3], *Поворотня І. Р.*[4], *Белькова А. І.*[5]**

Перспективи рециклінгу відходів шкіряної промисловості як джерела хромовмісної сировини: фізико-хімічний аналіз системи Fe–Cr–P–O

[1] ORCID: 0000-0001-5913-2284. Iron and Steel Institute of Z. I. Nekrasov National Academy of Sciences of Ukraine, Ukraine
[2] ORCID: 0000-0001-6413-4823. Iron and Steel Institute of Z. I. Nekrasov National Academy of Sciences of Ukraine, Ukraine
[3] ORCID: 0000-0002-8733-3216. Subsidiary Enterprise “Scientific and Design Institute “DNEPROENERGOSTAL”, Ukraine
[4] ORCID: 0000-0001-5872-7403. Iron and Steel Institute of Z. I. Nekrasov National Academy of Sciences of Ukraine, Ukraine
[5] ORCID: 0000-0001-8519-9351. Iron and Steel Institute of Z. I. Nekrasov National Academy of Sciences of Ukraine, Ukraine
*Email: dntog@ukr.net

Abstract. *The paper considers thermodynamic and physicochemical regularities of phosphorus behavior in multicomponent systems of Fe–Cr–P, Fe–Cr, Fe–P, Cr–P and Fe–Cr–P–O when using chromium-containing man-made raw materials, in particular substandard ores and leather industry wastes. The analysis of the current state of the raw material base of chromium in Ukraine is carried out and the expediency of attracting alternative sources of chromium-containing raw materials is substantiated. The literature data on phase equilibrium, thermodynamic properties and features of the formation of phosphide and oxide-phosphate phases in these systems is summarized. It has been established that the main problem of the use of man-made raw materials is the increased content of phosphorus, which negatively affects the properties of the metal. It is shown that solid-phase reduction creates favorable conditions for controlling the distribution of phosphorus between the metal and slag phases. The influence of temperature, charge composition and interatomic interaction on the stability of phosphide phases and the efficiency of dephosphorization has been determined. Particular attention is paid to the role of the magnetic state of iron and the conditions for the formation of solid solutions and intermetallics in the Fe–Cr–P system. The results obtained can be used to develop energy-efficient technologies for the processing of chromium-containing waste and substandard ores in order to reduce import dependence and increase the environmental safety of metallurgical production.* ***The purpose of the work*** *is to study the thermodynamic and physicochemical patterns of phosphorus behavior in the Fe–Cr–P, Fe–Cr, Fe–P, Cr–P and Fe–Cr–P–O systems when using complex chromium-containing raw materials (substandard ores and leather industry wastes), as well as to substantiate the possibility of controlled phosphorus removal in order to improve the quality of the obtained metals and alloys.* ***Research methodology:*** *A systematic analysis of the scientific and technical literature on phase equilibrium and thermodynamic properties of Fe–Cr–P, Fe–Cr, Fe–P, Cr–P, Fe–Cr–P–O systems was carried out. composition of the charge and reducing medium for the distribution of phosphorus between phases.* ***Scientific novelty:*** *The relationship between the parameters of the interatomic interaction (ZY, d, tgα, ρl) and the thermodynamic stability of phosphide phases has been established.* ***Practical significance:*** *The expediency of using leather industry waste as an alternative source of chromium for metallurgy has been substantiated. Approaches to reducing the phosphorus content in the pro-*

© Степаненко Д. О., Тогобицька Д. М., Семірягін С. В., Поворотня І. Р., Белькова А. І., 2026
© Stepanenko D. O., Togobytska D. M., Semiryagin S. V., Povorotnya I. R., Belkova A. I., 2026

This is an Open Access article under the CC BY 4.0 license https://creativecommons.org/licenses/by/4.0/

cessing of complex raw materials, which allows to improve the quality of steel and ferroalloys, have been proposed. The optimal temperature and thermodynamic conditions for the implementation of dephosphorization processes have been determined. The results can be used in the development of energy-efficient technologies for solid-phase recovery and recycling of waste. It helps to reduce Ukraine's import dependence on chromium-containing raw materials and increase the environmental safety of production.
Keywords: *waste recycling, leather industry, chromium-containing raw materials, Fe–Cr–P–O system, thermodynamic modeling, ferrochrome, chromium utilization, phase transformations.*

Анотація. *У роботі розглянуто термодинамічні та фізико-хімічні закономірності поведінки фосфору в багатокомпонентних системах Fe–Cr–P, Fe–Cr, Fe–P, Cr–P та Fe–Cr–P–O при використанні хромовмісної техногенної сировини, зокрема некондиційних руд і відходів шкіряної промисловості. Проведено аналіз сучасного стану сировинної бази хрому в Україні та обґрунтовано доцільність залучення альтернативних джерел хромовмісної сировини. Узагальнено літературні дані щодо фазових рівноваг, термодинамічних властивостей і особливостей утворення фосфідних та оксидно-фосфатних фаз у зазначених системах. Встановлено, що основною проблемою використання техногенної сировини є підвищений вміст фосфору, який негативно впливає на властивості металу. Показано, що твердофазне відновлення створює сприятливі умови для керування розподілом фосфору між металевою та шлаковою фазами. Визначено вплив температури, складу шихти та міжатомної взаємодії на стабільність фосфідних фаз і ефективність дефосфорації. Особливу увагу приділено ролі магнітного стану заліза та умовам утворення твердих розчинів і інтерметалідів у системі Fe–Cr–P. Отримані результати можуть бути використані для розробки енергоефективних технологій переробки хромовмісних відходів і некондиційних руд з метою зниження імпортозалежності та підвищення екологічної безпеки металургійного виробництва.* ***Метою роботи*** *є дослідження термодинамічних і фізико-хімічних закономірностей поведінки фосфору в системах Fe–Cr–P, Fe–Cr, Fe–P, Cr–P та Fe–Cr–P–O при використанні комплексної хромовмісної сировини (некондиційних руд і відходів шкіряної промисловості), а також обґрунтування можливості керованого видалення фосфору з метою підвищення якості отриманих металів і сплавів.* ***Методика дослідження:*** *Проведено системний аналіз науково-технічної літератури щодо фазових рівноваг і термодинамічних властивостей систем Fe–Cr–P, Fe–Cr, Fe–P, Cr–P, Fe–Cr–P–O. Застосовано метод оцифрування графічних даних (діаграм стану, залежностей) для формування репрезентативних вибірок. Виконано аналіз міжатомної взаємодії на основі концепції спрямованого хімічного зв'язку з використанням параметрів (Z^Y, d, tgα, ρl). Проведено порівняльний аналіз впливу температури, складу шихти та відновлювального середовища на розподіл фосфору між фазами.* ***Наукова новизна:*** *Встановлено взаємозв'язок між параметрами міжатомної взаємодії (Z^Y, d, tgα, ρl) та термодинамічною стабільністю фосфідних фаз.* ***Практична значимість:*** *Обґрунтовано доцільність використання відходів шкіряної промисловості як альтернативного джерела хрому для металургії. Запропоновано підходи до зниження вмісту фосфору при переробці комплексної сировини, що дозволяє підвищити якість сталі і феросплавів. Визначено оптимальні температурні та термодинамічні умови для реалізації процесів дефосфорації. Результати можуть бути використані при розробці енергоефективних технологій твердофазного відновлення та рециклінгу відходів. Сприяє зменшенню імпортозалежності України щодо хромовмісної сировини та підвищенню екологічної безпеки виробництва.*
Ключові слова: *рециклінг відходів, шкіряна промисловість, хромовмісна сировина, система Fe–Cr–P–O, термодинамічне моделювання, ферохром, утилізація хрому, фазові перетворення.*

Introduction

The current state of ferrous metallurgy is characterized by the search for innovative solutions to increase profitability and minimize man-made impact on the environment. The global market situation causes the transformation of the production structure and changes in the positions of key players in the segments of high-quality metal and pig iron [1-3].

One of the promising areas is the attraction of non-traditional materials, in particular waste from the leather industry, as well as substandard ores containing chromium. The choice of chromium is motivated by its irreplaceable role in the production of high-alloy and specialized steels - such as stainless, Cr–Mo alloys, heat-resistant materials and tool alloys, which are in demand in the domestic market. Chromium is one of the most important alloying elements in ferrous metallurgy, which increases the corrosion resistance, heat resistance, wear resistance and hardness of steel. Chromium-containing steels are widely used in power engineering, aviation and automotive industries, chemical engineering, as well as in the production of stainless steels. Chromium-containing steels are of particular importance due to their advantages, namely: increased corrosion resistance in aggressive environments; stability of the structure at high temperatures; increasing the durability of parts and structures; the possibility of reducing the weight of structures due to higher strength characteristics.

Ukraine is experiencing a shortage of its own raw material base of chromium due to limited reserves of deposits [4]. The main manifestations of chromite mineralization are concentrated in the massifs of the Middle Buzhzhia (interspersed ores, lenses, chromium-nickel weathering crusts). The development of the Kapitanovske deposit [5], which can partially meet the needs of metallurgy, with chromite ore is promising. At the same time, the deposits available in Ukraine (in particular, the Middle Buzhzhia) are characterized by a low content of Cr_2O_3 (9–25 %) and an increased amount of impurities of iron, nickel and silicates [5]. This creates significant technological barriers. In particular, traditional beneficiation methods (gravitational, magnetic) are effective only at a content of ≥30–35 % Cr_2O_3. An additional problem is the fine-grained structure of ores, which complicates separation even when using modern equipment.

One of the promising wastes containing a significant amount of chromium oxide, about 70%, is ash from leather production waste [6]. These wastes are considered as potential raw materials for the production of ferrochrome [7, 8].

It has been established [9, 10] that ash of leather production, due to its biogenic origin, is marked by a

high concentration of phosphorus-containing compounds. The use of such raw materials within the framework of traditional ferroalloy production technologies will lead to the inevitable transition of phosphorus into the melt, which will lead to its increased content in finished alloys [11].

Despite the need to solve the problem of phosphorus removal, the involvement of leather production waste in recycling has a comprehensive positive effect. In particular, this contributes to increasing the level of occupational safety and health, reducing the environmental burden on industrial regions, as well as minimizing environmental pollution, which generally improves life safety indicators [12].

Thus, although waste can replace part of the traditional raw materials, its use in classic smelting schemes has significant limitations.

One of the most promising areas is the use of technologies for solid-phase reduction of complex charge containing waste. The essence of the technology is that the reduction of chromium and iron oxides occurs not in melt conditions, but in the solid phase, at temperatures lower than the melting point of the charge. For iron oxides ($Fe_2O_3 \rightarrow Fe_3O_4 \rightarrow FeO \rightarrow Fe$), the initial stages of transformation usually begin as early as ~300–400 °C (especially in hydrogen reduction), intensive conversion to metallic iron often occurs in the range of ~500–900 °C depending on the reducing agent (H_2, CO or carbon agents), particle size, and charge porosity [13]. For chromium oxides (Cr_2O_3 and chromite), solid-phase (carbothermal or gas-phase) reduction usually requires higher temperatures: the initial stages of reduction and formation of chromium carbides/carbonitrides are observed at ~800–1100 °C, and the complete reduction of Cr_2O_3 to metallic chromium in a "pure" carbothermal process often begins to occur closer to 1200 °C and above [14]. The main advantages of solid-phase Recovery should be attributed [15-17]:

- the ability to control diffusion processes and create conditions for the oxidation of phosphorus;
- reducing the transition of unwanted impurities, in particular phosphorus, to the metallic phase and directing it to the slag phase;
- reduced energy consumption due to lower process temperature;
- the possibility of processing substandard ores and leather industry waste.

Thus, solid-phase recovery allows you to combine environmental and economic advantages – rational use of waste, reduce the burden on the environment and at the same time obtain a precursor, followed by the production of steel and ferroalloy.

Materials and methods of research. A significant number of scientific studies have been devoted to the study of multicomponent systems Fe–Cr–P, Fe–Cr–P, and Fe–Cr–P–O [18-25]. The accumulated array of data on phase equilibrium and physicochemical properties of these systems has become the basis for modern technology of steel smelting and optimization of their chemical composition.

At the same time, despite the in-depth study of the main phases, a number of complex compounds potentially formed in such systems remain insufficiently studied. In particular, the study of their physical and chemical nature in the context of phosphorus removal from melts is of particular relevance, since a deep understanding of the mechanisms of formation of these compounds is critically important for the development of effective methods of dephosphorization and obtaining high-quality metal products.

As the accumulated scientific and practical experience of scientists [18-25] shows , the study of complex multicomponent systems in metallurgy, such as Fe–Cr–P, Fe–Cr, Fe–P, Cr–P, Fe–Cr–P–O, requires the use of a whole range of experimental and analytical methods. The main features and factors that are the key to successful experimental phosphorus reduction in these systems include:

1. **High temperatures and reactivity.** Iron, chromium and phosphorus in melts actively interact with oxygen, nitrogen and crucible materials. Experiments require the creation of an inert or reducing atmosphere (argon, vacuum, hydrogen), which complicates the design of equipment and increases the cost of research. High temperatures (more than 1500 °C) lead to intensive evaporation of phosphorus and its compounds, which makes it difficult to accurately determine concentrations [18, 19].
2. **Fragility of phosphide phases.** Compounds such as Fe_3P and $(Fe,Cr)_3P$ often have a brittle structure and can be destroyed during machining of samples, and such fine phosphides are difficult to fix during quenching due to their tendency to dissolve during rapid cooling [19, 20].
3. **Problems of fixing the phase composition.** To construct phase diagrams, it is necessary to fix equilibrium structures, but metastable phases often occur in multicomponent systems. Slow cooling allows to achieve equilibrium, but causes segregation of impurities and isolation of secondary phases. . In the work of Bernhard et al. [18] it has been shown that even for relatively simple binary and ternary Fe–P and Fe–C–P systems, there are significant discrepancies between experimental phase fields and predictions from thermodynamic models. The authors note that with slow cooling, a coarse-crystalline structure is formed with pronounced segregation of phosphorus along the grain boundaries, which complicates the fixation of equilibrium phases. Rapid quenching, on the other hand, results in the preservation of metastable phosphide phases (e.g. Fe3P or Fe2P), which should not be present in real equilibrium. Thus, the data obtained depend on the method of fixing the structure, which complicates the construction of reliable phase diagrams. In a study by Cao et al. [19] it is emphasized that even when using CALPHAD modeling, the Fe-P system requires adjustment due to the difficulty of obtaining pure experimental data. The authors note that equilibrium phase ratios are highly dependent on the cooling rate and in a number of experiments phases are recorded that are the product of

non-equilibrium crystallization. This confirms that thermodynamic optimization should take into account the possibility of fixing metastable structures and adjust experimental data using model calculations.

4. **Complexity of working with oxygen in the Fe–Cr–P–O system.** In the presence of oxygen, complex oxide-phosphide inclusions are formed, the composition of which is difficult to predict. When studying such inclusions in laboratory conditions, their change in the analysis process is often observed (especially in an electron microscope due to heating with an electron beam) [21-23].

5. Chromium in the Fe–Cr system forms solid solutions in iron in a wide range of concentrations. Experimental difficulties are associated with **the high temperature of liquidus and the tendency of chromium to oxidation**, however, vacuum melting or melting in an inert gas atmosphere is necessary to obtain pure samples [24, 25].

6. Phosphorus in the Fe-P system is limited soluble in α-iron, which leads to segregation at grain boundaries. In experiments**, it is difficult to reproduce the uniform distribution of phosphorus, especially at high temperatures, due to its volatility** [18, 19].

7. **Chromium phosphides in the Cr-P system are characterized by high hardness and thermal stability.** Their synthesis requires temperatures above 1300 °C and strict control of the atmosphere, otherwise Cr oxidation and the formation of Cr_2O_3 occur [20].

8. **In the triple system Fe–Cr–P, complex interactions between phases are observed, which depend on the ratio of elements.** Obtaining pure three-component alloys requires a complex technology that excludes the ingress of carbon and oxygen [20]. In particular, in the Fe–Cr–P–O system, the formation of multicomponent inclusions containing oxides and phosphates requires complex analysis – optical metallography, X-ray phase analysis, scanning electron microscopy.

9. **The problem is the instability of some inclusions in contact with air or moisture** [21-23]**.**

Research results and discussions. The review of modern information on the behavior of phosphorus in Fe–Cr–P, Fe–Cr, Fe–P, Cr–P, Fe–Cr–P–O systems was aimed not only at collecting a theoretical scientifically grounded review, but also at forming reliable representative data samples, as an important component for modeling and predicting physicochemical interactions with an appropriate focus on the removal of phosphorus into the slag phase. As a result of the literature review, it was noted: that a significant amount of information is not in an unconventional format (tables of chemical compositions), but in graphic representations, dependencies and state diagrams. That is why to create a representative sample of data, the method of digitizing data was used while maintaining their initial accuracy of fixation by researchers (Table 3).

Based on the concept of directed chemical bonding [26, 27], the dependence of the standard enthalpy of formation (ΔH) of the Fe-P alloy on the phosphorus content at temperatures of 298 K and 900 K according to the data [28] was analyzed. This approach allows to identify correlations between thermodynamic parameters and phosphorus concentration in the Fe-P system, which is represented through the parameter of the interatomic interaction tgα, which describes the gradient of change in the radius of the ion from its charge (Fig. 1).

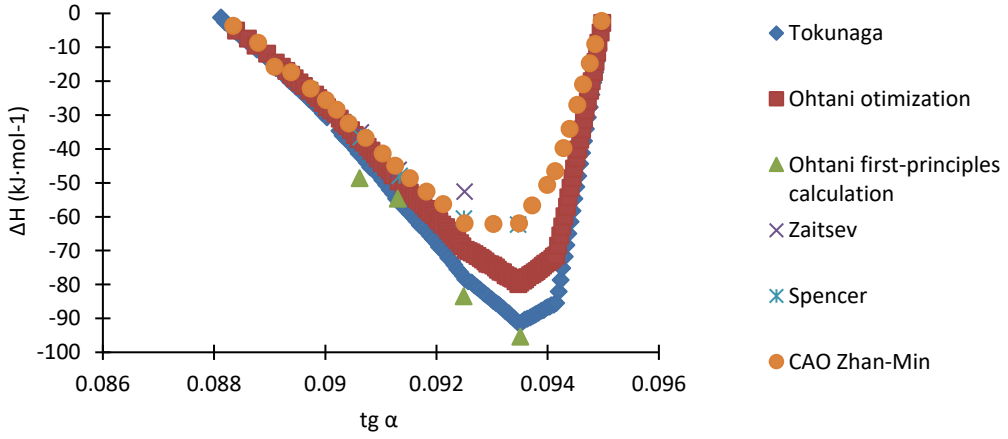

Figure 1 – Dependence of the standard enthalpy of formation (ΔH) of an alloy of the Fe-P system according to data [28] on the parameter of the interatomic interaction tg(α).

The high correlation between the results presented in the paper [28] and the obtained calculation data confirms the expediency of using the parameters of the interatomic interaction as criteria for the reliability of the results. In particular, *the tgα parameter* almost completely reproduces the course of the curves described by the authors [28]. Similar trends and dependencies persist at a temperature of 900 K. It has been established that an increase in the absolute value of the negative enthalpy of the formation of a compound indicates its higher thermodynamic stability relative to the initial simple substances.

With an increase in the phosphorus content, its charge increases, which is reflected by the *parameter*

tgα in Fig. 2, at the same time, the weighted average internuclear distance of ions in the system, represented by the *parameter d*, is minimal at its maximum content, which testifies in favor of the formation of strong interatomic bonds with the partner, in particular iron.

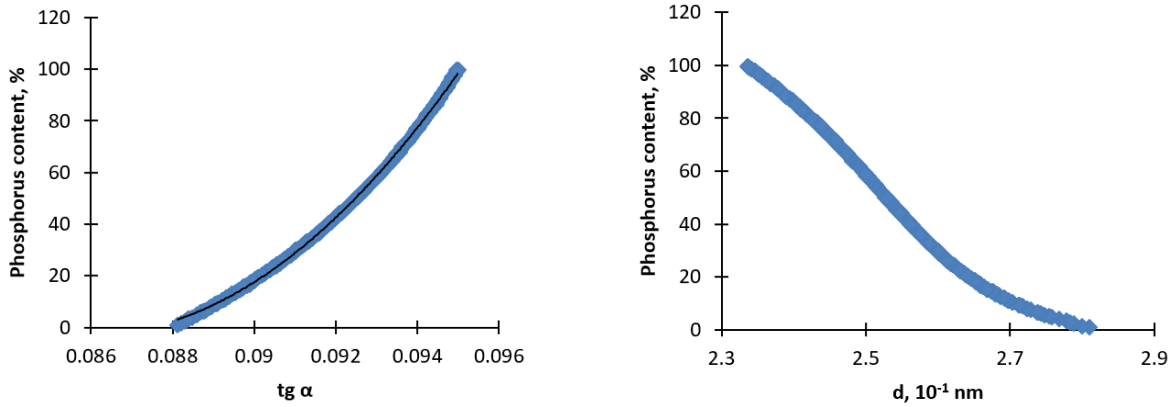

Figure 2 – Relationship between changes in phosphorus content and parameters of interatomic interaction.

The results obtained confirm that the regulation of the parameters of interatomic interaction in Fe–Cr–P–O systems allows creating thermodynamically grounded conditions for the effective reduction of iron and phosphorus. The formation of stable phases in the reduction process creates the necessary prerequisites for their further extraction from complex oxide systems.

The relevance of further developments is reinforced by the lack of comprehensive research in this area. In particular, in domestic scientific practice, the issue of disposal of leather production waste is usually considered only in the environmental aspect, which neutralizes their value as a source of chromium-containing raw materials for metallurgy. The analysis of world publications also confirms the lack of attention to the technological potential of such waste. Thus, the introduction of recycling of ash from leather production waste will not only partially provide enterprises with important chromium-containing raw materials, but will also lay the foundation for the formation of new global trends in the field of rational environmental management.

Conclusions

The analysis of literature data of domestic and foreign scientists made it possible to find a promising way to obtain chromium, in particular, it is the use of leather production waste, but it should be noted a significant number of related issues that need to be solved for the successful implementation of the recycling scheme. Namely, the removal of a significant phosphorus content by directing it to the slag phase.

The limiting factors that should be taken into account for conducting experimental studies on phosphorus removal in Fe–Cr–P, Fe–Cr, Fe–P, Cr–P, Fe–Cr–P–O systems (high temperatures and reactivity, fragility of phosphide phases, problems of fixation of phase composition, and others) have been described and systematized.

A representative sample of data has been created, including data on Fe–Cr–P, Fe–Cr, Fe–P, Cr–P, Fe–Cr–P–O systems using the technique of digitizing graphic data while maintaining their initial accuracy of fixation.

The relationship between enthalpy at temperatures of 298K and 900K and phosphorus content has been investigated through the prism of the concept of directed chemical bonding. A significant discrepancy between the presented authors and the dependencies obtained by us was revealed, which testifies in favor of using the parameters of interatomic interaction to assess the reliability of the data obtained.

Reference

1. Dvulit, Z. P., & Andrusiak, K. A. (2023). Vyklyky metalurhiinoi haluzi ukrainy v umovakh sohodennia. *Menedzhment ta pidpryiemnytstvo v Ukraini: etapy stanovlennia ta problemy rozvytku,* 1(9), 261–268.
2. Hordieieva-Herasymova, L. Yu., & Krainiak, A. V. (2022). Funktsionuvannia pidpryiemstv metalurhiinoi haluzi Ukrainy: potochni vyklyky ta tendentsii diialnosti. *Ekonomika ta suspilstvo*, (44), https://doi.org/10.32782/2524-0072/2022-44-40
3. Tuboltsev, L. G., Chaika, O. L., & Babachenko, O. I. (2023). Prospects of technological development of metallurgical production in Ukraine due to the use of new technologies. Fundamental and Applied Problems of Ferrous Metallurgy, 37, 4–25. https://doi.org/10.52150/2522-9117-2023-37-4-25
4. Popov, A. S. (2011). Issledovanie vozmozhnosti obogashcheniia khromovykh rud Metalurhiia. Naukovi pratsi zaporizkoi derzhavnoi inzhenernoi akademii. 24, 26-29.
5. Hrinshput, V. O. (2006). Metalurhiini vlastyvosti khromitovykh rud Pobuzhzhia i rozrobka ratsionalnykh rezhymiv otrymannia vysokovuhletsevoho ferokhromu: Avtoref. Diss. 23 p.
6. Andini, S., Vegliò, F., Moro, F., & Felici, A. (2002). Chromium recovery from tannery waste by solid–liquid extraction. *Waste Management*, 22(8), 841–846. https://doi.org/10.1016/S0956-053X(02)00074-5
7. Famielec, S. (2020). Chromium Concentrate Recovery from Solid Tannery Waste in a Thermal Process. Materials, 13(7), 1533. https://doi.org/10.3390/ma13071533

8. Wenzel, B. M., Zimmer, T. H., Fernandez, C. S., Marcilio, N. R., & Godinho, M. (2013). Aluminothermic reduction of Cr2O3 contained in the ash of thermally treated leather waste. Brazilian Journal of Chemical Engineering, 30(1), 141–154. https://doi.org/10.1590/s0104-66322013000100016
9. González-Lucas, M., Peinado, M., Vaquero, J. J., Nozal, L., Aguirre, J. L., & González-Egido, S. (2022). Microwave-Assisted Pyrolysis of Leather Waste. Energies, 15(4), 1273. https://doi.org/10.3390/en15041273
10. Freitas, A. M., et al. (2020). Biochar as Influenced by Feedstock Variability: Implications and Opportunities for Phosphorus Management. *Frontiers in Sustainable Food Systems,* 4, 510982. https://doi.org/10.3389/fsufs.2020.510982
11. Petrucci E., Fenoglio I., & Baricco M. Recycling of tannery waste for the production of chromium containing steels: Challenges and perspectives. Journal of Cleaner Production. – 2017. – Vol. 142. – P. 3170–3180. https://doi.org/10.1016/j.jclepro.2016.10.168
12. Petryshchev A.S., Semiriahin S.V., & Smirnov Yu.O. (2023). Pidvyshchennia rivnia bezpeky ta hihiieny pratsi pry ekolohichno spriamovanii pererobtsi vidkhodiv shkirianoi promyslovosti ta osoblyvosti yikh mikrostruktury. *Metal ta lyttia Ukrainy*, 31(3), 79–85. https://doi.org/10.15407/steelcast2023.03.079
13. Spreitzer, D., & Schenk, J. (2019). Reduction of iron oxides with hydrogen—A review. *Steel Research Internationa*l, 90(10), 1900108, 1–14. https://doi.org/10.1002/srin.201900108
14. Anacleto, N., & Ostrovski, O. (2013). Solid-State Reduction of Chromium Oxide by Methane-Containing Gas. Metallurgical and Materials Transactions B, 44(5), 1112–1121.
15. Zhou, Y. C., Chen, Z. Z., Gong, H. J., & Yang, Z. Y. (2021). Chromium speciation in tannery sludge residues after different thermal decomposition processes. *J. Clean. Prod.,* 314, 128071. https://doi.org/10.1016/j.jclepro.2021.128071
16. Tripathy, B. C., Ray, H. S., Das, R. P. (1991). Recovery of chromium from ferrochrome slag. *Minerals Engineering,* 4(7–11), 855.
17. Hryshyn, O. M. (2022). *Fizyko-khimichni osnovy otrymannia Fe-Cr hubchastykh lihatur.* Zhurfond.
18. Bernhard, M., Presoly, P., Fuchs, N., Bernhar,d C., Frie,s S. G., Kozeschnik, E., & Schmid-Fetzer, R. (2020). Experimental Study of High Temperature Phase Equilibria in the Iron-Rich Part of the Fe-P and Fe-C-P Systems. *Metallurgical and Materials Transactions A*, 51, 6087–6097. https://doi.org/10.1007/s11661-020-05912-z
19. Cao, W., Shim, J.-H., & Ohtan,i H. (2020). Thermodynamic Optimization of the Fe-P System. *Metallurgical and Materials Transactions B,* 51, 2710–2723. https://doi.org/10.1007/s11663-020-01939-0
20. Miettinen, J., Cao, W., Ohtani, H., Hillert, & M., Selleby, M. (2014). Thermodynamic Description of Ternary Fe-X-P Systems. Part 1: Fe-Cr-P. *Journal of Phase Equilibria and Diffusion*, 35, 473–484. https://doi.org/10.1007/s11669-014-0314-x
21. Darken, L. S.,& Muan A. (1956). Phase Equilibria in the System Fe-Cr-O. *Transactions of the Metallurgical Society of AIME*, 206, 119–127.
22. Seybolt, A. U. (1963). Observations on the Fe-Cr-O System. *Transactions of the Metallurgical Society of AIME*, 227, 1213–1218.
23. Dong, Y., & Jönsson, P. G. (2022). Challenges in the Determination of High-Temperature Phase Equilibria in Multicomponent Metallurgical Systems. *Journal of the European Ceramic Society*, 42, 5755–5766. https://doi.org/10.1016/j.jeurceramsoc.2022.08.032
24. Lee, B.-J., Sundman, B., Hillert, M., & Lukas, H. L. A (1999). Thermodynamic Evaluation of the Fe-Cr System. Calphad, 23(3–4), 485–495. https://doi.org/10.1016/S0364-5916(99)00019-X
25. Xiong W., Chen Q., Bratberg J., Ågren J. 2018. Revised Thermodynamic Description of the Fe–Cr System. Calphad, 62, 128–142. https://doi.org/10.1016/j.calphad.2018.06.003
26. Prykhodko, E. V. (2013). Prohnozyrovanye fyzyko-khymycheskykh svoistv oksydnikh system. Porohy.
27. Togobitska, D. & Belkova A. (2024). New approach to evaluating the thermodynamic consistency of melts in the “Metal-Slag” system based on interatomic interaction parameters. *Lithuanian Journal of Physics*. 64(1), 58-71 https://doi.org/10.3952/physics.2024.64.1.6
28. Cao Z.-M., Wang K.-P., Qiao Z.-Yu, & Du G.-W. (2012). Thermodynamic Reoptimization of the Fe-P System. *Acta Physico-Chimica Sinica*, 28(1), 37–43. https://doi.org/10.3866/PKU.WHXB201111172

Надіслано до редакції / Received: 27.12.2025
Прорецензовано / Peer-Reviewed: 24.02.2026
Прийнято до друку / Accepted: 16.03.2026
Опубліковано / Published: 30.03.2026

ISSN 3083-7219 (Print), ISSN 3083-7227 (Online)
Теорія і практика металургії, 2026, № 1
Theory and Practice of Metallurgy, 2026, No. 1

https://doi.org/10.15802/tpm.1.2026.09

UDC 669.018.9:536.75:620.22

***Kamkina L. V.*[1,*], *Proidak Y. S.*[2], *Mianovska Y. V.*[3],
Guba R. M.[4], *Bezshkurenko O. G.*[5]**

High-entropy alloys. A new concept for the design of innovative structural materials

[1] ORCID: 0000-0002-8329-0917. Ukrainian State University of Science and Technologies, Ukraine
[2] ORCID: 0000-0003-1363-8081. Ukrainian State University of Science and Technologies, Ukraine
[3] ORCID: 0000-0002-5898-1169. Ukrainian State University of Science and Technologies, Ukraine
[4] ORCID: 0009-0003-2173-517X. Ukrainian State University of Science and Technologies, Ukraine
[5] ORCID: 0000-0002-3204-3780. Ukrainian State University of Science and Technologies, Ukraine
*Email: l.v.kamkina@ust.edu.ua

***Камкіна Л. В.*[1,*], *Пройдак Ю. С.*[2], *Мяновська Я. В.*[3],
Губа Р. М.[4], *Безшкуренко О. Г.*[5]**

Високоентропійні сплави. Нова концепція проектування інноваційних конструкційних матеріалів

[1] ORCID: 0000-0002-8329-0917. Український державний університет науки і технологій, Україна
[2] ORCID: 0000-0003-1363-8081. Український державний університет науки і технологій, Україна
[3] ORCID: 0000-0002-5898-1169. Український державний університет науки і технологій, Україна
[4] ORCID: 0009-0003-2173-517X. Український державний університет науки і технологій, Україна
[5] ORCID: 0000-0002-3204-3780. Український державний університет науки і технологій, Україна
*Email: l.v.kamkina@ust.edu.ua

Abstract. *Modern technologies require state-of-the-art materials that meet their conditions, regardless of operating conditions. Alloys with high entropy can replace traditional materials, work under impacts, dynamic loads, elevated temperatures, etc. These alloys are used for the manufacture of tools, molds, dies, mold casting in parts that require high strength, resistance to oxidation and wear, can also be used in environments with high corrosion resistance parameters (plumbing, marine conditions), in aggressive conditions and in the chemical industry. High entropy alloys are quite easy to investigate and control, and can be obtained by the same methods as traditional alloys, such as: casting, rapid melt quenching, film sputtering, electrolysis, and mechanical alloying. Electroslag remelting (ESD) can greatly improve the purity, hardening structure, and transverse mechanical properties of steel. However, the increasing demands on the mechanical properties of steel are prompting metallurgists to make more efforts to eliminate defects in steel microstructures such as shrinkage and segregation. The combination of directional crystallization technology with electroslag melting technology effectively eliminates macrosegregation in the cast ingot through a shallow molten metal bath controlled by directional crystallization. Increasing the strength of alloys can be achieved either by alloying a solid solution (elements in the internodes) or by isolating the solidification phases or artificially introducing microparticles. Curing phases (carbides, nitrides, carbonitrides, intermetals) can be endogenous (formed from elements introduced into the melt in a liquid state or during its solidification and subsequent cooling) or exogenous (usually introduced into the melt just before crystallization begins, and there is also an increase in size and deterioration in the distribution of solidification phases.*
Keywords: *high-entropy alloys, strength, hardening phases, electroslag remelting.*

Анотація. *Сучасні технології потребують сучасних матеріалів, які відповідають їхнім умовам, незалежно від умов експлуатації. Сплави з високою ентропією можуть замінити традиційні матеріали, працювати під ударами, динамічними навантаженнями, підвищеними температурами тощо. Ці сплави використовуються для виготовлення інструментів, форм, штампів, лиття у деталях, що потребують високої міцності, стійкості до окиснення та зношування, а також можуть застосовуватися в середовищах з високими параметрами стійкості до корозії (сантехніка, морські умови), у агресивних умовах та в хімічній промисловості. Сплави з високою ентропією досить легко досліджувати та контролювати, і їх можна отримати тими ж методами, що й традиційні сплави, такими як: лиття, швидке загартування плавом, розпилення плівки, електроліз і механічне легування. Електрошлакове переплавлення (ESD) може значно покращити чистоту, структуру загартування та поперечні механічні властивості сталі. Однак зростаючі вимоги до механічних властивостей сталі спонукають металургів докладати більше зусиль для усунення дефектів сталевих мікроструктур, таких як усадка та сегрегація. Поєднання технології напрямленої кристалізації з технологією електрошлакового переплаву ефективно усуває макросегрегацію в литому злитку через неглибоку ванну з розплавленим ме-*

© Kamkina L.V., Proidak Y.S., Mianovska Y.V., Guba R.M., Bezshkurenko O.G., 2026
© Камкіна Л.В., Пройдак Ю.С., Мяновська Я.В., Губа Р.М., Безшкуренко О.Г., 2026

This is an Open Access article under the CC BY 4.0 license https://creativecommons.org/licenses/by/4.0/

талом, контрольовану напрямленою кристалізацією. Підвищення міцності сплавів можна досягти або шляхом легування твердого розчину (елементів у міжвузлах), або шляхом ізоляції фаз затвердіння або штучного введення мікрочастинок. Фази затвердіння (карбіди, нітриди, карбонітриди, інтерметали) можуть бути ендогенними (утвореними з елементів, введених у розплав у рідкому стані або під час його затвердіння та подальшого охолодження) або екзогенними (зазвичай вводяться в розплав безпосередньо перед початком кристалізації, а також спостерігається збільшення розміру та погіршення розподілу фаз твердіння.
Ключові слова: *сплави з високою ентропією, міцність, фази загартування, переплавка електрошлаку.*

Introduction

Alloying has long been used to give materials the desired properties. It usually involves the addition of small amounts of secondary elements to the primary element. However, in the last decade and a half, a new alloying strategy has become widespread, involving the combination of several basic elements in high concentrations to create new materials called high-entropy alloys [1]. The multidimensional compositional space that can be explored with this approach is virtually limitless, and only tiny areas have been explored [2]. The materials science community, which is no longer safe at the corners and edges of triple phase diagrams, now finds itself in uncharted, hyperdimensional territory that is difficult to imagine, difficult to visualize, and difficult to systematically explore [3]. The concept of huge compositions and microstructures associated with alloys with several basic elements did not lose its relevance in the first 12 years. Significant progress has been made, and it continues to motivate new research questions and inspire new important scientific topics. The combinatorial enormity of this idea also poses the greatest technical challenge that this industry offers. Of the literally hundreds of millions of possible combinations of elements, barely a hundred have been studied so far.

Review of scientific information

Due to the multiplicity of base elements and multiple effects, they have different organizational structures and unique properties compared to traditional alloys, which opens up unlimited development potential and promising applications of wind farms. For almost 30 years of development, the methods for obtaining and studying wind farms have expanded significantly, the systems have been optimized, and the scope of their application has expanded. This article provides a comprehensive overview of the development of manufacturing processes, including wind farms in the form of blocks, coatings, wire, powders, and additive technologies. In addition, a number of research results on the critical properties of wind farms, such as mechanical properties, corrosion resistance, wear resistance and oxidation at high temperatures, as well as new functional properties such as radiation resistance, hydrogen capability and biocompatibility, etc., have been summarized [1].

Based on research on intermetallic structural materials [4, 5] and massive metallic glasses [6], the concept of "high-entropy alloys (HEA)" or "multiple-core alloys (MPEA)" was introduced in two papers independently published by J.W. Yeh et al. [7, 8] and B. Cantor et al. [9] in 2004. Since then, there has been an explosive development in the field of materials. According to the composition, HEA are defined as alloys consisting of at least 5 elements and a maximum of 13 elements. To expand the scope of alloy development, the molar fractions of each major element were >5% and <35% [10].

H13 steel is a prime example of Cr-Mo-Si-V hot-working tool steels known for their extreme strength, resistant red hardness, and extreme resistance to wear and thermal stress [11]. Its wide application in the manufacture of molds and dies can be explained by these exceptional properties. Traditionally, molds are made using casting and machining methods. However, these traditional production methods are characterized by low production rates and significant limitations in design flexibility. In recent years, laser powder cladding (LPBF), due to its unique advantages such as geometric design flexibility, the ability to create complex structures, which contributes to cost-effective product customization and provides excellent mechanical properties, has become a promising method for manufacturing metal components and is widely used in the aerospace, medical, automotive, and mold manufacturing industries [11].

Tool steels must not only provide wear resistance, but also have good toughness, which can guarantee a long service life under wear conditions [13, 14]. For example, tools for rolling panel machines, usually made of tool steels with a high chromium content [15], have good mechanical properties characterized by impact toughness as well as high wear resistance [16]. The main reason is that when a rolling tool is used to roll rocks, it undergoes abrasive wear under high load, and a large amount of heat is released due to instantaneous friction, resulting in a rapid increase in the surface temperature of the tool [17]. After rotation, the surface of the tool is immediately cooled by spraying water. In this way, the tool not only withstands wear and tear [18], but also withstands cold and hot fatigue. However, for some tool steels with a specific composition, wear resistance and toughness are contradictory. Under the condition of high wear resistance, the impact strength of steels is usually low [19]. Therefore, it is necessary to balance impact strength and wear resistance in order to improve tool life [25]. Broadly speaking, there are many methods to improve the conflicting mechanical properties of steel, such as ultra-pure cleaning, heat treatment, large forging ratio, etc. [20, 21]. However, on a technical level, tool and stamped steel for cutting tools has reached a certain limit. Therefore, the development of a new

and effective method that can improve the impact strength and wear resistance of steels is of high practical importance and industrial application [22]. Traditional methods for improving the complex mechanical properties of steel include adding metal elements to the steel die for alloying and optimizing the composition, developing new heat treatment processes, and developing new molding manufacturing processes. However, it is difficult to simultaneously increase the strength and strength of steel with these traditional methods [22]. The incorporation of trace ceramic particles into the steel matrix is an effective method to further improve the mechanical properties of steel due to its low cost and high performance [23]. One of the most attractive methods for increasing the strength of tool steel is to add ceramic rebar to a steel-based die, which has a low density and a homogeneous microstructure with better mechanical properties. Metal matrix composites have been developed due to their attractive properties such as high specific strength, modulus, thermal resistance and excellent wear resistance. Solid ceramic particles such as TiC and TiB2 are used to improve mechanical properties, temperature stability, and wear in steel composites. TiC is well known as a reinforcement in steel composites due to its desirable characteristics such as high melting point, low density, high modulus of elasticity, and good wettability with iron and steel matrices. Stable carbides coarsen more slowly than cementite and are therefore much more efficient than cementite at higher temperatures. Together with the solid martensitic matrix, the addition of TiC, which is thermodynamically stable in contact with the steel matrix [22, 25-27], there is a significant increase in stiffness, hardness, and wear resistance.

The paper [28] presents the results of a systematic study of the effect of the Cr/V ratio (0.2, 0.4, 0.6, 0.8 and 1.0) on the microstructure and tensile strength of high-vanadium high-speed steel. The results show that lower Cr/V ratios contribute to the formation of coarse block carbides of the MC type, which are gradually crushed and undergo spheroidization with an increase in the Cr/V ratio. The evolution of the matrix phase reveals a non-monotonic trend towards austenite content, peaking at approximately 40% for a Cr/V ratio of 0.6, while the martensite content is inversely related.

[29] The effect of the axial static magnetic field (ASMP) on carbides and mechanical properties of stamped H13 steel obtained by electroslag melting was investigated. An optical microscope (OM) and a scanning electron microscope (SEM) were used to analyze the solidification structure and morphology of carbides of electroslag melting ingots (ESD). To detect inclusions in ESP H13 ingots, the FEI Aspex Explorer device was used. Compared to conventional ESP, the application of ASMP in this study made the molten metal bath more superficial and gentle, resulting in a reduction in local solidification time and uniform distribution of solute atoms, which reduced the degree of segregation of elements and further inhibited the formation of primary carbides. The magnetically controlled electroslag remelting (MC-ESR) process not only crushed the structure of dendrites (which tended to grow parallel to the ingot axis) and carbides, but also improved the inclusion removal efficiency and mechanical properties of H13 steel ESP ingots.

Authors [30, 31] studies of microstructure and carbides in cast austenitic mold steel produced by traditional electroslag remelting (ESR) and continuous directional electroslag remelting (ESR-CDS) methods have been performed. In addition, the growth pattern of carbides was also considered. A combination of optical microscopy (OM) and scanning electron microscopy (SEM) was used to characterize the microstructure and carbides. Segregation was analyzed using an initial position analyzer (OPA) and electron probe microassay (EPMA). Electrolytically extracted carbides were analyzed using SEM and X-ray diffraction (XRD) to determine their three-dimensional microstructure and composition. The microstructure of the steel consisted of an austenitic matrix and primary carbides of the V8C7 and Mo2C types. Compared to traditional ESR, ESR-CDS contributed to the formation of a finer microstructure in cast steel, a smaller amount and smaller size of carbides in melted steel. Meanwhile, the segregation of alloying elements was reduced with ESR-CDS. Enrichment with carbide-forming elements was reduced due to directional solidification of ESR, resulting in a change in the morphology of V-rich carbides from rod-shaped to lamellar shape. The hardness and impact strength of the melted ingot (made with ESR-CDS) after heat treatment (solution temperature 1180°C for 2 hours, aging temperature 720°C for 2 hours) increased by 3-5 HRC and 4-6 J/cm2, respectively, compared to the results obtained with conventional ESR.

A thorough study is presented in the publication [32]. To analyze the curing and deposition behavior of primary carbides in H13 steel, the size, morphology, distribution, and type of carbides from the cooling edge to the center of H13 steel are studied using a scanning electron microscope (SEM), X-ray diffractometer, and Thermo-Calc thermodynamic software, and both carbide formation time under equilibrium conditions and non-equilibrium solidification are discussed. The results show that the primary carbides are distributed in the final curing of the steel, mainly including MC type V–Ti PC, V PC and M7C3 type Mo–Cr PC. From edge to center, the average area of primary carbide increases by 620.22 μm², with an increase of 3.53%. From the edge to the ¼ position, there are mainly V-rich and Mo–Cr carbides; at position 1/4, carbides rich in V-and Mo–Cr are interconnected; from position 1/4 to the center, there are three types of interrelated V–Ti PC, V-rich PC, and Mo–Cr PC carbides. Oxides promote MC-type precipitation, while sulfides promote M7C3-type precipitation. Thermodynamics shows that the pri-

mary carbide MC is not formed in equilibrium solidification, but is precipitated in a non-equilibrium state with a precipitation temperature of 1108°C at a solidification fraction of 0.9987.

Thermodynamic analysis of carbide formation with the participation of steel components H13 and D2.

UNS T30402 Type D2 steel is intended for the manufacture of tools used for cold processing of metals and other materials. It is characterized by a high content of carbon and chromium, has high resistance to abrasion. The steel is used for the manufacture of punching dies, mandrels, rolling dies, tools with high mechanical strength and toughness.

UNS T20813 Type H13 is intended for the manufacture of tools used for processing metals under pressure at temperatures above 300ºC. The steel is used for the manufacture of oil- and air-cooled mandrels and mandrels of extrusion presses, molds for injection molding.

Table 1 - Chemical composition of UNS T20813 Type H13 steel and the closest analogue 4X5MF1C.

Chemical element, %	UNS T20813 Type H13		4X5MF1C	
	Min.	Max.	Min.	Max.
C	0,32	0,45	0,37	0,44
Mn	0,20	0,60	0,20	0,50
Si	0,80	1,25	0,90	1,20
Cr	4,75	5,50	4,50	5,50
V	0,80	1,20	0,80	1,10
Mo	1,10	1,75	1,20	1,50
Ni		0,30	-	0,30
W		-	-	0,20
Cu		0,25	-	0,30
Ti		-	-	0,03
P	-	0,030	-	0,030
S	-	0,030	-	0,030
Fe	main element		main element	

Table 2 - Chemical composition of UNS T30402 Type D2 nd the closest analogue X12MF.

Chemical element, %	UNS T30402 Type D2		X12MF	
	Min.	Max.	Min.	Max.
C	1,40	1,60	1,45	1,65
Mn	0,10	0,60	0,15	0,45
Si	0,10	0,60	0,10	0,40
Cr	11,0	13,0	11,0	12,5
V	0,50	1,10	0,15	0,30
Mo	0,70	1,20	0,40	0,60
Ni	-	0,30	-	0,35
Ti	-	-	-	0,03
Cu	-	0,25	-	0,30
W	-	-	-	0,20
P	-	0,030	-	0,030
S	-	0,030	-	0,030
Fe	main element		main element	

According to the chemical composition given in Tables 1 and 2, the main carbide-forming elements are: V, Cr, Mo, Mn, Fe. The sequence and intensity of the formation of carbides of these elements are determined by the magnitude of their chemical affinity for carbon, which is clearly confirmed by the mutual arrangement of the corresponding temperature dependences on the Ellingham diagram (Fig. 1, 2).

The results showed that the primary carbides in cast H13 steel are mainly composed of Cr, Mo, V and Ti, and there are four types of primary carbides in the interdendritic zones of H13 steel: M2C type, enriched in Mo-Cr; eutectic M2C type, enriched in Mo-Cr; MC type, enriched in V, and MC type, enriched in V, with Ti and N.

In H13 steel, primary carbides significantly affect the tool life. The precipitation of primary carbides reduces the solubility of Cr, Mo and V in the solid

state in the matrix, thereby reducing the precipitation of secondary carbides during tempering and affecting the homogeneity of the microstructure. Uniformly dispersed nanoparticles are vital for the secondary strengthening of H13 steel. However, due to the high temperature stability of primary carbides, they cannot be removed during heat treatment. Large primary carbides can become sources of cracks, leading to thermal fatigue failure and reduced tool life.

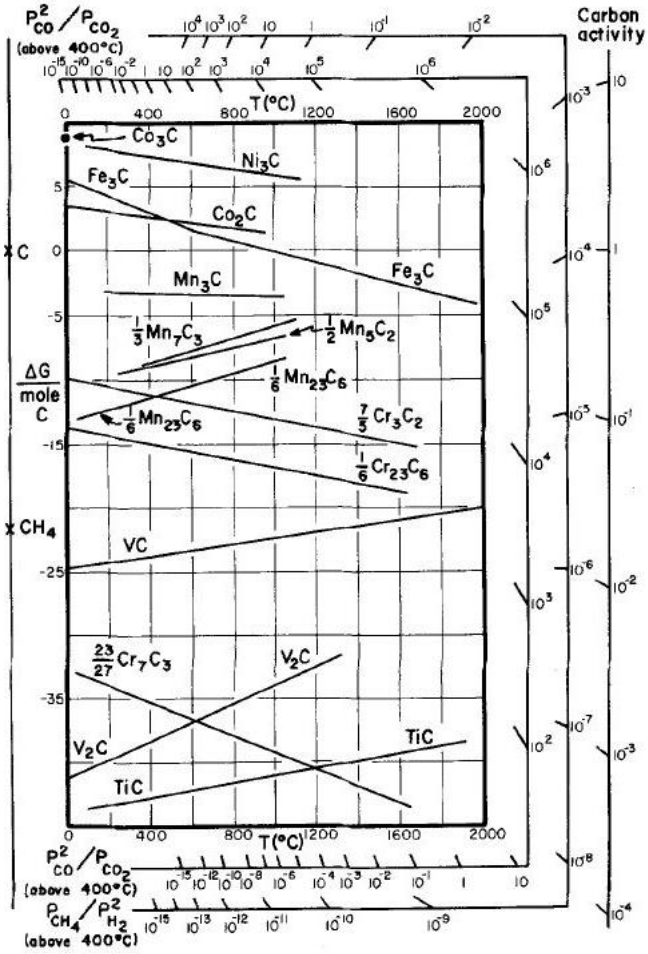

Figure 1 - Ellingham diagram for carbides of the first transition series.

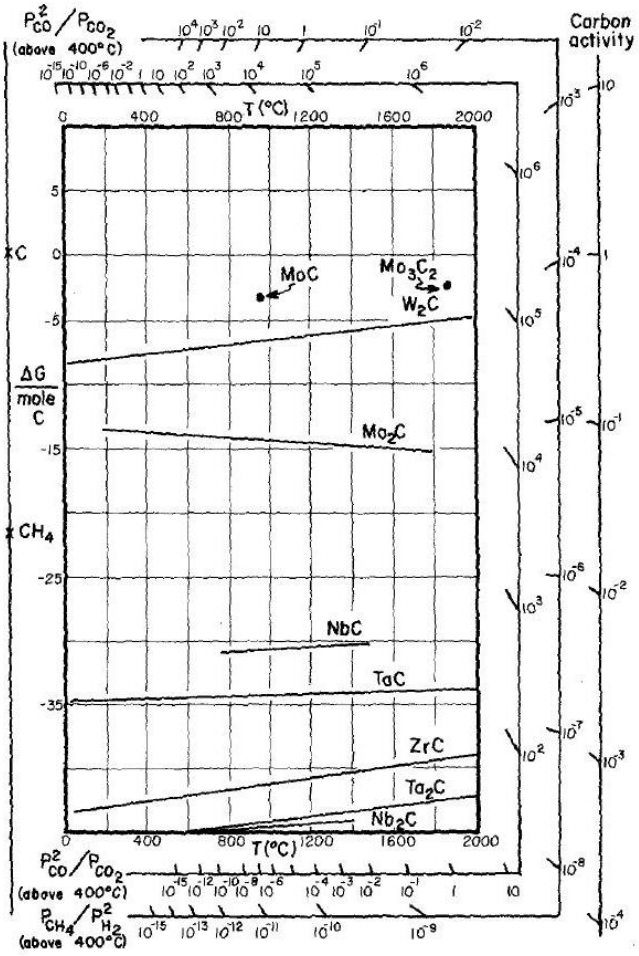

Figure 2 - Ellingham diagram for second and third transition series carbides.

Conclusions

At present, high-entropy alloys are a promising direction for the development of innovative materials. Modern technologies require the latest materials that will meet their conditions, regardless of the operating environment.

High-entropy alloys can replace traditional materials, they can work under shock, dynamic loads, elevated temperatures, etc.

High entropy alloys are suitable for the manufacture of tools, molds, dies, casting molds in parts that require high strength, oxidation resistance and wear resistance, can also be used in environments where high corrosion resistance parameters are required (plumbing, marine environments), in aggressive environments and in the chemical industry. High-entropy alloys are quite simple to investigate and control, they can be obtained by the same methods as traditional alloys, i.e.: casting, rapid melt quenching, film sputtering, electrolysis and mechanical alloying.

Electroslag remelting (ESD) can greatly improve the purity, curing structure, and transverse mechanical properties of steel. However, increasing demands on the mechanical properties of steel are prompting metallurgists to put more effort into eliminating steel microstructure defects such as shrinkage and segregation. The combination of directional crystallization technology with electroslag melting technology effectively eliminates macrosegregation in the cast ingot due to a shallow bath of molten metal controlled by directed crystallization.

An increase in the strength of alloys can be realized either by alloying a solid solution (elements in the internodes) or by isolating hardening phases or artificial introduction of microparticles. Hardening phases (carbides, nitrides, carbonitrides, intermetallics) can be endogenous (formed from elements introduced into the melt in a liquid state or during its solidification and subsequent cooling), or exogenous

(usually introduced into the melt immediately before the start of crystallization, and there is also an increase in the size and deterioration of the distribution of hardening phases. phases is 30-70% mass.

References

1. Yu, B., Ren, Y., Zeng, Y., Ma, W., Morita, K., Zhan, S., Lei, Y., Lv, G., Li, S., & Wu, J. (2024). Recent progress in high-entropy alloys: A focused review of preparation processes and properties. *Journal of Materials Research and Technology*, 29, 2689–2719. https://doi.org/10.1016/j.jmrt.2024.01.246

2. George, E.P., Raabe, D. & Ritchie, R.O. (2019). High-entropy alloys. *Nat Rev Mater* 4, 515–534 https://doi.org/10.1038/s41578-019-0121-4

3. Miracle, D. B., & Senkov, O. N. (2017). A critical review of high entropy alloys and related concepts. *Acta Materialia*, 122, 448–511. https://doi.org/10.1016/j.actamat.2016.08.081

4. Yang, T., Cao, B. X., Zhang, T. L., Zhao, Y. L., Liu, W. H., Kong, H. J., Luan, J. H., Kai, J. J., Kuo, W., & Liu, C. T. (2022). Chemically complex intermetallic alloys: A new frontier for innovative structural materials. *Materials Today*, 52, 161–174. https://doi.org/10.1016/j.mattod.2021.12.004

5. Pasini, W. M., Polkowska, A., Nowak, R., Bruzda, G., Kudyba, A., Jawańska, M., Zajusz, M., Górniewicz, D., Dworecka-Wójcik, J., Łazińska, M., Karczewski, K., & Polkowski, W. (2023). Boron Enhanced Complex Concentrated Silicides – New pathway for designing and optimizing ultra-high temperature intermetallic composite materials. *Journal of Materials Research and Technology*, 27, 6182–6191. https://doi.org/10.1016/j.jmrt.2023.11.056

6. Gao, K., Zhu, X. G., Chen, L., Li, W. H., Xu, X., Pan, B. T., Li, W. R., Zhou, W. H., Li, L., Huang, W., & Li, Y. (2022). Recent development in the application of bulk metallic glasses. *Journal of Materials Science & Technology*, 131, 115–121. https://doi.org/10.1016/j.jmst.2022.05.028

7. Yeh, J. W., Chen, Y. L., Lin, S. J., & Chen, S. K. (2007). High-Entropy Alloys – A New Era of Exploitation. *Materials Science Forum*, 560, 1–9. https://doi.org/10.4028/www.scientific.net/msf.560.1

8. Yeh, J. -W., Chen, S. -K., Lin, S. -J., Gan, J. -Y., Chin, T. -S., Shun, T. -T., Tsau, C. -H., & Chang, S. -Y. (2004). Nanostructured High-Entropy Alloys with Multiple Principal Elements: Novel Alloy Design Concepts and Outcomes. *Advanced Engineering Materials*, 6(5), 299–303. https://doi.org/10.1002/adem.200300567

9. Cantor, B., Chang, I. T. H., Knight, P., & Vincent, A. J. B. (2004). Microstructural development in equiatomic multicomponent alloys. *Materials Science and Engineering: A*, 375–377, 213–218. https://doi.org/10.1016/j.msea.2003.10.257

10. Zhang, Y., Zhou, Y. J., Lin, J. P., Chen, G. L., & Liaw, P. K. (2008). Solid-Solution Phase Formation Rules for Multi-component Alloys. *Advanced Engineering Materials*, 10(6), 534–538. https://doi.org/10.1002/adem.200700240

11. Wang, Q., Kong, D., Li, X., Zhou, S., & Zhang, Z. (2025). Additive manufacturing Cr-Mo-Si-V steel: Systematic parameter assessments, precipitation behavior of in-situ VC-M23C6 and strengthening mechanisms. *Materials Science and Engineering: A*, 919, 147504. https://doi.org/10.1016/j.msea.2024.147504

12. Stovpchenko, G., Medovar, L., Stepanenko, D., Jiang, Z., Dong, Y., & Liu, Y. (2023). Energy and environmental savings by and for steel lightweight. *ISIJ Int.,* https://doi.org/10.2355/isijinternational.ISIJINT-2023-230

13. Kou, S.-Q., Dai, J.-N., Wang, W.-X., Zhang, C.-K., Wang, S.-Y., Li, T.-Y., & Chang, F. (2022). Enhancement of Wear Resistance on H13 Tool and Die Steels by Trace Nanoparticles. *Metals* 12, 348. https://doi.org/10.3390/met12020348

14. Qiu, F., Liu, Ts., Zhang, X. et al. (2020). Application of nanoparticles in cast steel: An overview. *China Foundry* 17, 111–126 https://doi.org/10.1007/s41230-020-0037-z

15. Saucedo-Muñoz, M.L. (2021). Precipitation kinetics of carbides during cyclical and isothermal aging of 2.25Cr–1Mo steel and its effect on mechanical properties. J. Iron Steel Res. Int. 28, 1282–1290 https://doi.org/10.1007/s42243-021-00610-5

16. Huang, Y., Cheng, G., & Zhu, M. (2020). Effect of Ti Content on the Behavior of Primary Carbides in H13 Ingots. *Metals* 10, 837. https://doi.org/10.3390/met10060837

17. Zhou, Y., & Jiang, W. (2021). Effect of sliding speed on elevated-temperature wear behavior of AISI H13 steel. *J. Iron Steel Res. Int*. 28, 1180–1189. https://doi.org/10.1007/s42243-021-00644-9

18. Zhao Yi., Liu N., Zheng X., & Zhang N.. (2015). Mechanical model for controlling floor heave in deep roadways with U-shaped steel closed support. *International Journal of Mining Science and Technology*, 25(5), 713-720. https://doi.org/10.1016/j.ijmst.2015.07.003

19. Zhao, F., He, G., Liu, Y., Zhang, Z., & Xie, J. (2021). Effect of titanium microalloying on microstructure and mechanical properties of vanadium microalloyed steels for hot forging. *Journal of Iron and Steel Research International*, 29(2), 295–306. https://doi.org/10.1007/s42243-021-00629-8

20. Zhu, J., Zhang, Z., & Xie, J. (2021). Relationship between martensite microstructure and ductility of H13 steel from aspect of crystallography. *Journal of Iron and Steel Research International*, 28(10), 1268–1281. https://doi.org/10.1007/s42243-021-00595-1

21. Zhou, J., Shen, Y., & Jia, N. (2021). Strengthening mechanisms of reduced activation ferritic/martensitic steels: A review. International *Journal of Minerals, Metallurgy and Materials*, 28(3), 335–348. https://doi.org/10.1007/s12613-020-2121-1

22. Zhang, H., Wang, W.-X., Chang, F., Li, C.-L., Shu, S.-L., Wang, Z.-F., Han, X., Zou, Q., Qiu, F., & Jiang, Q. (2021). Microstructure manipulation and strengthening mechanisms of 40Cr steel via trace TiC nanoparticles. *Materials Science and Engineering: A,* 822, 141693. https://doi.org/10.1016/j.msea.2021.141693

23. Cho, S., Jo, I., Kim, H., Kwon, H.-T., Lee, S.-K., & Lee, S.-B. (2017). Effect of TiC addition on surface oxidation behavior of SKD11 tool steel composites. Applied Surface Science, 415, 155–160. https://doi.org/10.1016/j.apsusc.2016.11.164

24. Wang, Z., Lin, T., He, X., Shao, H., Tang, B., & Qu, X. (2016). Fabrication and properties of the TiC reinforced high-strength steel matrix composite. International *Journal of Refractory Metals and Hard Materials*, 58, 14–21. https://doi.org/10.1016/j.ijrmhm.2016.03.013

25. AlMangour, B., Grzesiak, D., & Yang, J.-M. (2016). Nanocrystalline TiC-reinforced H13 steel matrix nanocomposites fabricated by selective laser melting. *Materials & Design*, 96, 150–161. https://doi.org/10.1016/j.matdes.2016.02.022

26. Akhtar, F. (2008). Microstructure evolution and wear properties of in situ synthesized TiB2 and TiC reinforced steel matrix composites. *Journal of Alloys and Compounds*, 459(1–2), 491–497. https://doi.org/10.1016/j.jallcom.2007.05.018

27. Yong Z.(2019). History of High-Entropy Materials. https://doi.org/10.1007/978-981-13-8526-1_1

28. Du, Z., Tao, X., Wang, X., Li, H., Zhang, R., Zhou, Z., Zhang, S., Al-Hammadi, R. A., Zhou, Y., & Cui, C. (2025). Effect of Cr/V ratio on the microstructure evolution and tensile behavior of a high-vanadium high-speed steel. *Materials Science and Engineering: A,* 947, 149227. https://doi.org/10.1016/j.msea.2025.149227

29. Ma, C., Xia, Z., Guo, Y., Liu, W., Zhao, X., Li, Q., Qi, W., & Zhong, Y. (2022). Carbides refinement and mechanical properties improvement of H13 die steel by magnetic-controlled electroslag remelting. *Journal of Materials Research and Technology*, 19, 3272–3286. https://doi.org/10.1016/j.jmrt.2022.06.090

30. Qi, Y., Li, J., & Shi, C. (2018). Characterization on Microstructure and Carbides in an Austenitic Hot-work Die Steel during ESR Solidification Process. ISIJ International, 58(11), 2079–2087. https://doi.org/10.2355/isijinternational.isijint-2018-370

31. Zhang, Y., Zuo, T. T., Tang, Z., Gao, M. C., Dahmen, K. A., Liaw, P. K., & Lu, Z. P. (2014). Microstructures and properties of high-entropy alloys. *Progress in Materials Science*, 61, 1–93. https://doi.org/10.1016/j.pmatsci.2013.10.001
32. Dengping Ji, Wang, Y., Zhu, H., & Fu, J. (2023). Precipitation Behavior of Primary Carbide in H13 Bloom Die Steel. *Physics of Metals and Metallography*, 124(13), 1482–1491. https://doi.org/10.1134/s0031918x23600902

Надіслано до редакції / Received: 02.01.2025
Прорецензовано / Peer-Reviewed: 04.03.2026
Прийнято до друку / Accepted: 16.03.2026
Опубліковано / Published: 30.03.2026

CONTENT

ЗМІСТ

ТЕОРІЯ І ПРАКТИКА МЕТАЛУРГІЇ
науково-виробничий журнал

Засновник: Український державний університет науки і технологій

Видавець: Український державний університет науки і технологій

Головний редактор – проф. Пройдак Ю.С.

Комп'ютерна верстка – Безшкуренко О.Г.

Адреса і місцезнаходження видавця:
Український державний університет науки і технологій,
вул. Лазаряна, 2, м. Дніпро, 49010, Україна.
Тел.: +38-056-373-15-44, **Email:** office@ust.edu.ua

Сайт наукового видання: https://tpm.ust.edu.ua/

Підписано до друку 30.03.2026 року.
Формат 60x84 1/8. Тираж 100 примірників.

THEORY AND PRACTICE OF METALLURGY
Scientific and Production Journal

Founder: Ukrainian State University of Science and Technologies

Publisher: Ukrainian State University of Science and Technologies

Editor-in-Chief – Prof. Proidak Yu.S.

Page layout by O.H. Bezhkurenko

Publisher's address and location:
Lazariana Str., 2, Dnipro, 49010, Ukraine
Phone: +38-056-373-15-44, **Email:** office@ust.edu.ua

Journal website: https://tpm.ust.edu.ua/

Signed for printing 30/03/2026.
Format 60x84 1/8. Edition of 100 copies.